Development of a third rotational input on a force feedback joystick

Silvia Zamarrón Montoya

July 1, 2011

Acknowledgements

First of all, I would like to thank my supervisor at TECNUN, Jorge Juan Gil, who made my incorporation into DLR, where this thesis was carried out, easier, and, in the distance, was always available for everything I needed from him.

I must thank specially the help provided by Carsten Preusche, my supervisor at DLR, and by Michael Panzirsch, who was my gide and workmate during the development of the thesis. I thank also all my colleagues at DLR, who with professionalism, patience and kindness knew how to help me get through the difficulties.

Finally I thank my parents, who are always there for me, supporting and encouraging me to carry on.

Resumen

Habitualmente los joysticks con realimentación de fuerza incorporan dos grados de libertad que son suficientes para muchos usos. Sin embargo, hay casos en los que un tercer grado de libertad que también tenga realimentación de fuerza es útil como entrada, por ejemplo cuando surge la necesidad de controlar un robot móvil con cuatro ruedas independendientes. Este tipo de robot ha sido desarrollado en DLR: el *Robomobil*. Un joystick de tres grados de libertad sustituiría los elementos tradicionales de conducción (volante, freno y acelerador) y posibilitaría al conductor comandar los movimientos longitudinales, laterales y rotatorios independientemente.

Las ventajas de este sistema son muchas, tales como: la integración de los controles de conducción en un único aparato, la posibilidad de comandar movimientos independientemente, o el ser compatible en términos de direcciones, por nombrar algunos ejemplos.

El objetivo de este proyecto fue investigar qué tipo de entrada era adecuada para el tercer grado de libertad y cómo afectaba al control de un joystick de tres grados de libertad el acoplamiento de la cinématica del antebrazo humano. Teniendo esto en cuenta, se realizó un estudio de usuarios (un robot de siete grados de libertad emuló los distintos modos del joystick, y con un aparato háptico, el Spacemouse, se comprobó si era adecuado separar alguno de los grados de libertad en dos aparatos). Finalmente se llevó a cabo el diseño mecánico para la implementación del tercer grado de libertad rotacional en un joystick de dos grados de libertad existente en DLR.

Contents

List of Figures

List of Tables

List of Symbols

$a(a_i)$	Actual position of the steered car
$a(t_i)$	Actual position of the target car
d	Control error
$k(t_i)$	Applied force on the steering device
e_1	Minimum distance to edge parallel to the direction of the load
e_2	Minimum distance to edge perpendicular to the direction of the load
p_1	Minimum distance between screws parallel to the direction of the load
p_2	Minimum distance between screws perpendicular to the direction of the load
d	Diameter of the screw
t	Thickness of the part
A_s	The screw thread tensile stress area
A	Transversal area
v_{xa}	Steered longitudinal velocity
v_{ya}	Steered lateral velocity
ϕ_a	Steered angular velocity
v'_{xa}	Desired longitudinal velocity
v'_{ya}	Desired lateral velocity
ϕ'_a	Desired angular velocity
β	Slip angle
ϕ_i	Steering angle for a wheel i
ω_i	Angular velocity in a wheel i
x_i	location in the x axis of wheel i, with i=1,...,4
y_i	location in the y axis of wheel i, with i=1,...,4
x	location in the x axis of the car cog
y	location in the x axis of the car cog
θ	yaw angle of the car cog
$\vec{v_w}$	vehicle linear speed in absolute coordinates
$\vec{v_v}$	vehicle linear speed in relative coordinates
$\vec{\omega}$	yaw rate

Part I

Report

Chapter 1

Introduction

The objective of the present chapter is to set the bases of this Master's thesis. To that end, the lines below describe the main points of the process, which are a brief description of the company where the thesis was developed, the project specification and motivation, the followed methodology, and the outline of the memory.

1.1 Deutsches Zentrum für Luft und Raumfahrt

Deutsches Zentrum für Luft- und Raumfahrt e.V. (from now on DLR) is Germany's national research center for aeronautics and space. Its extensive research and development work in aeronautics, space, transportation and energy is integrated into national and international cooperative ventures. It is engaged in a wide range of research and development projects in national and international partnerships. In addition to conducting its own research projects, DLR also acts as the German Space Agency. As Germany's Space Agency, the German federal government has given DLR responsibility for the forward planning and implementation of the German space program as well as international representation of Germany's interests. Key industries, including materials technology, medicine and software engineering, all profit from innovations made by DLR in the fields of aeronautics and space.

Figure 1.1: DLR's logo

The modern DLR was created in 1997, but was the culmination of over half a dozen space, aerospace, and research institutes from across the 20th century. Nowadays approximately 6900 people work for DLR, and the center has 33 institutes and facilities throughout Germany: Augsburg, Berlin, Bonn, Braunschweig, Bremen, Cologne (headquarters), Goettingen, Hamburg, Lampoldshausen, Neustrelitz, Oberpfaffenhofen, Stade, Stuttgart, Trauen and Weilheim. In addition to these locations, DLR also has offices abroad.

The DLR budget for in-house research and development work and other internal operations amounts to approximately €770 million, of which approximately half comes from revenues earned by DLR. DLR also administers the space budget of the German government, which totals some €1047 million (2009).

In Oberpfaffenhofen, a town 20 km away from Munich, where this thesis was developed, the following DLR facilities can be found:

- Applied Remote Sensing Cluster

- German Remote Sensing Data Center (DFD)

- Remote Sensing Technology Institute

- Space Operations and Astronaut Training

- Flight Experiments

- Microwaves and Radar Institute

- Institute of Communications and Navigation

- Institute of Atmospheric Physics

- Institute of Robotics and Mechatronics

- Space Operations and Astronaut Training

- DLR School Lab

1.1.1 The Institute of Robotics and Mechatronics

The content of the present thesis is part of the research Project carried out at DLR's Institute of Robotics and Mechatronics' Department of Robotic Systems in collaboration with Sensodrive (spin-off of DLR) to develop a new Force Feedback Joystick. The work team is formed by Carsten Preusche (Team chief), Michael Panzschirz (Control coordinator), Stephan Lechner (Mechanical coordinator), Norbert Sporer (Electrical coordinator) and Bernard Schoer (Psicologist).

Nowadays around 150 people work on the Institute, and their projects are based on the integration of mechanics, electronics, and information technology up to 'intelligent mechanisms' and robots which interact with their environment. The 'integral' design optimization and 3D simulation of such systems and components before they are built plays a decisive role. The Institute is a worldwide leading institution in applied robotics research with focus on space robotics and technology transfer in industrial and service robotics, surgery and prosthetics.

Figure 1.2: Different projects carried out at the Institute of Robotics and Mechatronics

1.2 Motivation

Usually force reflecting joysticks (as desktop devices) incorporate two degrees of freedom, which are sufficient for most uses. However, in some cases a third degree of input and feedback is useful and necessary, e.g. in case of a car-like robot with four steerable wheels, a concept investigated by Oshima in [1]. This kind of robot has been developed at DLR (the Robomobil, ROMO), and works based on this new steering concept: the 4 Wheel Independent Steering (4 WIS). As its name indicates, each wheel receives a different command in order to reproduce the movement steered with a control device (see figure 1.3).

Taking the displacement of the car as a movement on the plane, just three coordinates are needed to fully describe its displacement. The idea is to replace the traditional steering elements (steering wheel, brakes and accelerator) with a 3 degree of freedom (henceforth labelled as 3DoF) Joystick which would make the user able to command longitudinal, lateral and yaw movement independently in terms of velocity, acceleration or even curvature. The exact position of the

center of gravity is known in each moment, fully defining the movement of the car.
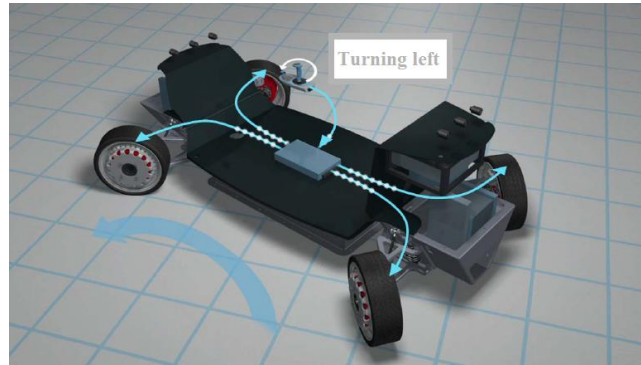
Figure 1.3: 4 Wheel Independent Steering

Advantages of this system are many, such as the absolute integration of the steering controls in a single device, the possibility to separately command movements, or the fact that it is compatible in terms of directions to name some examples.

Focus of this thesis is to investigate if the third degree of freedom can be applied and how the implementation can be done.

1.3 Methodology

The methodology followed during the development of the thesis is explained briefly in the following lines. It can be divided in three basic stages: the literature research, the user study design and implementation and the mechanical design.

Literature research was done in order to get familiar with concepts present at DLR, such as teleoperation, haptic devices and the kinematics of car-like robots.

Since the steering of the ROMO with a 3 DoF Joystick implied a whole new steering experience for the user and the human forearm kinematics may affect it, a user study was held up previous to the mechanical design stage to investigate these effects and the suitability of integrating the third degree of freedom. A driving simulator was conducted using DLR's Light weight robot, DLR's Spacemouse, and a virtual reality model of the ROMO.

The results of the study were used for the mechanical concept specification. The different options were weighed up, depending on the type of feedback provided by the third degree of freedom. Different sketches and calculations were made, and finally the optimal option was selected. The final phase of the Mechanical design consisted on implementing the new parts in the existing model of the 2 DoF force feedback Joystick in the computer aided design software Pro-Engineering Wildfire.

1.4   Memory outline

The present memory intends to follow chronologically the methodology carried out through the development of the thesis. To that end, it is divided in six different chapters.

The second chapter, the first chapter is the present introduction, the State of the art, shows the literature research done in the early stages of the thesis: familiarization with teleoperation and haptic technology, different 3 DoF haptic devices available, current situation of cars steered by sidesticks, as well as a deeper study on the DLR's ROMO was carried out.

On the third chapter the design and implementation of the user study is fully explained, describing the different steps taken to get from the model implementation in the simulator to the development of the study by the participants.

The mechanical design process is gathered on the fourth chapter: all the different options taken in consideration and the mechanical advantages and disadvantages they presented are documented. The final overview is explained, with the last three possible options. After getting more specific data to evaluate the configurations (providers were consulted, inertia and torque calculations were made), the optimal option to build the prototype was selected. In the last part of the chapter the design with Pro-Engineer is briefly explained and the final model is showed.

The economic budget can be found on the fifth chapter.

The conclusions and the outlook are listed in the sixth and last chapter.

In addition to these chapters an annex with several appendixes is attached. Each of them gathers topics which were useful for the development of the thesis, but not essential to follow the working out of the memory. The topics are: The kinematic analysis of a wheeled mobile robot, the instructions and questionnaires handed out during the user study, some calculus, and the drawings of the prototype parts.

Chapter 2

State of the art

This chapter gathers the literature study done on the first stages in order to get familiar with concepts necessary and useful for a good development of the thesis.

2.1   Teleoperations and haptic technology

The manipulation of an object can be done using bare hands, but sometimes it is not safe or possible, so the use of a tool is mandatory. Therefore a new concept called teleoperation came up, which is the manipulation of objects using robotic tools. It comprises a robot technology where a human **operator** holds on to an interface, called the **master** device, and gives force and movement commands to the system. According to [2], the remote robot, called the **slave** device, follows the motion of the operator and collects information from the remote site. The master device and the slave device are connected via a **controller** and a transmission line, sometimes with significant time delays [3].

The controller, usually also called the teleoperator, is the interface that communicates forces and movements between the human operator and a remote environment. Therefore the core of the model is how forces and movements are transmitted through the teleoperator, from the operator (F_h) to the slave (F_{sc}). F_{mc} is the force transmitted from the master device to the controller (which should be as similar to F_h as possible), and F_e is the force the environment transmits to the slave when they contact. The components the system consists of and the forces on each stage can be seen on Figure 2.1.

An very important concept which can be part of a teleoperator system is the force feedback. It means that the force generated at the slave when it interacts with the environment (F_e) is fed back to the operator in order to generate a real response in the manipulation tasks. The feedback is generated artificially by measuring the force at the slave robot and generating it with an additional actuator to the control equipment. The feedback can be controlled through indirect force control or impedance control (e.g. with a P.D controller) or through direct force control. By allowing the operator to feel the interaction forces from the remote environment certain tasks can be performed more reliably or faster according to [7] than without this feedback information. Actually, if we add force and/or distributed tactile feedback of sufficient range, resolution
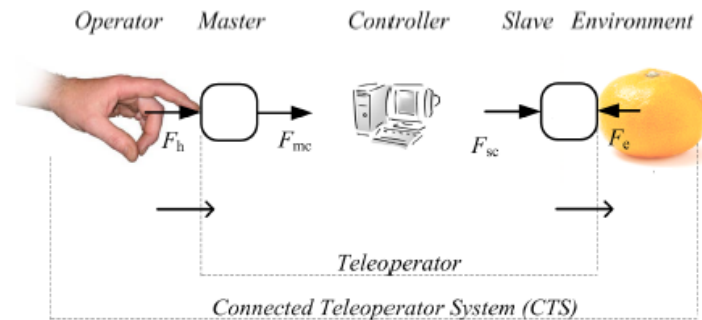
Figure 2.1: The teleoperator (Master-Controller-Slave) is in contact with the operator (left) and the remote environment (right). The whole system is the Connected Teleoperation System [3].

and frequency bandwidth to match the capabilities of our hands and other body parts, a large number of applications open up. Haptic technologies cover these issues.

With the processing power of modern computers it was also possible to generate virtual environments with which the operator could interact with, and the development of new master interfaces exploded. Force feedback can also be used in these virtual environments to generate the feeling of presence [2].

As it was mentioned above, the aim of haptic technology is to provide users with feedback information at the control tool on the motion and/or force that he or she generates. To enhance bilateral interaction between the user and simulation system, the haptic devices (which are the master in the systems) are introduced to provide both position and force information [4]. They are especially useful for tasks where visual information is not sufficient and may induce unacceptable manipulation errors (taking advantage of amplifying or reducing human-scale), for example, surgery or teleoperation in radioactive/harsh environments or with biological agents, in which safe human presence would be expensive to achieve and maintain. They can have other applications, such as fine compliant assembly or Virtual reality (VR) environment simulation. Consequently, multiple disciplines such as biomechanics, neuroscience, psychophysics, robot design and control, mathematical modeling and simulation, and software engineering converge to support haptics.

A haptic interface is needed to 'connect' the operator with the slave: it is a computer-controlled mechanism designed to detect motion of a human operator without impeding that motion, and to feed back forces or torques from a teleoperated robot or virtual environment. One intriguing theme in robotics research is the construction of a haptic interface and actuate the operator without significantly impeding the hand motion [5], i.e. the demand that the operator or subject be as unimpeded as possible in motion, yet be provided with forces and torques that are of high fidelity.

Not-force reflecting haptic devices, also called **passive** control devices, receive motor action commands from the user and display appropriate tactual images to the user. Computer keyboards, mice, trackballs, and even instru-

mented gloves available in the market can be thought of as relatively simple haptic interfaces, but they can only convey the user's commands to the computer, and are unable to give a natural sense of touch and feel to the user.

Three different resistance modes can be found on passive control devices: the **isotonic**, the **elastic** (also called isomorphic or spring-loaded), and the **isometric** mode, according to [6]:

- Isotonic devices have constant resistance and variable position.

- Isomorphic devices, in which as the stiffness of elasticity increases, the selfcentring effect increases accordingly, i.e. the device's resistive force.

- Isometric devices have constant position and variable resistance (which can increase up to infinite resistance).

[8] found that isotonic devices were more effective when position (or orientation) was being controlled directly, but that isometric devices worked better when hand motions were used to control velocity, as opposed to position.

On active control devices, [9] states that the desirable features of force-reflecting haptic interfaces are:

1. Low back-drive inertia and friction, and no constraints on motion imposed by the device kinematics.

2. The range, resolution, and bandwidth, both in terms of position sensing and force reflection, should match those of the human for the tasks for which the haptic interface is employed.

3. Ergonomics and comfort: Making the human user comfortable when wearing or manipulating a haptic interfaces is of paramount importance, since pain, or even discomfort, supersedes all other sensations.

Various kinds of haptic devices have been developed, such as data glove and pen-based and robot-based haptic interfaces [4]. Among them, the force-reflection joystick has the merit in its simplicity and generality. DLR's 2 DoF Force reflecting joystick is an example of this, and it is the device the third degree of freedom had to be integrated on.

2.1.1 Joysticks

Joysticks can be distinguished within desk-grounded masters (this kind of masters tend to be more compact, easier to install and less expensive than other force feedback systems). They have been used for many years as a simple and intuitive input devices for computer graphics, industrial control and entertainment (video games) applications [7]. These general-purpose joysticks typically have a two degree-of-freedom swing arm with a handle that is positioned by the user.

Usually two degrees of freedom are enough for the demanded tasks, and [10] states that the development of Joysticks or haptic devices with 3 or more degrees of freedom has not been widely run due to complexity, coupling of the degrees of freedom or lack of a field of application. However, the following are examples of 3 DoF sticks which have different feedback and tasks for the third degree of freedom. They were analyzed in depth to learn about design of haptic devices and their properties:

Russo's 3 DoF Force Output Joystick

The development of the design and implementation of this new type of force reflective joystick is described in [10]. It has three degrees of freedom that are actuated by both motor and brakes on each axis, which are uncoupled thanks to a novel kinematic design. Two of the degrees of freedom are actuated through a cardan joint, and the third degree of freedom, which is translational, is actuated through a sleeved cable transmission (which provides the system of high looseness). Control strategies are carefully designed to provide the system of accurate feedback.

The application of this joystick is the manipulation of physical models in virtual environments. The force feedback (achieved thanks to the use of a force torque sensor) is appropriate to display the inherent force information of these models necessary for a good performance of the user.

Logitech's Extreme 3D Pro Joystick

The joystick commercialized by Logitech as 'Extreme 3D Pro Extreme' is also a 3 degree of freedom device. The degrees of freedom are uncoupled, two of them are joint by a cardan joint and the third degree of freedom, which is rotational, has spring centered elastic feedback.

It is specially designed for its use in flight simulator games, but it can also be used in other games which require the rotational degree of freedom. The sensor is a magnetic sensor which works based on the hall effect.

Figure 2.2: Logitech's Extreme 3D Pro Joystick

SHaDe

A new type of haptic device using spherical geometry has been proposed by Birglen [11]. It is a three rotational DOF centerstick with a simple design and an ergonomic interface. The particular architecture of the Spherical Haptic Device (SHaDe) leads to several advantages, namely pure rotation around a point located inside the user's hand (therefore a 6 DoF-force torque sensor is needed), large workspace, and precise manipulation with wrist resting. Its basic kinematic properties are used for control and geometric optimization purposes in virtual environments and teleoperations. However, it has been observed that the control of the device by the user is difficult due to the parallel structure.
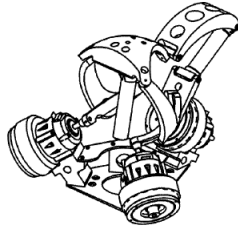
Figure 2.3: CAD model of SHaDe

The possibility of designing joysticks with more degrees of freedom based on various mechanisms is proved with devices such as the four degree-of-freedom, force-reflecting manipulandum by Millman [12] or the 6 DoF reflecting Joystick by Lindemann [13].

2.2 Stick-steered vehicles

As it was mentioned before, the present thesis deals with the idea of controlling DLR's ROMO using a joystick. The following lines show the literature study on the actual situation of the specific systems which are the stick steered vehicles, and the suitability of their use.

The sidestick-steering concept is widely used in the aircraft industry, due to the fact that fly-by-wire technology offered for the first time in aircraft development the possibility of removing conventional control column/wheel inceptors [14]. It gave the vision to fly an aircraft by fingertip inputs and providing 'ideal' stick force characteristics to the pilot over the whole flight process. Therefore the use of small control manipulators was a logical step when fly-by-wire flight control systems were developed. From the beginning small inceptors like sidestick or sidegrip systems were investigated. They were first introduced in military aircrafts and finally they were applied to civil transport aircraft as well. In order to avoid complex feel systems sidesticks in today's fly-by-wire aircraft have got fixed force/deflection characteristics with simple spring/damper systems in passive sidesticks [15].

The 'by-wire' systems have slowly reached other fields: one of the latest trends in automobile chassis control systems is to consider the steer-by-wire (SBW), which, as in the case of aircrafts, promise the potential for reduced weight, improved fuel economy, and improved packaging compared to their mechanical counterparts. In these systems the mechanical connection between the driver's steering wheel and the steering gear, or rack (which turns the road wheels), is replaced by an electrical control signal (see Figure 2.4). Since there is no longer a mechanical connection between the road wheels and the steering wheel in a steer by wire vehicle, the steering control device can be placed just about anywhere in the vehicle within reach to the driver (see Figure 2.5 for an example of stick displacement).

The main benefits of joystick steering in automobiles according to [16] are:

- Intuitive integration of longitudinal and lateral control, and therefore more
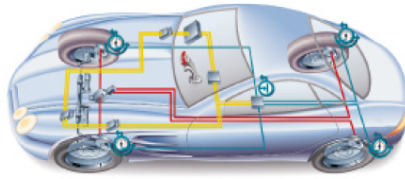
Figure 2.4: Drive-by-wire system

Figure 2.5: Automobile with two integrated joysticks

precise directional control.

- Faster reaction due to no use of feet.

- Greater space and flexibility to place the controls.

- Improved safety during a crash.

- Eliminating effects of friction, compliance, and lash.

- Getting feedback from state variables (speed, steering angle, etc.).

- Use of sophisticated vehicle dynamics control strategies.

In the last years several user studies ([16]-[19]) have been carried out investigating differences between steering cars with conventional steer elements and sidesticks. Although in most cases participants had a lot of experience driving with conventional elements and a similar control over joystick use would require of training, in general these user studies showed positive results concerning the sidestick steering: performances were at least equal, but clear advantage on the longitudinal steering and benefits in case of sidewind were observed. The stick-steering also demanded less work effort from the users.

The comparison between active and passive stick steering systems has also been an interesting research topic ([14] and [20] investigated this). The results

support the implementation of active sticks: the drivers' performance was significantly better and the work load was found to be lower than with passive systems.

[21] and [22] have also investigated the suitability of joystick control implementation in electric cars for disabled people, due to the reduced space needed for the device and the demanded limited range of motion. For example, Paravan is a German company which commercializes joystick steered vehicles specially designed for handicapped people.

2.3   DLR's ROMO

ROMO (ROboMObil), see Figure 2.6, is the robotic vehicle developed at the DLR Institute of Robotics and Mechatronics. It points toward the development of an innovative electro-mobility concept (studied in [1]) based on intelligent central control of four individual mechatronic 'Wheel Robots', which integrate the drive train, brakes, steering and dampers. The entire vehicle features ten independently controllable vehicle dynamics actuators. Apart from conventional forward/backward driving, the ROMO is able to rotate about a vertical axis (through the vehicle center or eccentric) or to move sideward (especially helpful for entering narrow parking bays), as [23] explains.

Figure 2.6: Virtual representation of DLR's ROMO

The mechanical power train is replaced by the wheel robots and an intelligent robot control concept provides the ROMO with unparalleled maneuverability: it can be driven with various degrees of autonomy, from partially to fully autonomous, i.e. from full manual control giving the driver input using a sidestick, to the point of autonomous navigation in an unknown environment without any human operator involvement.

The trend-setting module concept, which is composed of the front and rear chassis modules, the battery module and the body module with the central vehicle control unit, make ROMO a technology demonstrator for innovative vehicle dynamics control and energy management concepts; and a demonstration for the merge of robotics and electromobility [24].

Recently this robotic research vehicle has been put into operation facilitating research on a wide spectrum of scientific questions dealing with electric and autonomous mobility. Due to the high maneuverability of the vehicle new operation concepts for interactive driving are needed. Therefore, it is important to

distinguish the various motion operating modes, suitable reference motion parameterization and adequate filtering of the operator's inputs both depending on the operating mode. Furthermore, for turning on the spot the instantaneous center of rotation may be interactively set by the operator on a touch screen [23].

Chapter 3

User study

A driving simulator experiment was conducted with the aim of studying how the coupling of the human forearm kinematics affects the control of a 3-degree-of-freedom Joystick when steering a car in a virtual environment. Sixteen men participated in the study, all unexperienced with joystick driving. The driving tasks, divided in blocks depending on the degrees of freedom controlled, consisted of following the trajectory of a virtual target car. The differences in performance between having a separation in the lateral or the rotational steering and having all degrees of freedom integrated in the same device were investigated. The criteria for evaluating the study were objective performance data (comparison of actual and target trajectories and applied force on the devices), and subjective ratings in several questionnaires. The main results of the study were that performance with degrees of freedom integrated was more advantageous for lateral driving tasks, whereas in the case of rotational driving tasks, performances were better when the rotational degree of freedom was separated. In general, participants indicated that the driving experience was more intuitive, consistent and simple when the longitudinal and lateral degrees of freedom were integrated in the same device. At the end of the chapter a discussion about these results and design issues is provided.

3.1   Motivation

The motion of DLR's ROMO, as it was explained in the previous chapter, exhibits three independent degrees of freedom (see Figure 3.1). Currently, the joystick integrated in the ROMO for its steering is DLR's 2 DoF active Joystick, which appears to be sufficient since the lateral dynamics and yaw motion are coupled. However, a steering system where the 3 degrees of freedom are decoupled seems like a sensible idea. Furthermore, to optimize space and intuitiveness these decoupled three degrees of freedom, which are the primary controls, could be integrated in the same stick.

Since this whole concept of integrating the three degrees of freedom in the same device is completely new, some questions arise: Should it be wrist steered? Or just activated by a button? Is the coupling of the human arm kinematics a problem to steer the three degrees of freedom independently?

To our knowledge, no previous user studies had been held regarding this
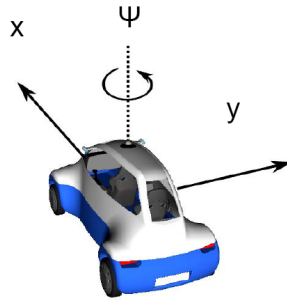
Figure 3.1: ROMO's 3 DoF

particular steering concept. Therefore an ergonomic evaluation study was conducted at the German Aerospace Center (DLR).

3.2 Method

This section provides a description of the experimental design, participants, and the experimental set-up.

3.2.1 Experimental conditions

Since the main objective of the study was to study the convenience and usability of having three degrees of freedom actuated by a single device, three different experimental conditions were implemented:

- Experimental condition 1. 3 DoF Joystick ('J'): The three decoupled degrees of freedom, i.e. longitudinal, lateral and rotational, were integrated in the same device. See Figure 3.2.
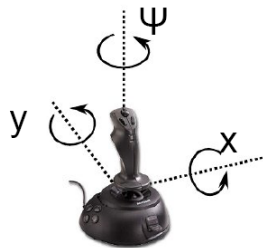
Figure 3.2: Experimental Condition 1

- Experimental condition 2. Separation of the lateral steering ('SL'): The lateral control was separated and implemented in DLR's Spacemouse and the other two decoupled degrees of freedom, i.e. longitudinal and rotational steering, were integrated in the Joystick. See Figure 3.3.
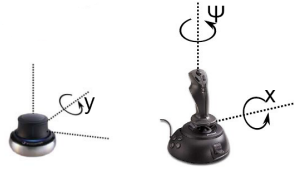
Figure 3.3: Experimental Condition 2

- Experimental condition 3. Separation of the rotational steering (SR): The rotational control was separated and implemented in DLR's Spacemouse and the other two decoupled degrees of freedom, i.e. longitudinal and lateral steering, were integrated in the Joystick. See Figure 3.4.
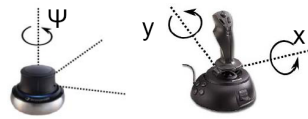
Figure 3.4: Experimental Condition 3

3.2.2   Input variable

Regarding the input variable associated to the control devices, two possibilities were carefully considered:

- The desired car velocity

- The desired car acceleration (reasonable input variable for the longitudinal movement according to [17])

If the input variable associated to the steering device was the desired acceleration, drivers just needed to steer the control device to provide the car with a new acceleration. Afterwards, the device was returned in its initial position and there was no more need of steering until a new acceleration was needed, and meanwhile the car went on with its displacement. However, if the input device was the desired velocity, it required a continuous and consistent steering (which

led to a higher operating effort), because no steering was equivalent to no car movement. This driving made it also more likeable to have the three degrees of freedom (or at least two) operated at the same time. Since the aim of the present study was to look at potential biomechanical couplings of the degrees of freedom, we chose the desired car velocity as the input variable.

3.2.3 Feedback design

As it will be described on a later section, for the study the feedback of the Joystick (which was integrated in one arm of DLR's Light Weight Robot) could be completely designed to get an active or pasive feedback modifying a number of different parameters. Since active feedback will be content of later user studies, the considered choices were the ones regarding passive feedback: isometric and isomorphic feedback. However, the Spacemouse had a isomorphic (elastic) feedback in all of its 3 degrees of freedom, so this was the type of feedback which was also chosen for the Joystick, so that both devices could be comparable in terms of feedback. Figure 3.5 shows esquematichally the steering concept with passive feedback, which suits the case of the present study, whereas Figure 3.6 shows the control loop with an active control device.
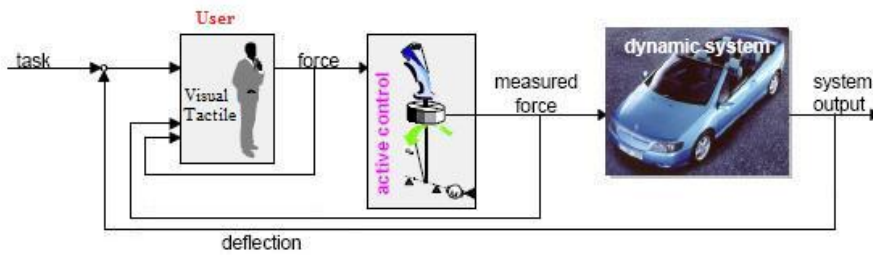
Figure 3.5: Control loop with a passive control device
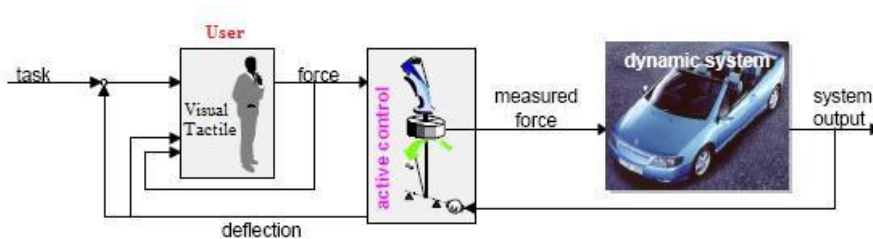
Figure 3.6: Control loop with an active control device

18

3.2.4 Driving task

The experimental design of the driving tasks for this study was based on a theoretical framework which is described in this subsection. As it was mentioned before, the experiment focused on the primary control of a vehicle equipped with one single control device or two. Primary control includes steering, braking and accelerating, and they are the driver's principal tools to get to a desired destination. That is the reason why before designing a driving task it is important to investigate about the human behaviour while steering a car.

In [21] the driving is said to be considered a cognitive motivated, regulated and controlled task. However, both perceptual and psychomotor abilities are required in order to carry out the driving task succesfully. While driving a car, the tasks can be high demanding on the driver, since they can vary from a simple tracking control to an extremely complex task. The task requirements can change from very low to extremely high with within less than fractions of a second. If the demands are low (usually at low velocities) the driver is able to plan and anticipate possible effects of his/her steering, and they say in [22] that the control of the car is carried out as a highly automated compensatory control. However, if the demands increase (at higher velocities) there is less time to plan and anticipate, so driving becomes more reactive and time becomes a critical factor. Keeping this in mind, it can be said that succesful driving seems to require adaptive driver behaviour including both compensatory and anticipatory control, and that depending on the situation, time may be a critical factor for the outcome of driving behaviour.

The three-level-model of the driving task (studied in [25]), see Figure 3.7, follows the idea of a hierarchical control structure. They assume that There is a communication between three levels where goals and criteria are defined at a higher level and the outcome of lower levels modifies goals at a higher level. The three levels can be distinguished by the task requirements, the time frame needed to carry them out and the cognitive process involved in each level.
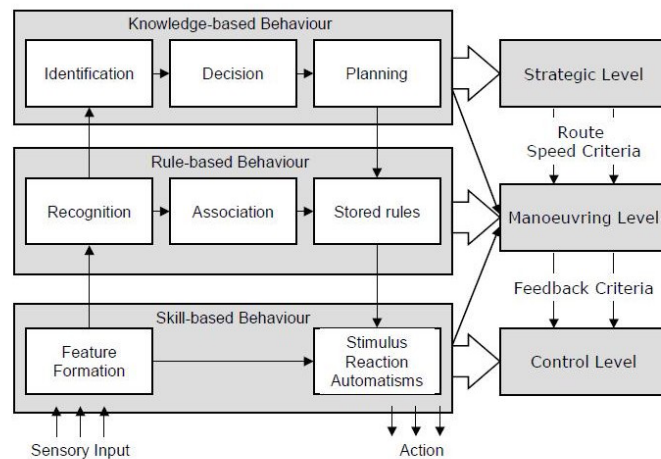
Figure 3.7: Three-level model [25]

The following lines briefly explain this driving model:

The lowest level is an operational, control level, where typically the steering wheel and the pedals are operated. The decisions made in this level are rather automatical within a very short time range as they are reactions that respond to external stimulus. Typical tasks on this level are lane keeping or gear shifting (matching or compensation tasks where the position needs to be corrected all the time) which are conducted without conscious information-processing by experienced drivers, and it could be supposed that different drivers would react the same way to the tasks.

The second level is a tactical, vehicle maneuvering level (also sometimes referred to like tactical or guidance level) referring to how traffic situations are mastered, these decissions are made within seconds. Typical manoeuvres are overtaking, turning or gap acceptance. Behaviour in this level is not only by motivational variables, but also by situational ones.

The third and highest level is a planning or strategic level. It comprises all processes concerning trip decisions, such as where, when, how to go, and so on. Decisions on this level are rare and take longest in comparison to the other levels. Due to their nature they are processed in a more or less aware mode, but become habits in case of constant repetition. It can be said that the number of decissions of this type taken on a trip are very few compared to the decissions taken in the other levels.

Given the hierarchical description of the driving task it was a good idea to match it to actual human behaviour. According to [26], human control structures are highly flexible and highly dependent on practice and experience, and they can be adressed in the hierarchical SRK model showed in Figure 3.8. This model discriminates between skill-based, rule-based and knowledge-based control.

	Strategic / Planning	Tactical / Maneuvering	Operational / Control
Knowledge	Navigating in unfamiliar area	Controlling skid	Novice on first lesson
Rule	Choice between familiar routes	Passing other vehicles	Driving unfamiliar vehicle
Skill	Route used for daily commute	Negotiating familiar intersection	Vehicle handling on curves

Figure 3.8: Michon's control hierarchy [26]

Since the results obtained in this study intended to be as general as possible, and the more spontaneous the drivers' reactions the better, the task design did not focus on neither knowledge based behaviour nor rulebased behaviour. This was easy because the driving experience with the primary controls presented was completely new for the participants. Therefore, tasks would require of the skill based behaviour, which matches with the control level in the three-level-model, so tasks were placed in the stabilisation plane. As mentioned before,

Figure 3.9: Steered car following target car

these tasks demanded a continuous correction of the position, which included:

- Control the track deviation (x and y)

- Control the yaw angle error (ψ)

As Huang in [27] states, these compensation tasks are performed at high velocities, and, unlike at low velocities, where you can control the error of position in foresight, the comparison of desired position and the actual position is absolute, not relative. Therefore we chose a type of simulation in which the path to follow could not be known in foresight (a circuit was not a suitable option, the driver could look ahead and decide his/her next step), instead, the choice was to create different trajectories of a target car, see Figure 3.9, which would be followed by participants. The objective was to reach the same position as the car in every moment. These trajectories required a one degree of freedom steering or a two degree of freedom steering, as it will be later explained in detail.

Six different blocks of tasks were designed. Four of these blocks just required to steer one degree of freedom, i.e. the steering was longitudinal, lateral or rotational. Since they had a learning objective, all participants performed these task-blocks first. Furthermore, within a task block, each task was repeated twice, and inside each block the differences between tasks were the velocity variations: each task required a higher velocity control than the previous one.

The other two task-blocks combined two degrees of freedom: The steering task was a combination of the longitudinal steering and the lateral steering (x and y) or the longitudinal steering and the rotational steering (x and ψ), respectively. Again, each task was repeated twice. In the case of the diagonal steering, the task had variations in the angle of the diagonal trajectory, whereas in the case of steering a curve, the variations were in the curvature of the cornering.

Table 3.1 and Table 3.2 summarize this:

1 DoF-Experimental tasks	
Task block	Degree of freedom
A1a - Longitudinal Displacement Forwards	x
A1b - Longitudinal Displacement Backwards	x
A1c - Lateral Displacement	y
A2 - Rotation	ψ

Table 3.1: 1 Degree of freedom experimental-tasks

2 DoF-Experimental tasks	
Task block	Degrees of freedom
B1 - Diagonal Displacement	x,y
B2 - Curve	x, ψ

Table 3.2: 2 Degree of freedom experimental-tasks

3.2.5 Experimental design

Since the objective of the experiment was to investigate differences when steering with all the degrees of freedom integrated in the same device and with the degrees separated in two different devices, participants were divided in two experimental groups: The lateral separation group, and the rotational separation group.

Participants

Sixteen right-handed, male DLR employees with an age range of 23-43 participated in the study. All subjects had taken part in a preliminary screening of senso-motor and fine motor skills. The subjects were assigned to the experimental groups in a way that both groups were comparable regarding participants' motor skills.

Lateral steering separation

The eight participants in the lateral separation group were divided in two subgroups (see Figure 3.10): Four participants of the group performed the six driving block tasks just using the 3 DoF Joystick first, i.e. there was no separation of the lateral steering. To investigate the effects of lateral separation, two of these tasks had to be repeated in the second part of the experiment. Therefore, the Spacemouse was introduced. The participants first used it to perform the learning task, that is, the block task of the pure lateral steering. The last block task, that of the diagonal steering, required the use of both the Joystick and the Spacemouse: the Joystick to steer in the longitudinal direction and the Spacemouse to steer in the lateral direction.

```
1.Person      A1 A2 | B1 B2 | A1c B1
3.Person      A2 A1 | B1 B2 | A1c B1
                    ‿‿‿‿‿     ‿‿‿‿
                      J         SL

2.Person      A1 A2 | B1 B2 | A1c B1
4.Person      A2 A1 | B1 B2 | A1c B1
...                 ‿‿‿‿‿     ‿‿‿‿
                      SL        J
```

Figure 3.10: Lateral separation group

The other four participants performed the six driving block tasks using the 3 DoF Joystick and the Spacemouse first. This was done to control for potential order or time effects (like learning, fatigue). The Joystick was used to steer in the longitudinal direction and the rotational steering, and the Spacemouse to steer in the lateral direction. In the second part of the experiment the pure lateral displacement and the diagonal steering were performed with the 3 DoF Joystick.

Rotational steering separation

Analogously, the eight participants of the rotational separation group were divided in two subgroups (see Figure 3.11): Four participants of the group performed the six driving block tasks using the 3 DoF Joystick in the first place, there was no separation of the rotational steering. In the second part of the experiment, two of these block tasks had to be repeated, to observe which effect had the rotational separation, therefore the Spacemouse was introduced. The participants first used it to perform the learning task, that is, the pure rotational steering. The last task, the steering of a curve, demanded the use of both the Joystick and the Spacemouse: the Joystick to steer in the longitudinal direction and the Spacemouse to steer in the rotational direction.


```
1.Person      A1 A2 | B1 B2 | A2 B2
3.Person      A2 A1 | B1 B2 | A2 B2
                    ‿‿‿‿‿     ‿‿‿‿
                      J         SR

2.Person      A1 A2 | B1 B2 | A2 B2
4.Person      A2 A1 | B1 B2 | A2 B2
...                 ‿‿‿‿‿     ‿‿‿‿
                      SR        J
```

Figure 3.11: Rotation separation group

The other four participants performed the six driving tasks using both the 3 DoF Joystick and the Spacemouse first. The 3 DoF Joystick was used to steer in the longitudinal and the lateral direction, and the Spacemouse to steer in the

rotational direction. In the second part of the experiment the pure rotation and the steer of a curve were performed with the 3 DoF Joystick.

3.2.6 Driving simulator

The hardware of the driving simulator consisted of

- DLR's Light Weight Robot (LWR) with a 3 degree-of-freedom Joystick as the tool at the end-effector (see Figure 3.12). This robot has 7 degrees of freedom, which can be independently adjusted (taking care of singularities) to reach the desired position of the end-effector. It allows multiple configurations, not just in terms of position, but also in terms of force-feedback. This can be achieved thanks to the Human Machine Interface developed at DLR and whose function in this simulation will be explained later.

Figure 3.12: DLR's Light Weight Robot

- DLR's Spacemouse. See Figure 3.13. This haptic device has three degrees of freedom (x, y and θ, the yaw angle) with isomorphic feedback, i.e. the user can feel a small deflection in the X, Y or Z plane, depending on the steering direction. It includes 3 force torque sensors, one for each degree of freedom. The Space Mouse is an elastic device with slight movement (5 mm in translation and 4° in rotation). It is patented by DLR, the German aerospace research establishment, manufactured by Space Control Company, Malching, Germany and marketed by Logitech, Fremont, CA, USA.

- Screen where the simulation was showed.

- Table where the Spacemouse was placed.

- Chair where participants seat.

Figure 3.13: DLR's Spacemouse

Figure 3.14 shows the actual disposition of the elements, which intended to be as ergonomical as possible. The correct position of the participant was checked before starting every task and it was supervised during the task performance.
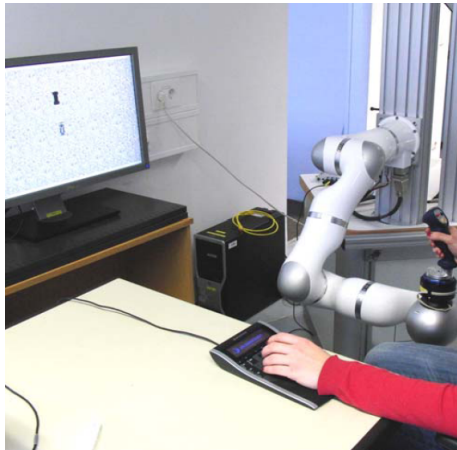
Figure 3.14: Driving simulator disposition

In this teleoperation system on a virtual environment the joystick and the spacemouse were the master devices, and the modeled ROMO was the slave.

The objective was to design the software to visualize the trayectories of both cars in the simulator screen: one car followed the inputs commanded by the user and the other one followed trajectories previously programmed and implemented in the simulation model. To do so Matlab Real Time Workshop, its simulation application Simulink and the visualisation program Instant reality were used.

The user study simulation run under Linux QNX realtime. Real time simulation systems like this are mainly used for testing and check out of control electronics and other components of complex modelled systems, which in the present case, was the ROMO. Therefore the model included vehicle kinematic and dynamic equations. The inputs of the model were obtained from exter-

nal devices (the Joystick placed at the LWR robot and the Spacemouse) each sampling time. Model equations were then solved within prescribed time intervals: this way a selected subset of variables could be computed and presented as outputs at the next sampling time. In order to implement real-time communication with external world and to schedule model execution exactly each sampling time, the present simulation software relied on the User Datagram Protocol (UDP): information packages were received from the external devices which were the Spacemouse and LWR robot, and information packages were delivered to the external device, the screen. Matlab Real Time Workshop addapted in the present case the Simulink off-line model to real time simulations on dedicated hardware.

The first steps of the Visualization design was the set-up of the LWR, since this robot per se was not designed to have a Joystick as the end effector tool, and in the cases it had one, the Joystick had two degrees of freedom, and not three, which is the present case. To that end, a new demo or user case was implemented: '3 DoF Joystick'.

To set the initial configuration of the LWR up, as well as to set some other parameters up (such as the damping and stiffness of the system) the Human Machine Interface (HMI) for the LWR designed on Simulink by Tomas Hulin at DLR was used and modified.

This HMI had already implemented four demos for different uses, but for all of them the general constants of the robot were defined and they were given values in a common block. These constants included, amongst others, the very important element for the kinematics of robots which were the different transformation frames. The transformation frames are 3x4 matrixes which allow the translation of coordinates from one physical point (a frame origin of coordinates) of the robot to another. Each of them is the joining of a 3x3 rotation matrix and a 3x1 translation array. The present robot, the LWR, had three transformation frames (see Figure 3.15 : the baseframe, the toolframe and the sensorframe (whose function was to transformate the forces measured by the force torque sensor to robot coordinates). The function of these frames was crucial, since measures (which were the user's steering commands) made by the sensor were translated to robot coordinates from the end-effector to the base of the robot, and these inputs were later transferred over UDP to Matlab Real Time Workshop, the visualization interface.

These frames were not modified, just one parameter was changed, regarding the type of end effector: it was defined to be a joystick (its mass influences the force measured by the sensor, so it muss be taken into account). Another important set-up was to determine the exact point to be the center of rotation of the Joystick.

In addition to the 4 previous demos, a fifth demo, called '3 DoF Joystick', was created specially for this study, which included 'The feed forward compensation' and the 'Spatial stiffness' blocks. The 'Feed forward compensation' block gave the applied torque as an output, after doing the homogeneous transformations. In the 'Spatial stiffness' block the damping and the stiffness of the system were realized, which were manually adjusted for each steering axis based on personal try and error trials. In this demo it was also stablished the feedback to be isomorphic.

The fourth demo, the 'Interpolator demo', was used to free and indepently move manually the 7 joints of the robot, and save the position to asigne it to
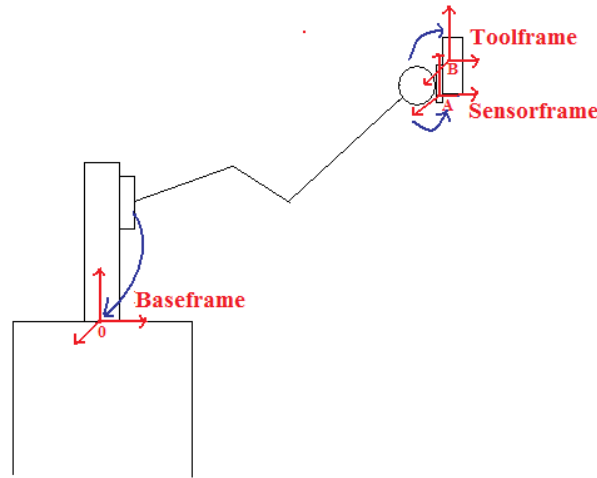
Figure 3.15: Transformation frames of the LWR

the fifth demo, so that the desired initial position of the end effector, where the Joystick would be placed, could be stablished. This was done manually to find an ergonomic position for the users to steer the Joystick.

Concerning the reception of data from the Spacemouse, the process was much more direct: this device has a 6 DoF force-torque sensor which measured the torques applied by the user on each of the three axis and could be automatically communicated via UDP to the 'Visualisation' program interface.

Input signals coming from the HMI hardware operating system, as well as the ones coming from the Spacemouse directly, needed to be interpreted, scaled and filtered. This was done in the 'Visualisation' program interface, which consisted of several blocks. Figure 3.16 is the flow chart which shows very schematically the steps followed both for the target car and the steered car before getting to the Visualization block inside the interface. The following are the steps followed before reaching the final visualization block of the interface:

1. The 3 input coordinates (in the current study they were the steered car absolut velocity in its center of gravity: v_x, v_y, ϕ) were received via UDP from one of the haptic devices, or from both. It was specified manually which of the 3 possible experimental conditions (see section 3.2.1 on page 16) was taking place so that the model got the coordinates from the correct input device.

2. The threshold (the minimum value the variable needs to reach so that it had any effect in the actual steering) was defined for each variable.

3. The input coordinates were scaled.

4. The velocity character of the input coordinates was optional: by default they were velocity inputs, but a manual selection block made it possible to define them as acceleration inputs.

5. After some other scaling the desired absolute velocity in the center of gravity (v_x, v_y, ϕ) and acceleration (this last was not used) were calculated.

6. The absolut linear velocity and rotational velocity were separated. Also β, the slip angle, was calculated.

$$\beta = atan(\frac{v_x}{v_y})$$

7. As later on will be explained in detail, the steering angles (ϕ_i) and angular velocities (ω_i) of the steered car wheels were calculated through kinematic equations. For the visualisation block we were only interested in the steering angles.

8. The so-called Double track model was implemented (developed by the designers of the ROMO), so dynamic elements were introduced, this way a more realistic velocity and position were calculated.

Finally, since the actual three coordinates of the centre of gravity of the car and the steering angles of the wheels were known, they were introduced as input values in the visualisation block.

The steps followed to watch the ghost car on the screen were different: The ghost car's trayectories were designed previously using time blocks and given constant accelerations within those blocks. Those blocks were 5 seconds long and depending on the task (see section 3.2.4 on page 21), acceleration remained constant from one to other or not. Before each task-block started, the number of the task was introduced manually. In the model, each time a demo was run, acceleration was integrated to get absolut velocity, and this absolut velocity was integrated to get absolut position. Absolut velocity went to a block like in the case of the Joystick steered car to get the wheel steering angles, so steps from 4 to 6 were also taken in this case.

As it can be seen on Figure 3.9, the visualization screen just showed two cars and the road they run through. The visualization program chosen was Instant reality, a high-performance Mixed-Reality (MR) framework which allows the developer to create applications by modelling and not just programming. Programming in X3D (sucesor to the Virtal Reality Modeling Languaje, VRML), allows not only the representation of 3D computer graphics, creating objects, shapes or textures, and defining visualization cameras through code lines, but also the integration of external x3d files. In the present case, developers of the ROMO provided us with the model of the car in x3d format. It was introduced as a external object in the programm.

The effect of seeing the target car as a 'ghost car' was achieved modifying the transparency characteristics all the objects have.

Every sampling time the inputs for the the programm were the different positions of both cars' centers of gravity, as well as the steering angles of their wheels. The Kinematic analysis to obtain these input data is fully developed in Appendix A of the Annex.

3.2.7 Procedure

The study took place in the Institute of Robotics and Mechatronics of the German Aerospace Center (DLR) between the 8th and the 18th of January of 2011.
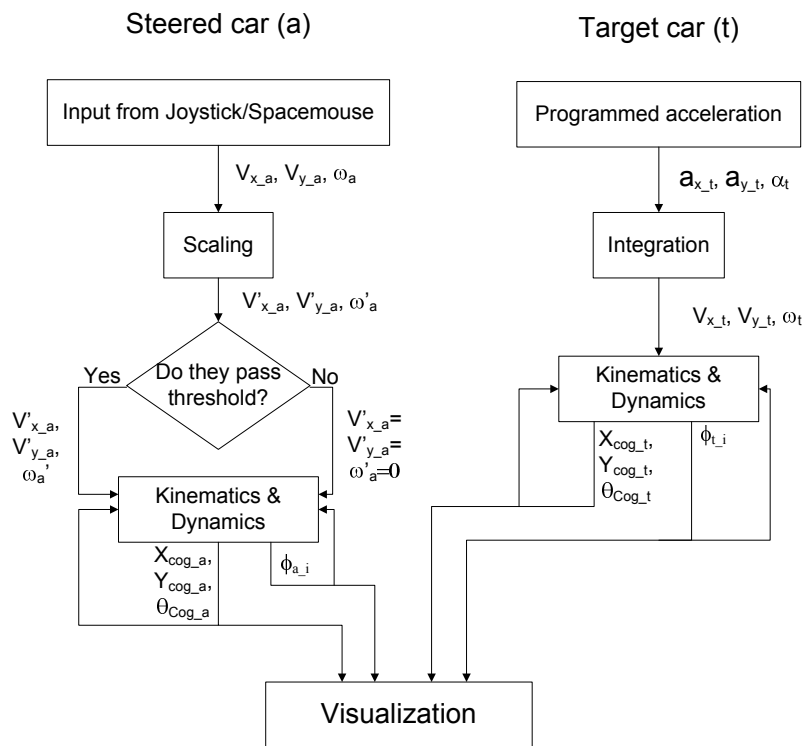
Figure 3.16: Visualization interface flow chart

The different tasks were previously designed, an implemented in the simulation, as it was explained in the previous subsection, but since for each participant the order of the tasks was different, they had to be carefully commanded manually from the computer. Different data about technical incidences during the experiment was collected.

A written instruction, introducing the study and its aim, the different devices, and the experimental task was given to each participant in the beginning. Before starting the experimental tasks, they were briefly explained to the participants.

After having finished a task block, participants filled out a questionnaire (NASA-TLX) measuring work load. Besides, the input devices were rated. After finishing the last of the six first task-blocks, in addition to the NASA-TLX, the System Usability Scale (SUS) was filled out by the participants. The aim was to collect opinions on topics such as the consistence of the system and the ease of use, for each driving system. After performing the last block a final questionnaire was given, which referred to this last block, but also about the whole experiment. Topics covered were for example previous use of the devices and comparison of both driving concepts.

Finally, participants could give freely their opinion on the different issues which had caught their attention, or ideas they would came up with. The questionnaires can be found in the Appendix B of the Annex (in german).

3.2.8 Statistical analysis

For each participant, the actual path followed (X and Y in meters and ψ in radians) and the force applied to the control devices (in Newtons for the longitudinal and lateral displacement and in Newtonmeters for the rotational displacement) were recorded by the simulator computer.

There are several parameters which can be obtained from the data recorded to evaluate the driver performance in a Experimental Study [20]. For the current study two were considered: the Control error (d) and the manipulating or operating effort (BA).

- Control error: The average distance between actual and target position.

$$d = \frac{\sum |a(a_i) - a(t_i)|}{n} \tag{3.1}$$

  with $a(a_i)$ the actual position and $a(t_i)$ the target position in meters in the case of the lateral and longitudinal steering. Therefore, the control error is calculated in meters. For the cases of rotational steering $a(a_i)$ and $a(t_i)$ are in degrees, and the control error has units of meters.

- Manipulating effort: The force applied to the device during the performance of each task is an indicator of the operating effort the task and the device demands.

$$BA = \sqrt{\frac{\sum [k^2(t_i)]}{n}} \tag{3.2}$$

  with $k(t_i)$ the applied force in Newtons in the case of the lateral and longitudinal steering. Therefore, the manipulating effort is calculated in

Newtons. When the tasks involved the rotation, the applied force was in Newton·meters, as well as the resulting manipulating effort.

Both individual and group means, and standard deviations were calculated for each driving block task. Then, a repeated measures analysis of variance (ANOVA) was used to analyse this data. The ANOVA analysis provides a statistical test of whether or not the means of several groups (in our case two different groups: tasks steered with Joystick and tasks steered with Spacemouse) differ significantly or not. A significance level of p=0.05 was used in the statistical tests.

3.3 Results

The presentation of the results has been divided into two sections which cover the most significant: The separation of the lateral displacement (divided into subsections Pure lateral displacement and Displacement in X and Y simultaneously) and the separation of the rotational displacement (divided into subsections Pure rotation and Cornering).

3.3.1 Separation of the lateral displacement

Due to technical problems, the data recorded from a test was deleted. This event was found too late to find a new participant, so the sample for the Separation of the lateral displacement got reduced from 8 to 7 participants. That is the reason why in the results showed below, in the case of the Separation of the lateral displacement the degrees of freedom are 6 (number of participants-1), whereas for the Separation of the rotational displacement the degrees of freedom are 7.
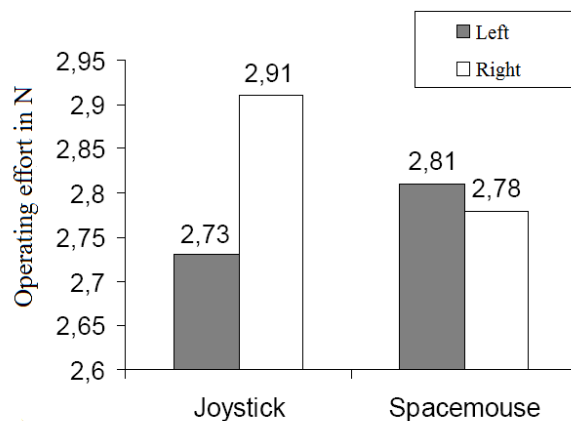
Pure lateral displacement

Figure 3.17: Pure lateral displacement. Operating effort. $F(1,6)=11.3$; $p<0.05$

When analysing the data referred to the operating effort for the pure lateral displacement, it must be pointed out that differences between steering effort with the Joystick and the Spacemouse were not significant. However, in the case of the Joystick control it was found that it required a significant higher effort to steer to the right than steering to the left. There was some previous evidence of this effect due to results of classical ergonomic studies. The reason of this not-symmetric behaviour is that the joints of the human arm work in such a way, that it is easier to turn in direction to the inner part of the arm. When steering with the right hand this results in a easier steering to the left, whereas if the steering is performed with the left hand, it comes easier to steer to the right. That could be the reason why in the case of the Spacemouse this effect was inverse, although the difference is not so high as in the case of the Joystick: the way the wrist has to rotate to steer the Spacemouse is more symmetric.
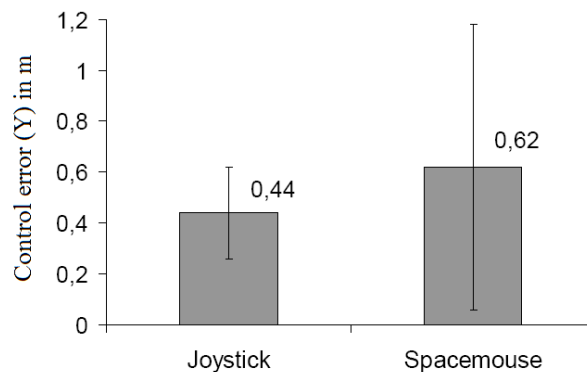
Figure 3.18: Pure lateral displacement. Control error

ANOVA indicated that the higher control of the error observed with the Spacemouse steering was not significant compared to the Joystick's. The high variance of the data obtained for the Spacemouse steering could appear because most of participants were using the Spacemouse for the first time, they were not used to it, and the learning period could had been not long enough. It was also observed that there was a big heterogeneity when it came to hold this device: some participants steered it just with their fingers, whereas others steered it with open hand. The high variance means a high dependency of the user skills, so when the user has low skills, the control error is higher. This does not seem to happen so often with the Joystick, meaning that the steer with the Joystick is more intuitive.

Displacement in X and Y simultaneously

The results for the Control of errors in the lateral direction for the case of the steering in the longitudinal and lateral direction simultaneously were not significant, but tendencial: the advantage was higher when using the Spacemouse. That is regarding the objective data, but regarding the subjective data, which was given by the users in the questionaries, the overall feeling was that the
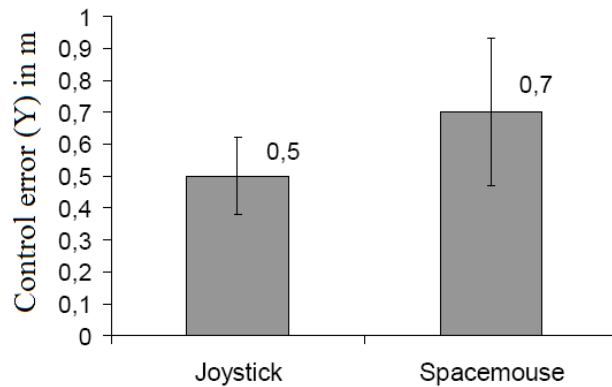
Figure 3.19: Displacement in X and Y simultaneously. Control error. $F_{(1,6)}$=5.7; p=0.05

complexity and consistence of the driving concept was worse with the Spacemouse. Thoughts were that driving in the X and Y directions simultaneously was more natural/intuitive and easier with both degrees of freedom integrated in the Joystick.

3.3.2 Separation of the rotational displacement

Pure rotation
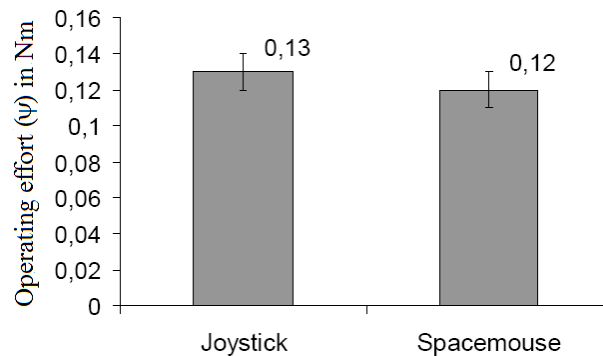
Figure 3.20: Pure rotation. Operating effort. $F_{(1,7)}$=4.8; p=0.07

For the pure rotation, a slightly (not significantly, since p=0.07) higher effort was observed when the steering device was the Joystick.

Focusing on the rotation direction, it must be pointed out that there is a significantly higher effort in the rotation to the right with the Joystick, because of the hand/arms biomechanical asymmetry mentioned before. In the case of the Spacemouse, this difference was not significant, but the effort was also a bit higher in the rotation to the right, because of the hands ergonomics when

33
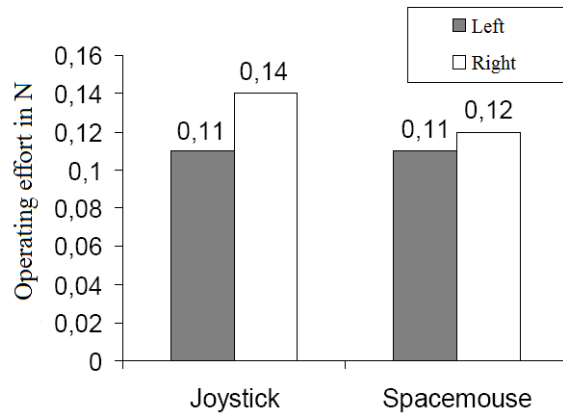
Figure 3.21: Pure rotation. Operating effort right/left. $F(1,7)=9.1$; $p<0.05$

holding the Spacemouse.
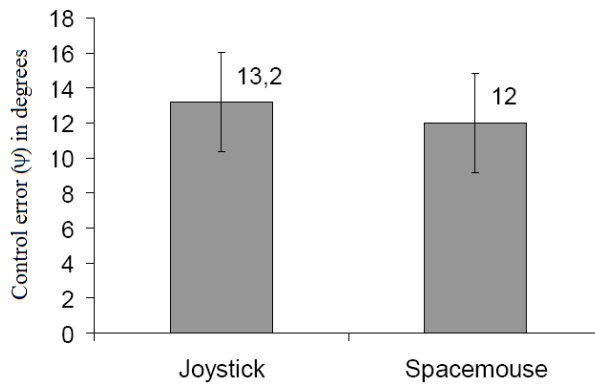
Figure 3.22: Pure rotation. Control error

The differece between the Correction of errors when steering the Spacemouse or the Joystick was not significant.

Cornering

The slightly lower operating effort in the longitudinal direction when driving a curve with the Spacemouse was not significant, according to ANOVA.

When the focus is upon the Operating effort in the lateral direction when driving a curve, it was found that the Operating effort was tendentially higher with the Joystick. ($F(1,7=3.7$; $p<0.10$))

It was found that there was a slightly higher Correction effort with the Joystick for the rotational degree of freedom, but according to the ANOVA, it was not significant.
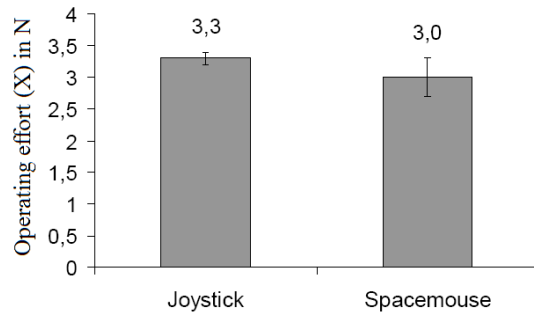
Figure 3.23: Cornering. Operating effort, longitudinal direction. F(1,7)=2.9; p=0.14
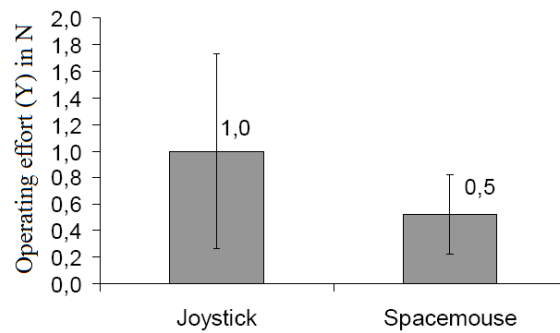
Figure 3.24: Cornering. Operating effort, lateral direction
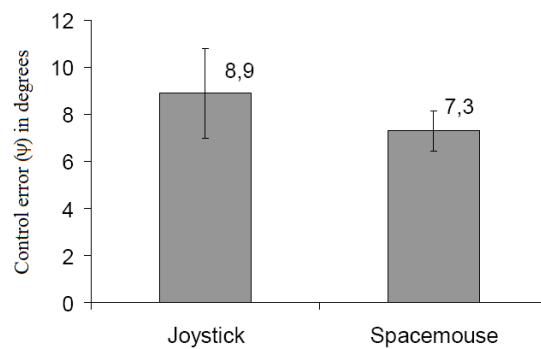
Figure 3.25: Cornering. Control error

Concerning the subjective opinions of participants, it required a higher effort to perform the tasks with the Joystick.

3.4   Conclusions

The following conclusions in relation to the separation of the degrees of freedom were drawn in view of the obtained results:

The joystick steering, that is, the integration of the degrees of freedom, turned out to be advantageous for the users in the case of the lateral translation: the control of the errors as well as the operating effort was low. Furthermore, participants found it really intuitive and less effort demanding.

Focusing on the rotation tasks, it must be pointed out that performances and sequential control were worse when steering the Joystick, in general it did not represent an advantage for the drivers' performances.

However, according to participants in the group of the Lateral separation, when answering about general steering feeling, the driving experience was significantly better when the degrees of freedom were integrated and not separated.

To sum up, both objective and subjective data supported the idea of integrating longitudinal and lateral steering. This may happen due to the fact that all of the participants had previously used Joysticks, which usually have those degrees of freedom integrated. A explanation for the not so positive objective results in the case of the rotational integrated steering, may be the human anatomical influence, the asymetry in the human arm joints. However, being this third degree of freedom a totally new concept for the regular driver, training and experience could get to better results.

Interesting points came out of this study which will be dicused on the next section. It also helped getting technical information for the starting point of the 'prototype design' phase: The steering torque applied by the users was obtained, as well as the range of angular movement.

3.5   Discussion

Given the results of the study, and supported by previous ones, the following are a series of points that should be taken into account for the design of a new steering device for the ROMO.

The human biomechanical asymmetry, which was reafirmed by this study and tends to have an impact in the right and left steering (both in the lateral and rotational steering), needed to be somehow compensated, by control technology or by the disposition of the stick inside the car. This way, the driver would have a much lower effort demanding driving experience.

A 2 DoF Sidestick should be considered. From an ergonomical point of view seems that it is not advisable to have 3 degrees of freedom activated at the same time, but not from a mechanical point of view either: there could be couplings between the degrees of freedom, i.e., they could interfere with each other and not be completely independent, which could lead to a not safe steering. Because of that a sensible solution would be to have the three degrees of freedom integrated in the same Joystick, but not active at the same time. They could be activated depending on the driving mode, because for a satisfactory and effective driving

experience they are not needed at the same time: the longitudinal and rotational degrees of freedom could be activated while in the driveway, and the longitudinal and lateral steering while parking, or viceversa.

Although it is a more expensive solution, and it requires more space inside the car, having 2 driving sticks would be a suitable option too. The reasons for this could be for example, on the one hand that the task of driving just with one hand could be very tiring, and on the other hand that simultaneous tasks appart from driving are very limited. There are also studies which suggest that two sticks instead of one give more redundancy to the movements, the ergonomics of the system is more intuitive, and that way the steering task becomes easier and requires lower effort from the driver [17]. From the point of view of security and human reactions, it is important to think on the reflex reaction of holding the stick and bringing it closer to the body in case of sudden and unexpected events. This would be understood as a brake in a one stick system, but if it was a two-stick system, it could be somehow compensated by control technology, so that when both sticks are brought towards the driver, the system understands it is a reflex human reaction and not necessarily a brake.

3.6   Further study

This is the first study held up at DLR regarding the steering of the ROMO, but as the 3 DoF Joystick prototype becomes a reality, new studies will be held up. The outlook will be:

- A full evaluation of this pilot study, with a deep knowledge of the training effect and the symmetry of the yaw axis will be held up.

- Regarding the sensitivity of the devices, since a lot of participants commented on this issue, it would be interesting to have a non-linear relationship between the input and the manipulated variable. The threshold (the minimum applied force value which has an effect on the steering device) should be variated too.

- Acceleration will be considered to be an input variable, which, as mentioned before is a reasonable input variable for the longitudinal movement acording to [17]. Once the arm kinematics are not to be evaluated, an interesting option would be to have the possibility to steer the car providing a desired acceleration. Effects on having this option active in all cases, or having the option to decide between which input variable we want to use, the desired velocity or the desired acceleration, could be investigated. As a matter of fact, in the current control implementation of the ROMO, for longitudinal dynamics, pushing the stick forward is interpreted as speed command at low speeds but as acceleration command otherwise.

- Simulation controls with active feedback should be implemented, since force feedback which reflect true system behaviour makes the control performance and learning easier. It would be interesting to study which effect has the feedback in the ergonomics (meaning fatigue to the user), and in the coupling with the other degrees of freedom (get the answer to the question 'If I get feedback in the rotational DoF, do I move by mistake any of the other DoFs?')

- The more realistic a study is, the more significant the results are, therefore, the realism of the simulation could be improved, perhaps with a moving driving simulator, sidewind effects, and so on.

- An adaptation evaluation adressing preventive safety should investigate if the adaptation allows the driver to drive with sufficient safety margins.

Chapter 4

Mechanical design

After the user study, before all the data was computed and conclusions could be reached, the theoretical mechanical design phase started. In this phase important concepts about properties and design of haptic devices were studied and different options for the implementation of the third degree of freedom were evaluated.

However, it was not until the results from the study were obtained and evaluated, when the prototype phase started and three final different options were studied in detail. The user study not only gave information about the convenience of integrating the rotational degree of freedom (see conclusions on section 3.4 in page 36), but it also gave objective performance data which would be used as design starting point.

4.1 Generic specifications

A conceptual and generic design study was carried out in the first phase of the mechanical design. It was always kept in mind that the process of designing a haptic device involves mechanical, electrical and control design, and that there are some specifications and limitations that must be fulfilled during the whole process to achieve a high quality feedback, i.e. not reducing the transparency of the master-slace system.

The following points are the generic specifications a good haptic device has to fulfill according to [28]. They must be taken into account over all in the mechanical design phase, but it must be an objective for the other two fields (electric and control design) to maintain these standards or to cover and compensate the possible shortcomings the mechanical design has.

- reduced **friction** between its components. The user can notice this inner friction sometimes in form of vibrations.

- as limitated **mass** as possible, because all objects have inertia, i.e. resistance to acceleration or deceleration, which is proportional to their mass, as it is explained in [29]. This is an undesirable property, because it implies that the user should apply an additional torque to the torque necessary to move the mechanical system. Moreover, the lower the inertia of the system is, the higher bandwidth it has. A high bandwidth means a high

frequency, which is one of the main objectives of haptics: accuracy of the feedback is high as long as the achieved frequency is high also.

- high **stiffness**. Since the weight and the stiffness of a system are related, and as we mentioned above mass must be as low as possible, this should be managed with a material which has a high stiffness to weight ratio.

- **compactness**. The more compact (smaller distance d from the center of gravity of the system to the rotational center), the less inertia the system has, but also the generated torques in the system are lower, given the simple formula that relates the applied forces (F) in the system (in this case the force generated by the system mass) and the torques (T):

$$T = Fd \tag{4.1}$$

As it will be mentioned in a later section, this is more deeply studied for the 3 last options and can be found in the Appendix C of the Annex.

- reduced **backlash**. This undesired effect is usually given in the transmission systems, and it is described as the amount of lost motion due to clearance or slackness when movement is reversed and contact is re-established, which results in a small force.

- **backdrivability**. Backdrivability is an important property which is determined by two independent sources of resistive forces: an acceleration dependent component due to inertial effects and a velocity dependent component due to frictional causes. The selected components must guarantee the backdrivability of the system.

All these properties are important and must be covered on the final design, although the more elements the system has, the more difficult it is to fulfill the requirements. That is the reason why, in the case of the indirect drive, the design of transmissions is critical. A direct drive would avoid lot of these undesired effects: there is no lost energy and the steering is softer. All of this will be discussed in following subsections.

The design phase consisted on making several specific choices that influenced each of these attributes, such as the location and type of speed reduction, choice of materials, and type of motor.

4.2   DLR's 2 DoF Force Feedback Joystick

It was already mentioned the fact that the aim of the present thesis was to integrate a third rotational degree of freedom on an existing Joystick: DLR's 2 DoF Force-Feedback Joystick (See figure 4.1). This Joystick was designed in 2003, and since 2004 it is the haptic device used to command the Rockviss, a robot in the International Space Station (ISS) to evaluate mechatronic lightweight robot joint units for use in an On Orbit Servicing scenario (see [30]). The Force feedback in this case is crucial: the experiment consists on commanding desired robot positions while the contact forces are measured by the on orbit robot during the experiment and they are transferred to the Joystick. This way the operator feels the interaction similar to being remotely present.

Figure 4.1: DLR's 2 DoF Force-Feedback Joystick

The joystick was adapted, necessary cuts or holes were done on any of its parts (providing it was not the cut of a critic point in a part) but also to re-design any of the parts. The drawings of the new parts as well as the old modified parts were taken to DLR's Workshop once the design phase ended and after the end of the present thesis, to evaluate the feasibility of the manufacturing, and make the necessary changes (See Appendix D in the Annex for the final Drawings).

The joint mechanism in the 2 DoF Force Feedback Joystick is a cardan joint, actually one of the most used systems for joystick construction. The main innovation of this 2 DoF Joystick compared to the first vesion from 1999 is the transmission system, a capstan drive mechanism. It provides the Joystick of several improvements due to the low friction with which it contributes to the system. Owing to the fact that the capstan drive mechanism is one of the options for the transmission of the third degree of freedom, the low friction and other issues will be in following sections discussed and compared to other transmission systems.

As it can be seen in the Figure 4.2, the 2 motors of the system are grounded to the floor, which means that their weight is supported by it, not by the handle or any other part to which the user could be connected, so this weight and therefore the inertia are negligible for the user. As it was stated before, this fact also provides the system with a high bandwidth, which currently makes the communication between ground and the Rockviss have a small delay, so a high accuracy is achieved. A range of movement of ±20 was designed for the x and y axis.

Regarding the capstan drive mechanism transmission system, the ratio of the diameter pulley to the diameter of the capstan drum dictates the mechanical ratio, similar to a gear system, which is in this case 14.1:1.

Both motors are the same Faulhaber model, with a continuous torque of 40mNm (enough to realize the needed output torque of 1 Nm at the cardan joint), and they have a graphite commutation. This high quality motors have low ripple inside, the undesired effect which is the deviation of torque that can be generated due to misalignments of the rotors inside the motor, and low cogging torque, which is a torque due to the interaction between the permanent magnets of the rotor and the stator slots, thanks to the shape of the windings
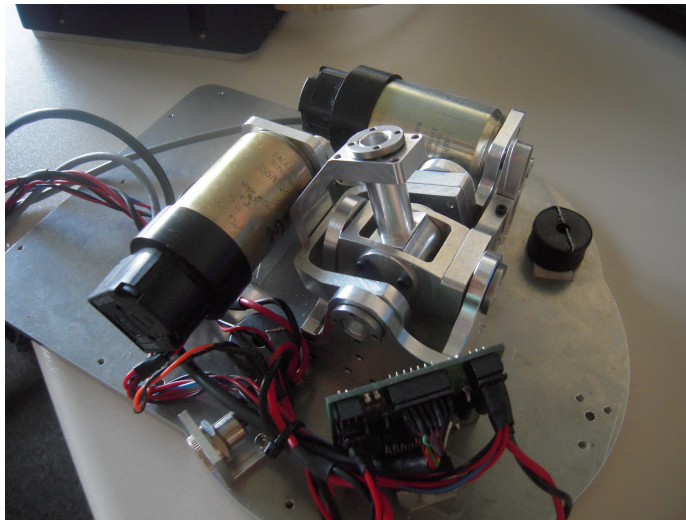
Figure 4.2: 'Skeleton' DLR's 2 DoF Joystick

inside the motor and the quality of the magnets, so a smooth torque is felt by the user. Furthermore, they have low cost and low power consuption. Therefore this high quality motors will be considered for the actuation of the third degree of freedom.

The motor torque is measured with incremental encoders placed in the back of the motors, with a resolution up to 1024 counts per revolution. Sensors are necessary in force feedback systems to measure the degrees the motor shaft has rotated due to the steering of the user. In the cardan joint they placed a potentiometer, to calibrate the joystick and get an absolute position reference.

4.3   Possible configurations for the third DoF

Many points must be taken into account during the mechanical design of a haptic device, and in the present case, since small forces or small deflections applied to the Joystick result in big movements in the slave system, it is crucial to select a good feedback system.

The question about the choice to make regarding the type of feedback arises: should it be active? Or is it enough if it is just passive? The degree of complexity varies from one option to another: for example, the passive sidestick's fixed force/deflection characteristics are just achieved with simple spring/damper systems.

As it was explained in 2.1 in page 7, the main difference between an active and a passive system is that in an active system information about the performance of the controlled element is felt in the device, whereas in a passive system this is not possible, although other information can be obtained, as it will be explained in following subsections.

Additional and desired features can be realized by active sidesticks but it is important to point out that active systems are more complicated and require
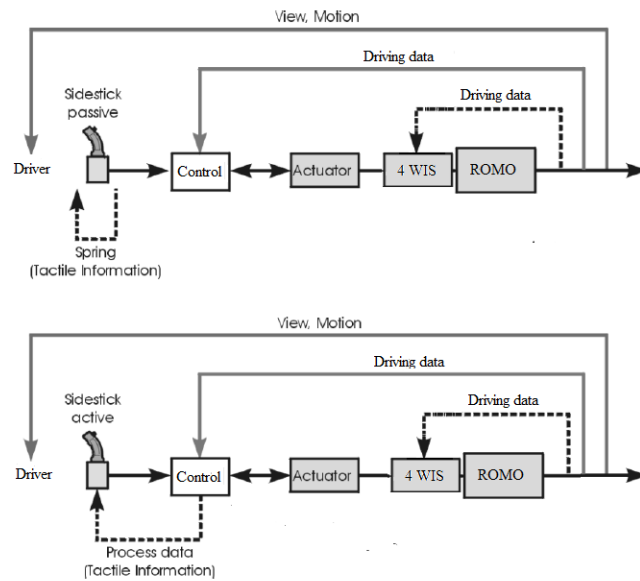
Figure 4.3: Tactile information situation for active and passive Joystick configuration

more technical effort to be as reliable as passive systems. Active systems are more complex and usually more expensive than passive systems, and a convincing technical solution which fits all the different requirements for control forces, volume, reliability and costs is the main objective, but sometimes the question whether active sidesticks are worth the additional effort is also not answered. The diagram in Figure 4.3 explains the differences between active and passive configurations.

Within an active configuration three different possibilities can be distinguished: the adaptive stiffness, direct drive (there are no intermediate elements between actuator and element steered by user) and indirect drive (the out force of the actuator needs to be increased by a transmission system).

Figure 4.4 summarizes schematically the different options regarding the different feedback design of a haptic device.

4.3.1 Passive configurations

As it was briefly explained in 2.1 in page 7 of the present memory, there are a number of possible passive configurations. Originally the elements used in passive configurations are springs, but as it will be explained in the corresponding section, also the degree of complexity can increase from a pure isometric behavior to a variable stiffness behavior changing the intrinsic lineal behavior of springs.

The following are the different types of passive configurations:

- Isometric

- Isotonic
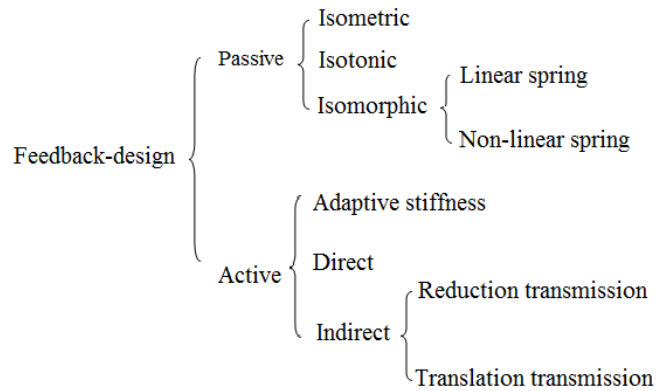
Figure 4.4: Possible feedback designs

- Isomorphic
    - linear spring
    - non-linear spring

Isometric

This configuration implies that an applied force on the device causes no deflection or movement on the stick. However, after brief consideration this option was dismissed, since it provides just visual feedback, which does not help to prevent actions (if the driver is just able to see what he/she just did, there is no chance to improve the performance), and no visual feedback concerning the joystick input.

Isotonic

This option is slightly better than the Isometric one, besides visual feedback, there is a deflection in the device, since this deflection is given provided a constant input force, so the user does not get the feeling of the magnitude of the applied force. It was also dismissed.

Isomorphic - Linear spring

The isomorphic configuration is the traditional solution implemented in most joysticks: it simply requires one torsion spring. Since all springs have a linear relationship between the applied torque (τ) and the spring elongation (θ) which is given by the spring's stiffness constant ($k(\theta)$)(see Equation 4.2), that is the feeling the user would get through the stick: a 'deflection' in the rotational third degree of freedom directly proportional to the applied force.

$$k(\theta) := \frac{\delta\tau(\theta)}{\delta\theta} \tag{4.2}$$

44

The spring could be placed inside the grip and above the cardan joint, or below it, both configurations would be feasible. These are the advantages concerning the assembly: after manufacturing a new shaft or rotating axis, it would be joined to a spring fixed on the cardan joint, allowing it to rotate. The mass added to the system by the spring would be almost negligible (the mass of the shaft would be added in the other systems too anyway), and since it is a centered system there would be no generated torques.

Isomorphic - Non-linear spring

The intrinsic nature of springs makes them all have a linear deformation, i.e. directly proportional to the force applied, as it was explained in the previous section. This deflection will be felt by the user, it is a improvement compared to the isotonic case, but it still gives not much information as desired about the magnitude of the applied force. That is the reason why it is interesting not to have this proportional behavior on the stick, but different depending on the applied force, provided by a non-linear behavior similar to the one showed in Figure 4.5.
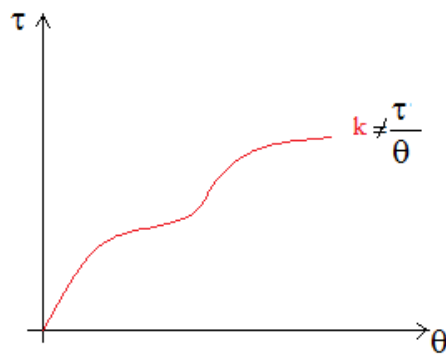
Figure 4.5: Non-linear spring behaviour

In Figure 4.6 the non-linear spring realization can be observed: a pulley deflects a linear spring relative to the string length given by the motor and link geometry. The relationship between string length and pulley deflection is non-linear, actually the height 'h' of the triangle relative to l/2 establishes the stiffness constant in each moment, different for every combination, but still fixed. It must be pointed out as an undesired side-effect the fact that the tendon going through the pulleys could suffer from friction, and therefore be translated to the user.

This configuration would require a slightly more complex system than the previous one: as it can be seen on Figure 4.6 it is needed a spring, a tendon, one moveable pulley and two fixed pulleys, but also a box, or a small platform to place these elements the way the mentioned figure shows. The positioning
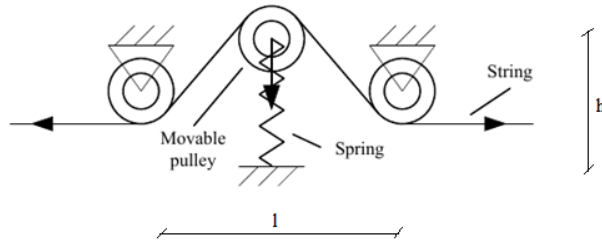
Figure 4.6: Non-linear spring behaviour realization

of this platform could be above or below the cardan joint. Above, due to space issues, it would be not centered, so a torque would be generated, whereas the positioning below could be done trying to make it as centered as possible.

As the complexity of the system grows and the effects get more positive for an effective steering, the mechanical undesired effects do so, as Table 4.1 shows.

| Type	Inertia	Friction	Compactness
Isometric	↓↓↓	↓↓	↑↑
Isomorphic	↓↓	↓↓	↑↑
Non-linear stiffness	↑	↓	↓

Table 4.1: Passive configurations

4.3.2   Active configurations

In an active configuration, as it has been mentioned before, the user is able to receive information through the steering device of the actual behavior of the slave system. In our case an active third degree of freedom would imply getting information about the yaw the car is performing in each case in form of an output torque in the joystick grip.

In all active systems the main element is the actuator (which could be an hydraulic actuator, an electromechanical system with servo-motors, electric torques or other means), which will produce the output torque. The generic diagram in Figure 4.7 [31] shows the elements present in an active configuration, not just the mechanical part, but also the electrical and control, since they all are connected and have to be in good harmony to provide a good feedback feeling. A force-reflection joystick consists of three major components: transmission mechanism, actuator, and sensor. The structure of the transmission mechanism determines its workspace, the actuator supplies the power, and the sensor detects system states and interactions with environments. The transmission mechanism and actuator together determine the manipulability, while the resolutions of the actuator and sensor specify that of the joystick. During the design process, we first evaluate current developments of these three components and then proceed with our design, respectively.

In haptics, due to the sometimes high maximum torques necessary but the small space for powerful actuators available, transmission systems are needed so that the motor output torques are amplified. When a transmission is necessary,
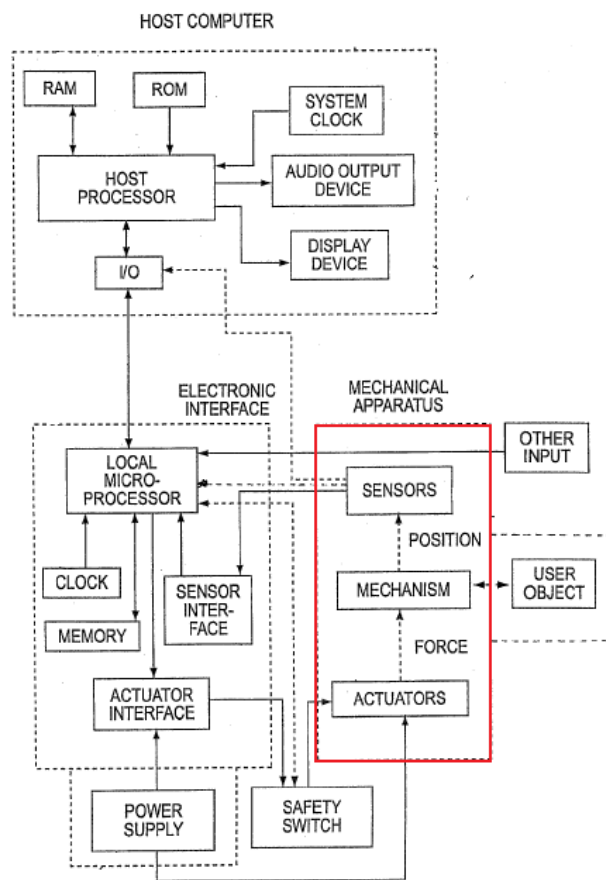
46

Figure 4.7: Active configuration. Relationship between electrical, mechanical and computer ([31])

the configuration is called indirect; when there is no need of a transmission, it is a direct configuration.

Adaptive stiffness

The non-linear spring approach is a good option. However, the advantage of adaptive stiffness is that it achieves to have a stiffness which can be modulated. For different force control tasks, different joint stiffness may be desirable, and this is what would be studied on the lines below.

The adaptive stiffness, which is sometimes also called adaptable compliance (compliance, $C = \frac{1}{k}$) is a topic of ongoing research that is being developed in the last few years in robotic applications, in particular in the human like robots joint design. Its aim is to achieve limb actuation similar to that of human muscles (which are able to show/develop a variable compliance depending on the situation), so that interactions between humans and robots are safer (see [34]).

Usually the software compliance is limited by sensor bandwidth and precision, model inaccuracy and motor dynamics. Technology which incorporates compliant behavior, mainly in hardware, may be used to overcome the drawback of the high joint stiffness. A possible solution to the problem is the variable stiffness actuation concept, which could also be used for the rotational degree of freedom of the joystick in the present Thesis. The joystick could be treated as a joint, and this concept could be implemented in the design, to get different feelings in the Joystick depending on the force applied, the steering case, and so on. Once the mechanical set-up is built, the control software would be implemented for each case.

It is important to point out that Joysticks with variable compliance have been designed in the past, like [35], but in that case the modifications of stiffness and damping came just from modifying the software algorithms, i.e. through control.

According to [36], three principal design paradigms currently exist in the development of variable stiffness for artificial muscles that have been adopted:

- The first approach consists of using compliant actuator systems such as pneumatic actuators.

- The second approach undertakes the development of electroactive polymers that deform when a voltage is applied.

- The third approach involves electromechanical devices typically comprising an electrical actuator and an elastic element in combination.

In the present Thesis just the last approach was brought to focus, the electromechanical one, and therefore research done at DLR regarding this concept in [37] was studied, where the so called antagonistic setup was developed.

In the antagonistic setup a non-linear torque-displacement characteristic of the elastic elements is essential for stiffness variation, due to the dependency of a mechanism's stiffness on the torque curve and the applied torque (see Equation 4.2 and Figure 4.9). As it was mentioned before, increasing the force of a linear spring does not increase its stiffness, therefore, flexibility at the joint level requires the inclusion of a nonlinear spring between the actuator and the joint.
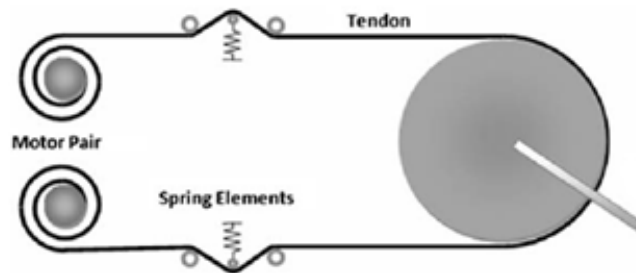
Figure 4.8: Adaptive stiffness behaviour realization through antagonistic setup (from [37])

Thus, these solutions must include a mechanism changing the linear properties of the spring, turning its behavior to nonlinear. As it was explained in the previous section, this can be achieved by a setup like the one Figure 4.6, where the height of the spring in each moment determines the stiffness constant. From now on this will be referred to as 'nonlinear spring element'.

To change the joint stiffness in the desired way, the elastic elements are elongated by driving the motors in opposite directions in the antagonistic setup. This increases the applied force to the elastic member, and as a result the stiffness of the link is increased too. Two motors, each of which is equipped with a nonlinear spring element, then can be used to increase the total stiffness (up to infinite stiffness) by pulling in counter directions, since their tendons are stiffly connected to each other via the joint that they are controlling (See Figure 4.8). This system requires a complete system design, including control strategies.

It is important to point out that due to the elastic elements, an undesired effect shows up: every motor action in an antagonistic system will induce vibration (as well as the friction mentioned before due to the tendon going through the pulleys).

The negative points of this configuration are on one hand, the need of two motors and the weight introduced by them in the system, and on the other, the quite large configuration with the springs (2 platforms) that it requires. This makes the specification of compactness not easy to fulfill. The need of two platforms each with its motor, would make this configuration symmetric, so that is a positive point, but still the configuration is not optimal enough, and the fact that it is a quite new concept makes it an interesting, but not very feasible option for the prototype.

Direct drive

As one can imagine, advantages of a direct system are many, such as:

- higher efficiency
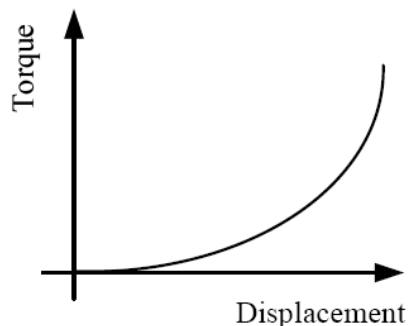- reduced noise
- longer lifetime

Figure 4.9: Adaptive stiffness: Increasing and convex torque-displacement profile

- faster and precise position
- no drive stiffness,
- no mechanical backlash
- no hysteresis
- no elasticity

According to [10], a direct drive also implies viscous friction and effective actuator inertia, since in the case of a indirect drive, viscous friction is amplified as much as the transmission-ratio, and inertia as much as the transmission-ratio squared.

The disadvantage for this type of configurations, is, anyway, that a large motor is necessary (which implies large weight added to the system) for a significant torque.

The configuration is this case would be accomplished by simply placing a powerful enough motor below the cardan joint and join its rotor to the shaft. Asymmetries would not be introduced and the system would be quite compact.

Indirect drive

When a direct drive is not a feasible option, or if different alternatives should be weighed up before making any decision, as in the present case, the indirect drive option must be also considered. As it was mentioned before, the transmission system is in these cases necessary because the output forces of the actuator demand a mechanical advantage. The disadvantages come out due to the different elements introduced, and all the advantages of the indirect drive turn out into the disadvantages of the direct drive system: less efficiency, noise, possible misalignments, and so on. However, once these undesired effects are accepted, the steps to follow are to look into all the options and see which present the best balance, as it will be later on discussed. The following transmission systems had been previously used in different Joystick designs ([31],[32] and [33] for example), so their use is extended and they have been proved to work.

- Planetary gear

- Toothed wheel/worm wheel

- Timing belt

- Cardan joint

- Capstan drive

Planetary gears

Planetary gears are devices which have a rotating velocity as an input, and give as an output this reduced velocity, thus, amplify the torque. They have three elements which make this possible: the sun gear, the planet carrier, and the internal gear, as seen in Figure 4.10. The use of planetary gears is a easy and simple solution from the point of view of assembling, since planetary gears are devices directly assembled to the motor shaft, and whose shaft is coaxial with it. The advantages of this transmission system are:

- high power density

- large reduction in small volume

- coaxial shafting

- compactness and outstanding power transmission efficiency

- a efficiency loss of 3% per stage
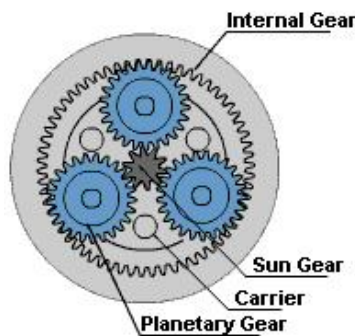
- high stability

- stiffness

Figure 4.10: Planetary gear

However, the main disadvantage they have is a crucial undesired effect for haptic devices: due to the fact that the minimum reduction is very large (1:30) backlash appears, a loss of motion. This problem should be minimized as much

as possible, because when the turning movements have to be precise both forwards and backwards, backlash makes the user feel undesired movements. Other disadvantages to take into account are:

- high bearing loads

- inaccessibility

- design complexity

- feeling of the harmonic revolutions by the user

An important element is the diameter of the shaft, because the smaller the diameter, the smaller the reduction ratio, and the bigger the backlash. And the inherent backlash that the planetary gear has is unluckily felt by the user amplified by the transmission ratio.

Toothed wheel and worm wheel

Toothed wheels are typical transmission systems, used in many mechanical configurations, whose working principle is the meshing of two toothed gears in order to transmit a torque (see Figure 4.11). The gears introduce some backlash in the system, and users might be able to feel the interlocking and grinding of gear teeth during their rotation when manipulating the handle.

Worm wheels (see Figure 4.12) are not always passively backdrivable, they are not backdrivable if the worm pitch angle is less than the friction cone angle, so the transmission ratio is limited by the backdriveability requirement.

Due to these facts, they both were not a good option to consider and they were dismissed.

Figure 4.11: Toothed wheel

Figure 4.12: Worm gear

Timming-belt

The timing belt is another type of transmission, in which alike the toothed wheels, where the teeth of the two shafts are in contact, in this case the toothed shafts are in contact through a belt (see Figure 4.13).

For the basis of calculation (an analysis was carried out to study the feasibility of the system, see Appendix A in the Annex) and keep a working order, it is assumed the following good conditions, which will make it to be a maintenance free operation:

Figure 4.13: Timing belt

- Tooth strength: The specific tooth shear strength depends on the rotational speed. Time belt drive is correctly designed when not exceeding tooth shear stress. In this case it is not necessary to apply a safety factor.

- Tension cord strength: It is the permitted tensile load of the belt cross section. The belt drive is correctly designed when the maximum permitted tensile load on the steel cord is not exceeded under operation conditions.

- Flexibility: Minimum number of teeth, minimum diameter.

A very important point in this systems is the pre-tension, which is intended to guarantee a minimum tensioning force at the slack span side to ensure smooth tooth meshing into the driven pulley. It is influenced by the stiffness of the belt, the belt length and the circumferential force, among others, and consequences of a faulty pre-tensioning setting can be that the tooth , the belt brakes, or reduction of the transmitted power.

The quite high demanding conditions were not worth the performance of the system, so it was also dismissed.

4.4 Cable drive

This option was considered due to the good performance of this transmission system in the DLR 2 DoF Joystick and properties such as high efficiency and very low friction mentioned in [31]. There is no need of electrically controlling it, and it is assumed that there is a linear relationship between the force applied by the user and the current going through the motors, which is easy to measure. A closer look can be taken in the generic example showed in Figure 4.14, taken from [31]. This is the only transmission system which is not on sale by any provider, so the mechanical properties depend mainly on the mechanical design and the manufacturing process.

The Table 4.2 summarizes properties of the reviewed transmission systems.

Cardan joint

The last option studied was the assembly of a cardan joint inside the existing cardan joint. The great advantage of this system is that the third actuator can
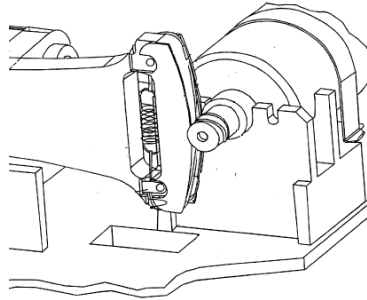
Figure 4.14: Detail of a capstan drive mechanism transmission system (from [31])

	Tooth gear	Timing belt	Cable & Pulley	
Slipping	No	No	If stressed, no	
Ratio	Constant	Constant	Constant	
Friction	High	-	Low	
Prize	Expens. manufacture	Cheap	cheap	
Lubrication	Yes	No	No	
Vibrations	-	Cheap	No	
Backlash	Yes	No	No	
Assembly	Easy	Not fixed	Medium	
Others		Long life	Thread in pulley	
		Not stiff		
Efficiency	60-70%	90%	98%	

Table 4.2: Transmission systems: Decision matrix

be grounded close to the cardan joint, and this way the motor would not add any inertia to the system. The transmission system, is not a reduction transmission (there is no need of reduction since the motor is grounded and its size is not a problem) but a direction transduction. The axis of the motor can be horizontal, and the transduction translates the rotation motion to the position the saft has each moment. The disadvantages of the system are, however, the possible couplings of the degrees of freedom, and the difficulty in the assembly: it must be very accurate so that there are not misalignments and the rotation is well translated. The degree of difficulty, as well as the fact that the existing cardan joint needed to be redesigned, made us reject it for the present prototype.

4.5   Prototype phase

Once all the options and their advantages and disadvantages were studied, and combining them with results from the user study, it was decided that the third degree of freedom of the joystick would be active (as it was mentioned in Chapter 2, according to previous User studies concerning the feedback in the steering, the performances were better when active feedback was provided). Decoupling the tactile information from the driver could lead to problems of awareness

about the situation of the ROMO. Specifically in a critical situation, with high workload, this additional force feedback information can contribute to enhance both situational awareness and driver's acceptability because force sensation is natural, very fast and does not influence mental workload. Therefore in combination with other indications (visual, motional) additional tactile information gives a more complete information about the situation for the driver.

After studying all the different active options presented in the previous pages of the present memory, it was decided that just three configurations offered the possibility to fulfill better the characteristics we were looking for in our haptic device (specified in 4.1) and which were more feasible to be constructed as a prototype:

1. A direct configuration

2. A indirect configuration

   (a) provided of a planetary gear
   (b) provided of a cable transmission system

The mechanical specifications were the starting point in this phase, obtained from the user study:

- Torque:

  - Maximum torque: 3Nm
  - Rated torque: 1Nm

- Range of rotation: $\pm 8^{\mathrm{o}}$

In order to fulfill the specifications and reach a optimal performance of the third degree of freedom, actual external providers were consulted for the necessary elements: actuators, encoders and bearings (to avoid friction between rotating shaft and fixed elements). The next sections describe the different options found.

4.5.1 Actuators

As it was explained in 4.3.2, the active system are provided with an actuator to transfer the desired force to the user. Usually in haptic solutions brushless DC motors are considered, mainly due to their high reliability and simple control of motor speed.

The studied brushless motors were featured in the catalogues of Sensodrive, Maxonmotor and Faulhaber (this last was consulted due to the good performance on the 2 DoF Joystick). Main aspects to look at were the peak and the rated torque, but special attention was paid to other aspects, such as the stall torque, to whether they included a encoder or not, and to their weight, as Table 4.3 shows.

After studying the table and all the variables, it was decided that the best choice was to use a Robodrive motor, since they were lighter and they were more reachable because Robodrive is a Spinoff from DLR, and the Institute already had some motors. A disadvantage may be their low compactness and

	Robodrive		Maxonmotor		Faulhaber
	ILM 70x18	ILM 50x8	EC 60	EC 45	4490B
Stall torque	-	-	6820mNm	3160mNm	2750 mNm
Peak torque	4Nm	0,9Nm	840mNm	318mNm	-
Rated torque	1,25Nm	0,28Nm	-	-	202mNm
Friction torque	-	-	-	-	202mNm
Encoder	No	No	No		
Weight	340g	86g (360g)	2450g	1150	750g
Shaft diameter	42mm	30mm	60/12mm	45/10mm	44/6mm

Table 4.3: Actuators: Decision matrix

big diameter. However, the diameter would be reduced by introducing in the motor's hollow shaft a manufactured shaft with different diameters along its length.

For the direct drive system the chosen motor was the ILM70x18, and for the indirect drive systems, the ILM50x8 (which required a reduction ratio of at least 3.6:1 to obtain the 3Nm maximum torque).

4.5.2 Encoders

Since the range of movement was very small ($\pm 8^{\circ}$), high resolution of the encoders was needed. Encoders make it easy to control the real rotation speed of the motor, because they convert angular position to digital code (digital pulse) or to analog, by current or voltage signals. When not very big transmission ratios are used, sometimes it is just necessary to measure the current going through the actuator, because it is proportional to the applied torque. However, in cases as the present, where the accuracy must be high, the use of a high resolution encoder is recommended. Resolution in encoders is represented by bits, but the parameter which helps get a better feeling of the actual resolution is the minimum angle step.

A X bit resolution means 2^X steps, so the angle step ($\Delta\theta$)is:

$$\Delta\theta = \frac{360}{2^X \text{steps}}$$

It is important to point out that if the system has a transmission, this step is reduced as much as the transmission ratio.

In spite of the existence of different technologies to measure torques (SAW sensors, strain gauges), the most commercially extended type of rotational encoders are the optical encoders and the magnetic encoders, which differ on their characteristics and the working principles, although the idea behind the working principle is esentially the same: rotating disks create lines of code depending on the rotation angle, which have to be interpreted. The number of rings in the disk is related to the resolution of the encoder: the number of rings is equal to the number of lines received by the receiver, meaning a resolution in bits equalt to that number. A brief review of these two types of encoders is given in the next subsections.
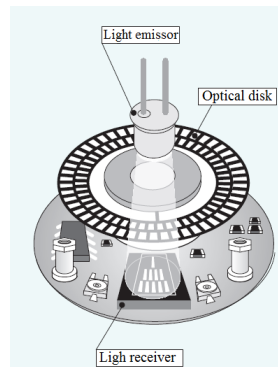
Figure 4.15: Working principle of an optical encoder

Optical encoders

Properties:

- They are delicate: their parts can be put out of action by oil, dirt or dust.
- They are bad with misalingments.
- They need low temperatures.
- They are usually used for slow and not very frequent rotations.
- Low cost

Figure 4.15 shows the actual configuration of a optical encoder, and its working principle can be easily understood: light emitted by the light emissor passes througth the codified disk (codified with the binary Gray code), and the light receivers get the information. This information gets into an electronic circuit, which will interpret it.

Magnetic encoders

Properties:

- Work at very high velocities
- They bare harsh environments
- Usually are very precise
- They are very robust
- Medium cost

Their working principle: Ferromagnetic disks with a pattern of magnetized and not-magnetized areas produce 0-1 pulses when magnetized or not magnetized areas pass next to magnetic head.

Another point to take into account is that encoders can be absolute or incremental. Incremental encoders need calibration before starting the use, because

they give the angle with reference to a known point, not the absolute angle like absolut encoders do. Generally incremental encoders provide a better resolution at a lower cost than the absolute, and their electronics are more simple because they have less output lines.

The choice was to use a magnetic encoder, although their price was a bit higher, its characteristics would assure the accuracy needed. The chosen one was a magnetic resistive encoder of 85 bit resolution, provided by Robodrive.

Bearings

The mechanism would be a rotating shaft going through a modified cardan joint. To assure the relative radial movement between both elements, but the lack of movement in the axial direction, as well as providing the parts of low friction, bearings were used. In fact, in the configuration of the 2 DoF two small bearings were used to maintain the axial position. These bearings stayed in the same place, but since they were not enough to assure the correct fixation of the now larger axis, two more bearings would be added. Regarding their disposition, one would be placed in the modified cardan joint, and the other one in the part which would be connecting the shaft to the motor board. Following the providers instructions, one of the bearings would be placed with a free fitting, whereas the other would be completely fixed.

The type and size of the bearings, the form and design of the assembly and the fixing mechanisms affect to the efficiency and reliability of the mechanism, so they must be chosen very carefully. To select the more suitable bearing type the following must be taken into account:

- Available space

- Loads

- Misalignments

- Precision

- Velocity

- Stiffness

- Life

- Friction

In the present case the most important factors are the limited space and the low friction, and since the supported loads will not be in any case very high, and they will be mainly radial, the selected type of bearings was ball bearings. The selected bearings were sealed, to avoid the introduction of dirt, and avoid the introduction of another element to prevent this.

4.5.3 Final overview

Once the common external elements were studied and selected, the following three options were considered in more detail:

Direct drive

This configuration is the most simple and its elements are:

- the ILM70x18 motor and a manufactured base for it

- the rotating axis

- the modified cardan joint where the axis would be introduced

- a way to join the motor with its base to the cardan joint (the joint would support all the weight in all the cases)

Indirect drive - System with a planetary gear

In the present case, the elements are:

- the ILM50x8 motor and a manufactured base for it

- a planetary gear and a fixing to the cardan joint

- the rotating axis

- the modified cardan joint where the axis would be introduced

- a way to join the motor with its base to the cardan joint

To select the optimal planetary gear, our specifications should be the necessary maximum continuous torque, the maximum peak torque and a diameter smaller than 32mm (the diameter of the rotor of the Robodrive motor is 32 mm). An extra specification was the reduction ratio: it should not be less than 3.5, but it should be as low as possible to avoid high backlash. This conditions made the search for a suitable planetary gear difficult, the best options are summarized in Table 4.4.

Label	Diameter	backlash	Ratio	Cont. T	Max. T	Weight	Efficiency
Maxonmotor	22 mm	1º	3,8:1	2Nm	2,5Nm	51g	84%
Maxonmotor	22 mm	1,2º	14:1	2,4Nm	3Nm	6Kg	70%
Faulhaber	22-26 mm	≤1º	9,7:1	3,5Nm	4,5Nm	116g	80%
Faulhaber	22-26 mm	≤1º	3,71:1	1,5Nm	3Nm	107g	88%

Table 4.4: Planetary gears: Decision matrix

Assuming that the most important points were the efficiency and the backlash, the most suitable options seemed Faulhaber's planetary gear, the one with a 88% efficiency, which also had a low weight, as well as suitable torque ranges.

Indirect drive - System with cable transmission/ capstan

- the ILM50x8 motor and a manufactured base for it

- the cable transmission system with the tightening mechanism

- the rotating axis

- the modified cardan joint where the axis would be introduced

- a way to join the motor with its base to the cardan joint

The design of the transmission would be done following the design of the one of the 2-DoF Joystick, which already had an optimized design, although the size of the new part would be much smaller. Although other mechanisms exist to tighten the cable and prevent it from loosening (such as springs), it was also followed the idea of the previous Joystick to use a screw. It is important to point out that this transmission system has a high efficiency, and viscous and Coulomb friction effects are minimized, according to [10].

The transmission system was chosen to have a 5:1 reduction ratio. Since a 10 mm motor shaft diameter seemed reasonable (it would be later manufactured, the only condition was that it had to be smaller than 32mm), the radius of the transmission part in contact with the motor shaft would be 50mm. Distance between the motor's shaft center and the rotating axis center would be:

$$\frac{10}{2} + \frac{50}{2} = 30mm$$

The minimum diameter of the cable in order to avoid the flexion should be 12-20 times smaller than the motor shaft, it was chosen a diameter of 0.6mm.

Final decision

The final decission was taken considering the general assembly and the type and number of elements needed for each option.

The introduction of the motor and the other elements in all of the three cases changed the center of gravity of the original Joystick, and it also created torques and moments of inertia. These had to be taken into account and were calculated (see Appendix C in the Annex) for each case.

The matrix in Table 4.5 summarizes the most important points to take into account when making the definitive election of motor and type of transmission.

The option number 2a was quite fast dismissed, the fact that the planetary gear introduces backlash to the system was a clear and very important disadvantage. So the choice was either option number 1 or option number 2b, direct or indirect system. A lot of points had to be weighed up:

- option number 2b introduced more elements, and therefore more complexity to the system, but a clear advantage of this system was the high encoder resolution, as mentioned before increased as much as the transmission ratio. The generated torque was higher than that of the option number 1, but easy to compensate.

- option number 1 is a compact configuration, but the high weight of the motor introduces quite high inertia to the system.

Finally the option chosen was the number 2b: Robodrive's motor with the cable transmission system. The lack of backdriveability, and the good experience with this transmission system in the DLR 2 DoF Joystick were crucial to make this decision.

	Motor	Reduction Ratio	Torque (Nm)	Resolution (bit)	Total M (g)	M (Nm)	J $(\frac{g \cdot m}{s^2})$	Others
1	ILM 70x18 (800g)	No	Cont 1.25 Max 4	85	800 bearings motor base	0.109	1.151	+ no backlash +low friction -inertia
2.a	ILM 50x8 (360g)	1:3.8 or 1:3.71	Cont: 1.5 Max 3	310	360 270 bearings motor base	0.086	0.6358	-backlash
2.b	ILM 50x8 (360g)	1:5	Cont: 1.4 Max 4.5	425	360 bearings motor base	0.18	0.632	+no backlash +low friction +compact -off-center. mass

Table 4.5: Final overview: Decision matrix

4.6 Design with Pro-Engineering Wildfire

We were provided with the Pro-Engineering Wildfire model of the previous Joystick (see Figure 4.16), in which we would have to assembly the new parts. That was the starting point.
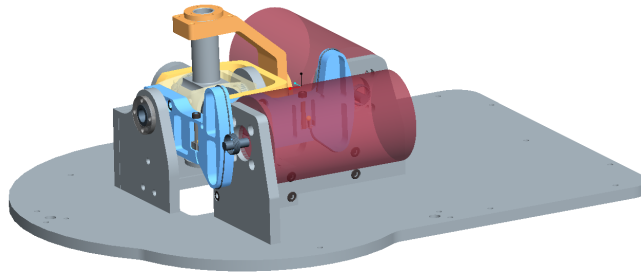

Figure 4.16: 2 DoF Force Feedback joystick: Pro-Engineer model

Although the general design was clear and sketches had been made, the first step to take once the final design was chosen was to decide whether the optimal position for the motor was the back or the front part. Since the disposition of elements would be completely symmetric respect to the YZ plane, and the only element which would break the symmetry in the XZ plane would be the motor, it was estimated which position would be helpful in terms of driving due to the torque generated by it.

It was first considered placing the motor in the back part (see Figure 4.17). When steering forward (applying a force to the front), the torque in the cardan joint due to the motor would increase, but would be compensated by that of the applied force. When steering backwards, the torque generated by the motor would be decreased, and added to that created by the applied force.

If the motor was placed on the front part, the oposite effect happened.

The positioning of the motor in the front part was clearly more beneficial, so it was the chosen location.

Once this was clear, the design process with Pro-Engineering Wildfire started. Parts were created, assembled to the previous Joystick model (showed in Figure 4.16), redesigned and so on, until the final mechanism was built. During the whole process points which were thoroughly considered were:

- Minimize the mass of the system, making the parts stiff and resistant but small.

- Make it as compact as possible.

- Avoid the collisions with the parts built already for the previous Joystick.

- Try to avoid or minimize the number of previous parts to be modified.

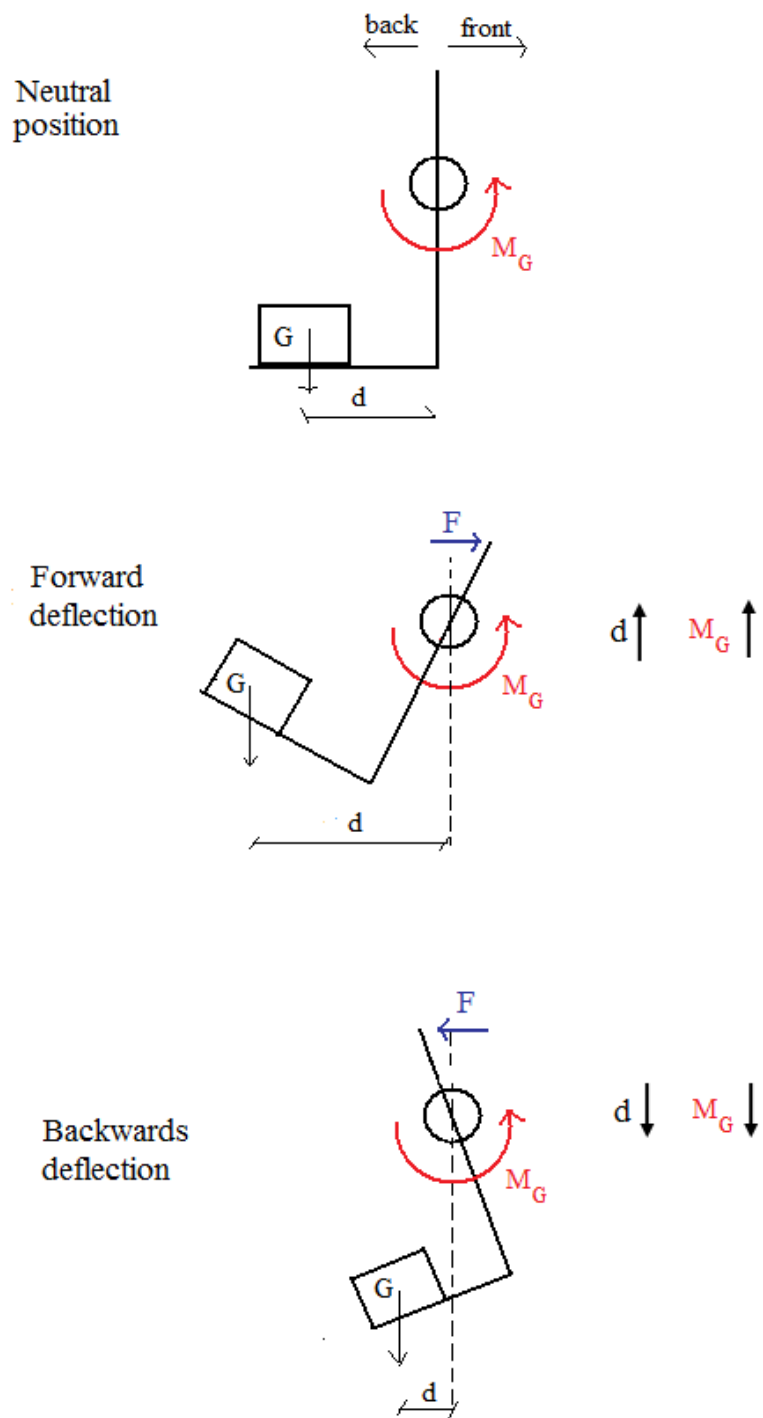- Avoid stress concentrations making the parts as round as possible.

Figure 4.17: Genrated torques for motor placed in the back

- Design simple geometries, easy to manufacture.

Obviously, the first part from the previous Joystick which had to be modified was the base. A squared hole was made on it, to allow the movement of the rotating axis. The collisions were easy to detect because Pro-Engineering Wildfire allows the movement of the assemblies according to the defined movement range. In the present case the movement range in the x and y axis was defined to be ±20. As the parts were assembled, the mechanism was made to move, allowing the detection of possible collisions and the later part redesign.

Information was collected from previous sketches to design the 2 DoF Joystick to investigate which parts were important for the mechanical sustain, which ones were not, and which screws could be taken away without causing instabilty in the system, and so on. Just three parts from the previous Joystick were finally modified: one of the bearing containers and two motor holders (see Drawings in the Appendix D of the Annex).

The material to manufacture all the parts was an alloy of aluminum, copper, magnesium and lead (F34), providing the prototype of high stiffness, but with the minimum weight, because, as it was mentioned above, minimizing mass was a concern throughout the design process.

The designing phase finished with a total of nine new designed parts, one part redesigned (the cardan joint) and three existing parts needed a cut to avoid collisions. The final design Pro-Engineering Wildfire model is showed in Figure 4.18. The last step was to prepare the drawings to submit them to the Workshop. They can be found attached in Appendix D of the Annex.

The next subsections give brief information of the steps followed for the design of the most important parts.

4.6.1 Rotating shaft

The length of the rotating shaft was intended to be as short as possible, in the upper end to keep it below the casing, and in the low end to keep the motor as close to the cardan joint as possible and generate the minimum torque.

Since it is in contact with a number of standardized elements such as rings and bearings, the axis was designed carefully taking into account the demanded tolerances. Phases were made in both ends of the axis to introduce the fitted elements avoiding their damage.

To avoid the stress concentration in places where bearings or the transmission system were placed, DIN509 E undercuts were practiced.

A helping drawing with the axis and the elements attached to it and the fittings can be found on Appendix D.

Cables had to go through the axis from the grip to the circuit which is grounded in the base of the Joystick, so part of the axis needed to be hollow.

4.6.2 Motor board

The motor board was a very simple board with a hole to fit the motor, and the necessary phase made for the fitting, which can be seen on Figure 4.20. The compactness of the assembly between the motor and the board is showed in Figure 4.21.
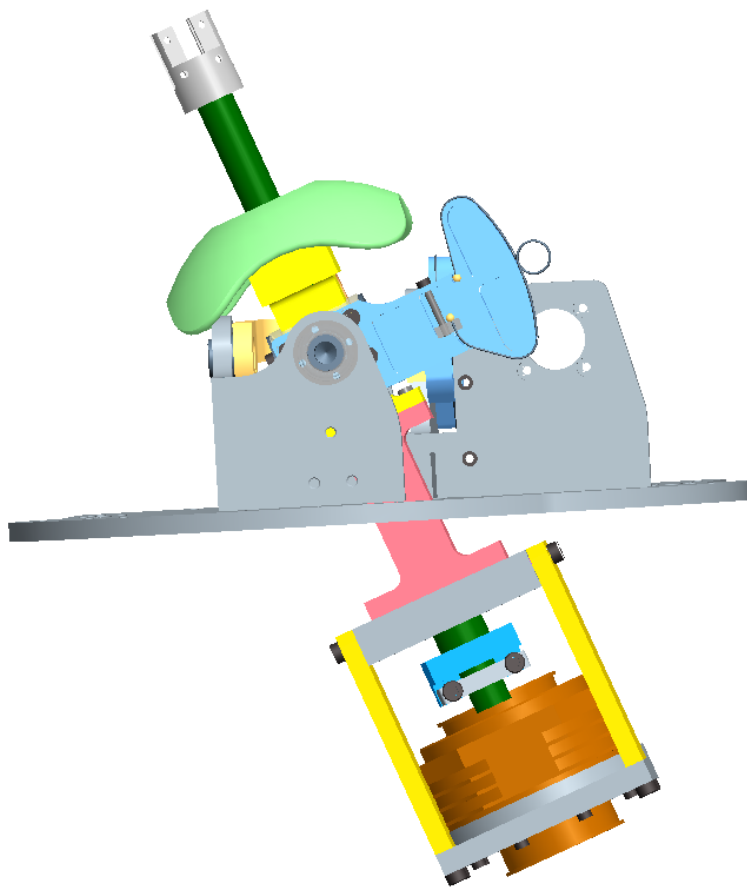
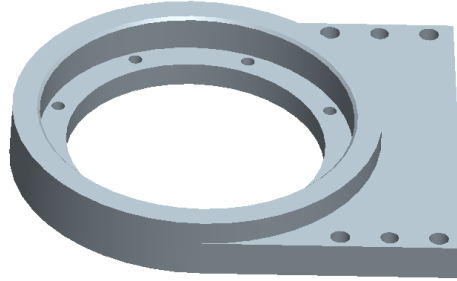Figure 4.18: Model of the prototype in Pro-Engineer Wildfire

Figure 4.19: Rotating axis

Figure 4.20: Motor board

4.6.3 Cardan joint

The cardan joint is a key part, since it is what can be called the 'heart' of the system. The original cardan joint had to be modified, to introduce the rotating shaft through it, and also to place one of the bearings (the smaller one, the one with the loose fitting). Figure 4.22 shows different phases of the designing process, starting from the actual part of the 2 DoF Joystick, and finishing with the final option. The different options were rejected following the basis of this design phase: minimizing the material quantity, making it as compact as possible, and trying to avoid asymmetries. As it can be seen, the third design and the fourth had elongations to join this part directly to the motor board. However, this option was rejected because they were difficult to manufacture, and the stiffness of the joining would be difficult to guarantee, because bending could happen. Finally it was decided to have an intermediate part between the motor board and this cardan joint (See 4.6.6). There is also a transition from cylindrical forms to more squared, the reason being to simplify the manufacturing process.

4.6.4 Bearing board

The bearing board was also a key element: it was an indirect joining part between the board motor and the cardan joint and therefore it had plenty of screws and pins, but it also contained a bearing, which taking advantage of the space available, was the bigger one. An undercut was also designed for the bearing to rest.

4.6.5 Transmission system

The parts which form the transmission system are the more complex and need of high manufacturing accuracy to perform the high quality reduction function. The system is formed by the main part and the tightening mechanism, which are showed in Figure 4.26. The stress concentration was an important issue in this
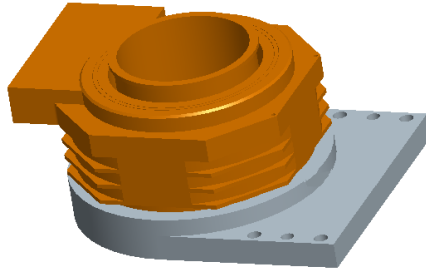
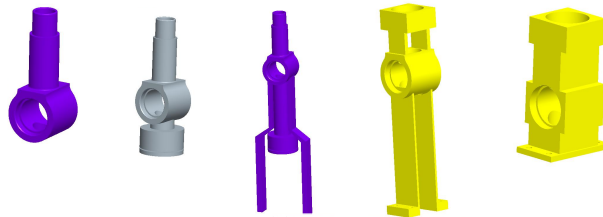Figure 4.21: Motor board with motor casing assembled

Figure 4.22: Different phases of the design from the original to the final griff-bolzen

part, because of its reduced size and the number of different forms introduced. The solution to avoid these stress concentrations was to add material whenever it was possible.

The range of movement ($\pm 8^{\text{o}}$) could be controlled mechanically, with a hard stop, but after considering it, it was decided that the controlling would be electrical.

The cable has 5 windings around the motor axis, as it can be seen in Figure 4.27, which shows a closer look of the transmission system in the assembly. Another advice was that the cable's diameter should be 12-20 times smaller than the motor shaft's diameter, so the cable's diameter was chosen to be 0.6mm. The point of maximum tension in the cable would be the turning of the cables, so this turning was made as open as possible.

The problem of joining the transmission system to the axis having no relative movement at all between these two parts was solved with a fitting and another adjustable part.
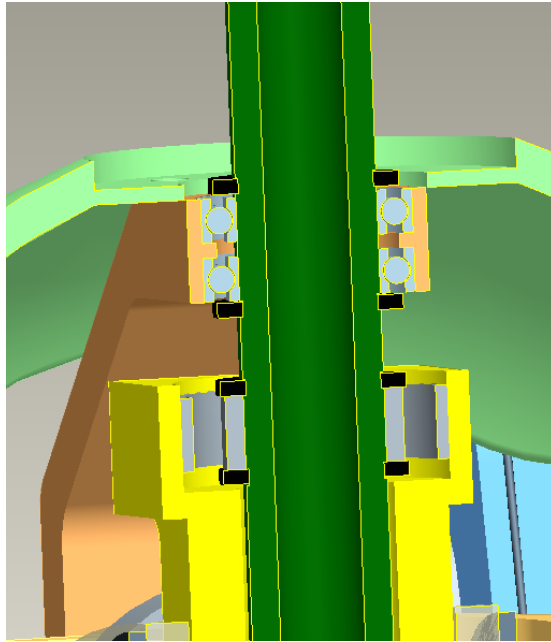
Figure 4.23: A section of the assembly

4.6.6 Bars

The function of this part was to connect the cardan joint with bearing board, as well as protecting the shaft. It was originally just one part, and later it was considered to make it be two parts, very thin to avoid collisions. They were made thicker to avoid the bending due to generated torques, and finally it was decided to use a single piece again, with a hole inside for the axis, and an additional hole to take out the cables.

4.6.7 Standarized elements

The selection of the standardized elements was done during the designing process, doing the covenient changes in the parts to adjust to the demanded tolerances and the space available needed for them, following the providers specifications. Appendix D of the Annex contains the list of all the standardized elements and the position of the joining elements in the manufactured parts.

Joining elements

Once all the parts and their weight were known, the procedure was to select the normalized joining elements. All the screws were socket head cap screws DIN912 in the standard grade 8.8, with the following tensile yield strength (f_{yb}) and tensile ultimate strength (f_{ub})

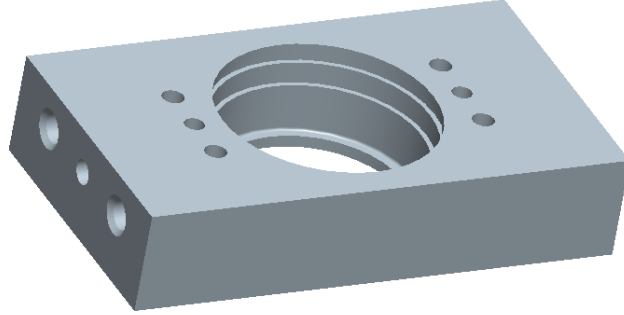$$f_{yb} = 640 \text{ N}/mm^2$$

$$f_{ub} = 800 \text{ N}/mm^2$$

Figure 4.24: Bearing board

The selected screw, in order to support the applied loads, according to [38], should fulfill the next three conditions with a security factor of M_b=1.25:

- Yielding

$$F_{v,Sd} \leq F_{v,Rd} \tag{4.3}$$

with

$$F_{v,Rd} = \frac{0.6 \cdot f_{ub} \cdot A_s}{\gamma_{Mb}} \tag{4.4}$$

- Crushing

$$F_{v,Sd} \leq F_{b,Rd} \tag{4.5}$$

with

$$F_{b,Rd} = \frac{2.5 \cdot \alpha \cdot f_u \cdot d \cdot t}{\gamma_{Mb}} \tag{4.6}$$

- Traction

$$F_{t,Sd} \leq F_{t,Rd} \tag{4.7}$$

with

$$F_{t,Rd} = \frac{0.9 \cdot f_{ub} \cdot A}{\gamma_{Mb}} \tag{4.8}$$
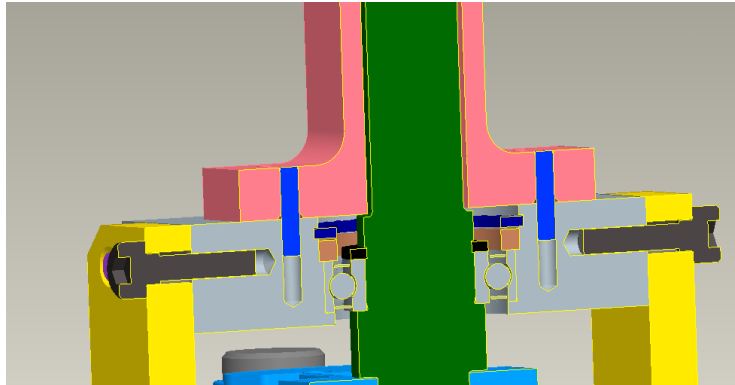
where, in each case

- d : Diameter of the screw
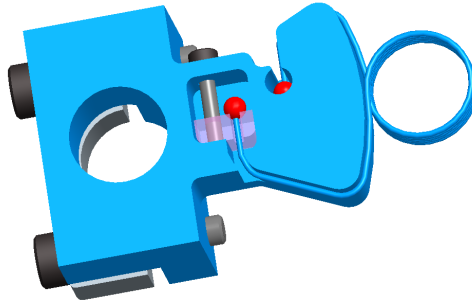
Figure 4.25: A section of the assembly

Figure 4.26: Assembly of the transmission system

- t : Thickness of the part

- As : The screw thread tensile stress area

- A : Transversal area

and α the minimum value between

$$\frac{e_1}{3 \cdot d_0} \text{ or } \frac{p_1}{3 \cdot d_0} - \frac{1}{4} \text{ or } 1.0 \tag{4.9}$$

(with e_1, p_1 and d_0 explained in next section)

To calculate the minimum distance from the last line of screws to the edge parallel to the direction of the load (e_1) equation 4.10 was used, minimum distance to the edge perpendicular to the direction of the load (e_2) was calculated using equation 4.11, and the minimum distance between screws parallel to the direction of the load(p_1) and the minimum distance between screws perpendicular to the direction of the load(p_2) was designed following equation 4.13. See Figure 4.29 for aclaration.
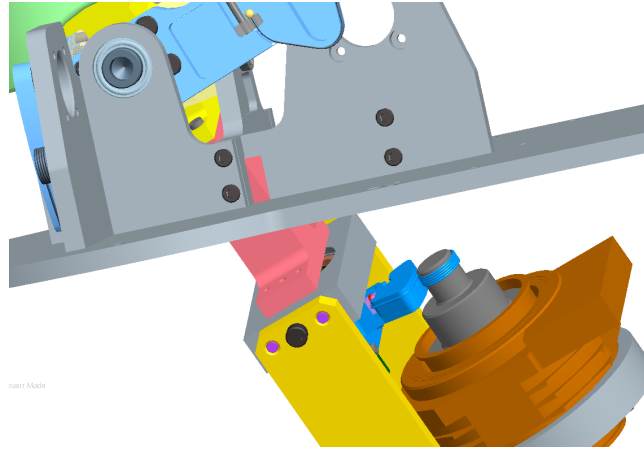
Figure 4.27: Detail of the prototype assembly

$$e_1 \geq 1.2 \cdot d_0 \tag{4.10}$$

$$e_2 \geq 1.5 \cdot d_0 \tag{4.11}$$

$$p_1 \geq 2.2 \cdot d_0 \tag{4.12}$$

$$p_2 \geq 3 \cdot d_0 \tag{4.13}$$

with d_0 the diameter of the hole.

Regarding the length of the screws, it must be guaranteed that they are at least $2 \cdot d_0$ introduced in the screwed part.

However, the use of screws was enough to assure the good joint between the parts, but not to avoid the relative torques which may be created between key parts. To do so, ISO 2338 cylindrical pins were used to reassure the joint between the cardan joint and the bars, and between the holders and the motor board. Their diameter was selected in function of the available space, and the minimum distance with the nearer screws. Tolerances for the holes were found in tables. Like in the case of screws, a minimum introduced length of $2 \cdot d_0$ must be guaranteed.
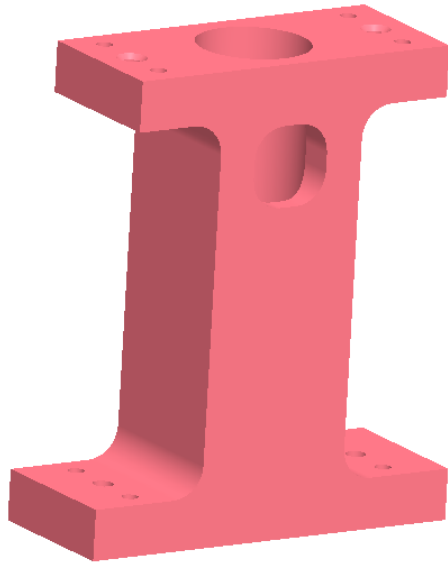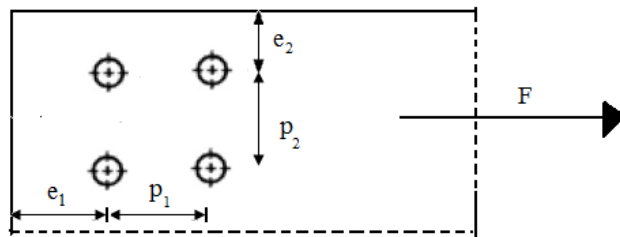
Figure 4.28: Bars

Figure 4.29: Hole distances

Chapter 5

Economic budget

From the beginning of the development of the thesis, the time and the cost linked to the production of the Joystick prototype was taken into consideration. At all the steps within the whole process the choices were made to reach the best solution, but as an engineer, the difficult job was to get an optimal quality/economic cost ratio.

Table 5.1 gathers the economic budget of the whole Project. Specific costs were calculated using administrative data from DLR. As far as the time amounts are concerned, although they do not measure the exact invested time, they are a good approximative description.

CONCEPT	COST
EMPLOYEES	4450€
Project supervisor	100 hours x 67€/hour
Engineering student	1000 hours x 3.78€/hour
INFORMATION SYSTEMS	1107€
Hardware (DELL computer)	1000hoursx0.75€/hour
Matlab	75hoursx1.48€/hour
OS (Linux & Windows)	free
Pro-Engineer Wildfire	200hoursx1.23€/hour
PROTOTYPE CONSTRUCTION	6225.52€
Standardized elements	125.52€
Part manufacturing	4000 €
Robodrive motor+encoder	2100 €
OFFICE MATERIAL	50€
TOTAL	**11832.52 €**

Table 5.1: Economic budget

Chapter 6

Conclusions and outlook

6.1   Conclusions

A good electric and control design does not always assure the good behaviour of a haptic device. The base, the device itself, and therefore the mechanical design has to meet some requirements so that it works properly. Through the different phases of the thesis, information was gathered about these needs, and in particular for the case of a joystick which would be used to steer a wheeled mobile robot. Some of the issues to take into account were:

- Mass

- Friction

- Stiffness

- Compactness

- Backlash

- Backdriveability

The user study, which took place to study the kinematics of the forearm and see if there were couplings in the degrees of freedom, was useful to prove that users found satisfactory the joystick steering for a virtual model of the ROMO. Objective data, control of the error and demanded effort, supported this fact, in particular for the longitudinal and lateral steering. The rotational degree of freedom turned out to be a too new steering concept for the users. But, since for a normal steering three degrees of freedom are not needed at once, it was considered it would be beneficial to implement the three degrees of freedom in a single device, not having all active at once. The ROMO is a project on which they are investigating different aspects of wheeled mobile robots, and it seems it would be positive to implement this new steering option, so that developers at DLR are able to implement new electric and control circuits. Visitors to the Institute could be able to observe and experience how is the feeling of driving with this new Joystick.

The user study also provided information about the performance when steering the third degree of freedom which would be used as specifications for the prototype.

After studying the different feedback options for Joysticks, and based on bibliography which recomended the active feedback for a more satisfaying driving esperience, three last active options were considered. These options had a motor, a sensor, and in two cases a transmission system. After studying several points such as the total mass of the system and the generated torque, the one which better covered the requirements was chosen for the prototype.

When finally designing the different parts, the following was considered:

- Minimize the mass of the system and make it compact.

- Avoid the collisions with the parts built already for the previous Joystick.

- Avoid stress concentrations making the parts as round as possible.

- Design simple geometries, easy to manufacture.

The parts were designed with the CAD software Pro-Engineer and implemented in the existing model of the DLR 2 DoF Joystick.

6.2 Outlook

The last step of the thesis was the preparation of the drawings of the different parts of the prototype to take them to the workshop, therefore this thesis has been the first phase of a project which will be still developed in the future.

Once the prototype is manufactured, and the electric and control circuits implemented, a new user study will be designed and carried out, considering different feedback options, and evaluating if the requirements for a good haptic feeling are fullfilled. If the results are positive, a new device will be designed based on this work, and will be implemented in the actual ROMO. The different studies and tests will prove in the future if the 3 DoF Joystick is a feasible steering device for wheeled mobile robots for public use, or if the device is just useful for research purposes.

Part II

Annex

Appendix A

Kinematic analysis

A.1   Introduction

For simulation purposes, the kinematics of wheeled mobile robots (WMR) that we care about are the rate kinematics, and in particular, the forward kinematics: translading the desired total linear and angular velocity of the vehicle center of gravity into the velocities ω_i and steer angles ϕ_i of the wheels. This problem is solved in the general case by appealing to the physics of rigid body motion, and the mathematic of moving coordinate systems, following the studies done in [39].

It is important to point out that this kinematic approach is not just followed for simulation purposes, but it is actually followed to control the real ROMO, because given the desired horizontal ROMO motion (which is 'decided' and steered by the driver) then from a control engineering viewpoint the challenge is to provide eight valid actuator command signals to the four wheels to make the car movement possible. At this, the vehicle should perform the desired motion as precisely as possible while external disturbances are rejected, safety is maximized, and energy consumption and tire wear are minimized. As a matter of fact, 'Global chassis control' simultaneously addressing these goals is a significant part of scientific work at DLR [23]. However, the ROMO should be drivable interactively even without the considerable effort implied by 'Global chassis control'. An efficient simple feed-forward actuator control has been proposed as an alternative which can later be consolidated with global chassis control and serve as a fallback system. This alternative is the approach which has been called 'Geometric control', based on kinematics of the vehicle, carrying on the idea behind Ackermann steering (see Figure A.1), which will be explained in the last part of the present section.

It is known that using kinematic relations, from the actual motion request, the linear reference velocity

$$\left(\begin{array}{c} v_{x,ref,i} \\ v_{y,ref,i} \end{array} \right) \tag{A.1}$$

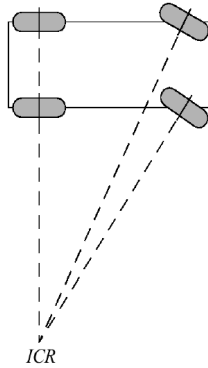at any location of the vehicle can be computed, particularly at the wheel loca-

Figure A.1: Ackerman steering and ICR

tions, which is our objective

$$\left(\begin{array}{c} x_i \\ y_i \end{array} \right) \text{ for i=1,...,4} \tag{A.2}$$

The linear vehicle acceleration is in the case of the ROMO motion assumed sufficiently small such that all three horizontal inertial forces/torque can be neglected. Setting them to zero yields three equations, however eight actuator command signals are searched for and thus the control allocation problem is underdetermined (see [40] for illustration). From the remaining fivedimensional solution space we deliberately choose the solution where all eight horizontal tire force components are zero. Hence all longitudinal and lateral tire slips are zero. Consequently, the steering angle of each wheel is aligned with the respective local reference velocity and the wheel rotational speeds directly follow from the quotient of speed and wheel radius (this settlement will be later on conveniently used). Of course, the assumption of vanishing inertial forces does not even hold for many low speed maneuvers. Nevertheless, (like Ackermann steering for the conventional vehicle) the simple geometric control approach only needs geometric vehicle parameters and works well as an approximation over a notable portion of the physically feasible motion operating domain.

To sum up, according to [41], it is important to take into account the following limitations for the construction of the kinematic model before starting the kinematic analysis:

- The robot moves on a planar surface.

- The contact points of the car with the floor are those 4 point where each wheel is in contact with the floor.

- There are no flexible/deformable elements in the robot's structure (including the wheels), and wheels are connected by rigid frame (chassis)

- Wheels have one or no directioning axis, that way this is always perpendicular to the floor.

79

- No frictions are taken into account, between vehicle's mobile parts, or with the ground. No friction for rotation around contact point either.

- Pure rolling, v_c=0 at contact point.

- No slipping, skidding or sliding.

Equations will be reached for a general case, in terms of generic geometric values. Afterwards the actual values of the ROMO geometry will be introduced (The ROMO uses axially symmetric assembly of the wheel robots with reference to the vehicle center, and the wheelbase is 2W = 2.4 m whereas the track width measures L= B = 1.5 m), much more suitable since this is written as code in the Simulink model afterwards, and it is preferable to have expressions in function of variables.

As mentioned above, this approach is the direct or forward kinnematics approach, the one we are interested in for the visualisation, but inverse kinnematics, that is, the reverse, compute the linear and angular velocity of the center of gravity given the steer angles and wheel rotation rates (estimated with sensors in the ROMO wheels), is taken into account in the actual ROMO for control purposes.

A.1.1 Frames and representations

In order to go on with an accurate kinematic analysis, the following frames of reference, see Figure A.2, must be defined:

- W: World, fixed to the environment.

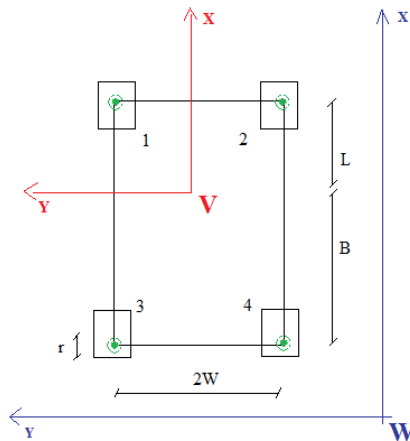- V: Vehicle, fixed to the Center of Gravity (Cog) of the car.

Figure A.2: Frame for the WMR - World and Vehicle

The planar motion has three degrees of freedom (as it was stated before, apart from conventional forward/backward driving the ROMO is able to rotate

about a vertical axis, which can be through the vehicle center or eccentric, and it can also move sidewards). For their representation over time three independent scalar variables are necessary. Many triple combinations of physically meaningful quantities are conceivable which allow the unique definition or representation of planar vehicle motion. If not the position is given directly but speed or even acceleration, then all other representations can be uniquely computed from there using standard kinematic relations.

$$\text{Position in the plane: } \begin{pmatrix} x \\ y \end{pmatrix} \quad \text{(A.3)}$$

$$\text{and yaw angle: } \theta \quad \text{(A.4)}$$

can be joined together in a vector $\vec{q}$, which is the state vector describing generalized coordinates of the robot:

$$\vec{q} = \begin{pmatrix} x \\ y \\ \theta \end{pmatrix} \quad \text{(A.5)}$$

These coordinates are of the vehicle frame with respect to the World frame (see Figure A.2) and they fully determine the position of a car-like-robot (See Figure A.3).
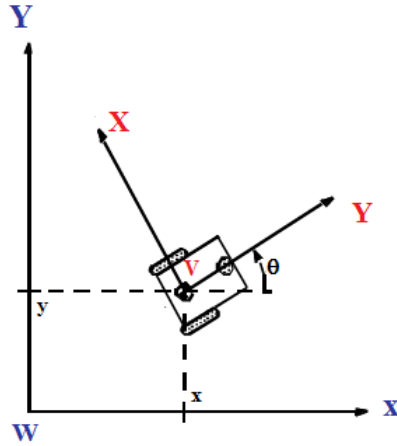

Figure A.3: The WMR's position is fully determined

In the same way,

$$\text{vehicle linear speed } \vec{v_w} = \begin{pmatrix} \dot{x} \\ \dot{y} \end{pmatrix} \quad \text{(A.6)}$$

$$\text{and yaw rate } \vec{\omega} = \dot{\theta} = \omega \vec{k} \quad \text{(A.7)}$$

can be joined together in a vector $\vec{\dot{q}}$, which is the state vector describing generalized velocities of the robot:

$$\vec{q} = \begin{pmatrix} \dot{x} \\ \dot{y} \\ \omega \end{pmatrix} \qquad (A.8)$$

Since, like the vector of generalized coordinates, this vector is defined with reference to the World frame, a change of frame from the Vehicle frame to the World frame needs to be done in order to later be able to operate just with absolute velocities:

$$\vec{v_w} = \begin{pmatrix} \dot{x} \\ \dot{y} \end{pmatrix} = \begin{pmatrix} cos\theta & -sin\theta \\ sin\theta & cos\theta \end{pmatrix} \begin{pmatrix} v_x \\ v_y \end{pmatrix} \qquad (A.9)$$

With

$$v_v = \begin{pmatrix} v_x \\ v_y \end{pmatrix} \qquad (A.10)$$

the linear velocity of the car expressed in the Vehicle frame, the velocity which can be computed in the car.

A.1.2   Wheels

The i-th wheel rotates with an angular velocity ω_i and the linear velocity component forms a ϕ_i angle with the longitudinal direction, as illustrated by Figure A.4 in a general case.
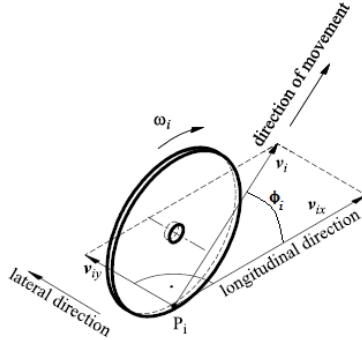

Figure A.4: Velocities of one wheel

For simplicity, as [42] states, the thickness of the wheel is neglected and it is assumed to be in contact with the plane at point P_i. As said before, the slip is neglected, so

$$v_i = v_x \qquad (A.11)$$

which will be taken into account later. So, once the two vector of generalized coordinates and velocities are defined, the objective is to compute the 4 wheels configuration vector:

$$\left(\begin{array}{c} \omega_i \\ \phi_i \end{array} \right) \tag{A.12}$$

A.2 Analysis

Suggested by [43], to get the 4 wheels configuration vector, classical kinematics of the rigid body will be followed, which states that the velocity of a point q can be related to the velocity of point p of the same body through the angular velocity of the body, ω,

$$(\frac{d\vec{r}}{dt})_{fixed} = (\frac{d\vec{r}}{dt})_{moving} + \vec{\omega}\mathrm{x}\vec{r} \tag{A.13}$$

Then, the velocity on each wheel can be calculated, with the yaw rate, the angular velocity ω between the frame V and W, taken into account:

$$(\frac{d\vec{r_1}}{dt}) = (\frac{d\vec{r_w}}{dt}) + \vec{\omega}\mathrm{x}\vec{r_{v1}} \tag{A.14}$$

$$\vec{v_1} = \vec{v_w} + \vec{\omega}\mathrm{x}\vec{r_{v1}} \tag{A.15}$$

Which is the linear velocity of the wheel 1 expressed in terms of absolut, with reference to the World frame. The same can be applied to the other 3 wheels:

$$\vec{v_2} = \vec{v_w} + \vec{\omega}\mathrm{x}\vec{r_{v2}} \tag{A.16}$$

$$\vec{v_3} = \vec{v_w} + \vec{\omega}\mathrm{x}\vec{r_{v3}} \tag{A.17}$$

$$\vec{v_4} = \vec{v_w} + \vec{\omega}\mathrm{x}\vec{r_{v4}} \tag{A.18}$$

The $\vec{v_w}$, the absolut linear velocity of the car, can be expressed in the World frame in the x and y direction with its two components: $\dot{x}\vec{i}$ and $\dot{y}\vec{j}$. The angular velocity $\vec{\omega}$ is always perpendicular to the plane, so it is $\omega\vec{k}$. Then, the velocity of the wheels can also be expressed by means of the World frame, if the geometry of the car $\vec{r_i}$ is also taken into account (see Figure A.5):

$$\vec{r_{v1}} = \left(\begin{array}{c} x + L \\ y + W \\ 0 \end{array} \right) \tag{A.19}$$

$$\vec{r_{v2}} = \left(\begin{array}{c} x + L \\ y - W \\ 0 \end{array} \right) \tag{A.20}$$

$$\vec{r_{v3}} = \left(\begin{array}{c} x - b \\ y + W \\ 0 \end{array} \right) \tag{A.21}$$

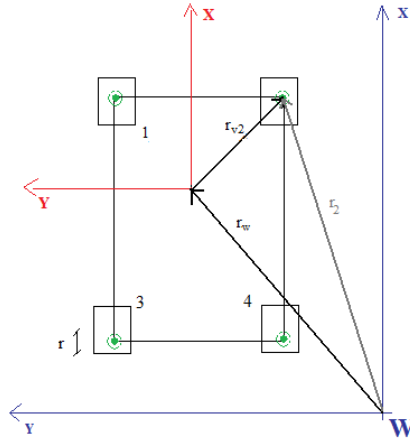$$\vec{r_{v4}} = \left(\begin{array}{c} x - b \\ y - W \\ 0 \end{array} \right) \tag{A.22}$$

Figure A.5: Position vector for Wheel 2

$$\vec{v_1} = \begin{pmatrix} \dot{x} \\ \dot{y} \\ 0 \end{pmatrix} + \begin{pmatrix} 0 \\ 0 \\ \omega \end{pmatrix} \times \begin{pmatrix} x+L \\ y+W \\ 0 \end{pmatrix} = \begin{pmatrix} \dot{x} \\ \dot{y} \\ 0 \end{pmatrix} + \begin{pmatrix} x-\omega W \\ y+\omega L \\ 0 \end{pmatrix} = \begin{pmatrix} \dot{x}+(x-\omega W) \\ \dot{y}+(y+\omega L) \\ 0 \end{pmatrix}$$
(A.23)

Similarly, velocity for the other 3 wheels would be calculated:

$$\vec{v_2} = \begin{pmatrix} \dot{x}+(x+\omega W) \\ \dot{y}+(y+\omega L) \\ 0 \end{pmatrix} \tag{A.24}$$

$$\vec{v_3} = \begin{pmatrix} \dot{x}+(x-\omega W) \\ \dot{y}+(y-\omega b) \\ 0 \end{pmatrix} \tag{A.25}$$

$$\vec{v_4} = \begin{pmatrix} \dot{x}+(x+\omega W) \\ \dot{y}+(y-\omega b) \\ 0 \end{pmatrix} \tag{A.26}$$

That way, the velocities of the wheels expressed in components

$$\begin{pmatrix} v_{x1} \\ v_{y1} \\ v_{x2} \\ v_{y2} \\ v_{x3} \\ v_{y3} \\ v_{x4} \\ v_{y4} \end{pmatrix} = \begin{pmatrix} 1 & 0 & x-W \\ 0 & 1 & y+L \\ 1 & 0 & x+W \\ 0 & 1 & y+L \\ 1 & 0 & x-W \\ 0 & 1 & y-b \\ 1 & 0 & x+W \\ 0 & 1 & y-b \end{pmatrix} \begin{pmatrix} \dot{x} \\ \dot{y} \\ \omega \end{pmatrix} \tag{A.27}$$

$$v = H\dot{q} \tag{A.28}$$

84

Since it is considered a simplified case of the wheeled mobile robot for which the longitudinal slip between the wheels and the surface can be neglected, based on work done in [44], the following relation can be developed:

$$v_i = r_i \omega_i \tag{A.29}$$

$$\vec{\omega_1} = \frac{v_1}{r_1}\vec{k} = \frac{\sqrt{v_{x1}^2 + v_{y1}^2}}{r_1}\vec{k} \tag{A.30}$$

$$\vec{\omega_2} = \frac{v_2}{r_2}\vec{k} = \frac{\sqrt{v_{x2}^2 + v_{y2}^2}}{r_2}\vec{k} \tag{A.31}$$

$$\vec{\omega_3} = \frac{v_3}{r_3}\vec{k} = \frac{\sqrt{v_{x3}^2 + v_{y3}^2}}{r_3}\vec{k} \tag{A.32}$$

$$\vec{\omega_4} = \frac{v_4}{r_4}\vec{k} = \frac{\sqrt{v_{x4}^2 + v_{y4}^2}}{r_4}\vec{k} \tag{A.33}$$

The steering angle of each wheel can also be calculated, because, since the wheel is assumed to roll without slipping, the local speed is aligned with the wheel steering angle:

$$\phi_1 = atan\frac{v_{y1}}{v_{x1}} \tag{A.34}$$

$$\phi_2 = atan\frac{v_{y2}}{v_{x2}} \tag{A.35}$$

$$\phi_3 = atan\frac{v_{y3}}{v_{x3}} \tag{A.36}$$

$$\phi_4 = atan\frac{v_{y4}}{v_{x4}} \tag{A.37}$$

A.3   ICR and ROMO operating modes

Although it is a concept which was not taken into account in the visualisation kinematic model to make it simple, there is a concept developed in the ROMO which is very important and should be taken into account in next visualisations: The adequacy of using the instantaneous center of rotation (ICR) for motion control, as it was investigated in [45]. The planar horizontal motion of a vehicle (as seen from above, cf. Figure A.7) can at any time be considered as the rotation about a virtual point in that plane which is called the instantaneous center of rotation. This is also assumed by the Ackerman steering. As it was stated before, since the wheel is assumed to roll without slipping, the local speed is aligned with the wheel steering angle, and, as a matter of fact, the perpendiculars to all velocity vectors (regardless of the considered location) of a moving rigid body intersect in the ICR. Therefore, we can state that the ROMO body ICR is located somewhere on the straight line which is formed by the prolongation of the wheel rotation axis being perpendicular to the local
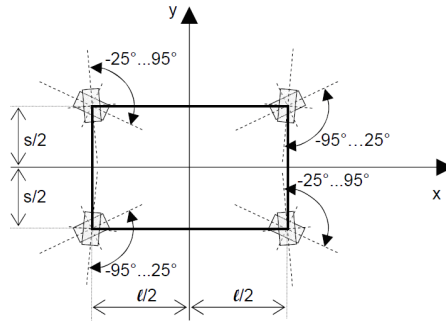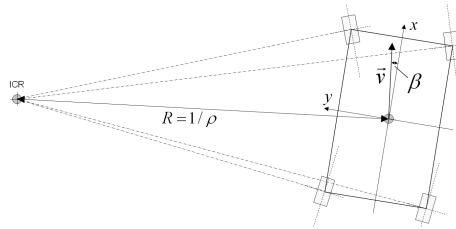
Figure A.6: ROMO geometric parameters

Figure A.7: Instantaneous center of rotation (ICR) in vehicle fixed coordinate system

velocity. However, the location of the ICR is restricted to the white area visible in Figure A.8 due to the limited steering angle range: the steering angle have ranges of -95° to 25° (front left and rear right wheels) and -25° to 95° (front right and rear left wheels), ilustrated with Figure A.6). In the present simulation thus limited steering angle was in fact not taken into account: ideally a range of 360º is available for the wheels so that they can turn freely.

Figure A.9 extends the consideration by taking into account all four wheels at the same time by forming the union of the corresponding invalid ICR sets. The remaining white regions thus indicate the set of all possible ICR locations, which is split into three discontiguous regions (0, 1, 2) corresponding to separate operating modes.
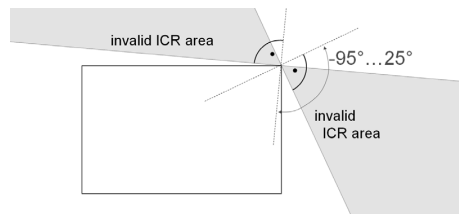

Figure A.8: Invalid area (gray) for the vehicle body's ICR regarding steering angle limits at the front left slip-free rolling wheel and zero tire slip
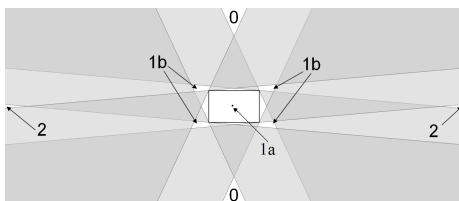
Figure A.9: The white regions form the valid set for the vehicle's ICR when simultaneously regarding the steering angle limits of all four wheels rolling with zero tire slip

- region 0: represents conventional 'pure' longitudinal driving. The two parts (sectors) of region 0 are connected via infinity. The opening angle of the two sectors indicates the margins which are effective for variation of the chassis side slip angle. Mobile solid point.

- region 1: The vehicle rotates on the spot if the ICR lies in region 1a. In the neighboring regions 1b the vehicle turns about an ICR which is out still close to the vehicle corners. Mobile solid point.

- region 2: 'Pure' lateral driving. Not mobile solid point.

As a conclusion, it can be said that the reference motion for geometric control needs to be specified such that the vehicle's ICR lies in one of the valid operationally meaningful regions as shown in Figure A.9. This suggests the direct use of the vehicle's ICR for parameterization in the kinematic model of the desired vehicle motion.

It is also important to point out that since in every moment all planar motions can be described as a pure rotation around the ICR, as it was stated above, the direction of the velocity in any point p of the ROMO will have a perpedicular direction to the line joining p and the ICR, and its modulus and sense will be given by the following vectorial product (expresed in the ICR frame):

$$\vec{v}_p = \vec{\omega} \mathrm{x} \vec{r}_p^{icr} \tag{A.38}$$

As it was mentioned before, this concept should be taken into account in next visualisations, since the assumption of any possible motion is not correct, as it was demonstrated in lines above.

Appendix B

Instructions and questionaries

The following pages contain the instructions about the user study given to participants, as well as the questionaries they filled.

Instruktion _(tl)

Vorab vielen herzlichen Dank für die Teilnahme!

Im folgenden Experiment sollen alternative Bedienelemente zur Steuerung eines Automobils untersucht werden. Das zu steuernde Fahrzeug ist dabei in der Lage, alle Räder unabhängig voneinander zu bewegen, wodurch unterschiedlichste Fahrmanöver wie Rotationen auf der Stelle oder Seitwärtseinparken möglich werden.

Ihre Aufgabe im Experiment wird es sein, ein Fahrzeug in einer Simulation mit einem Joystick zu bewegen, der an einem Leichtbauroboter installiert ist.

Die Steuerung des Fahrzeugs in Längsrichtung erfolgt durch Vorwärts- (Beschleunigen) bzw. Rückwärtsbewegung (Bremsen) des Joysticks (Drehung um die Y-Achse, siehe Abbildung). Das Drehen des Fahrzeugs (Gieren) wird durch Drehung des Joysticks um die Vertikalachse (Z-Achse) kommandiert. Das Seitwärtsfahren wird mit zwei unterschiedlichen Bedienkonzepten realisiert:

A) Bewegung des Joysticks nach links bzw. rechts (Drehung um die X-Achse):
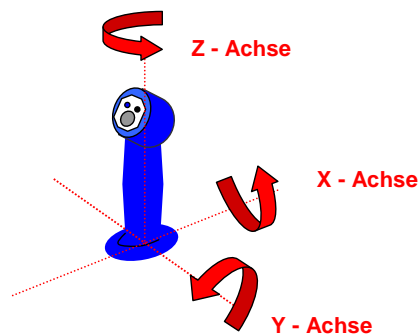
B) Bewegung einer *zusätzlichen* Spacemouse nach links bzw. rechts
   (Drehung um die X-Achse)
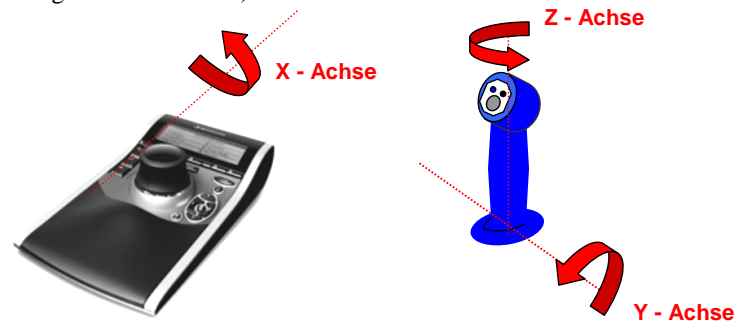
In dieser Bedingung steuern sie Längs- und Drehbewegung mit der rechten Hand über den Joystick und die Seitwärtsbewegung des Fahrzeugs mit der linken Hand über die SpaceMouse.

Im Experiment werden Sie sowohl mit Bedienkonzept A als auch B das simulierte Fahrzeug steuern. Dabei werden Sie unterschiedliche Fahraufgaben wie die Geradeausfahrt, Rückwärtsfahrt, Rotation auf der Stelle, das Seitwärts- und Schrägfahren und Kurvenfahrten zu bewältigen haben.

Während der verschiedenen Aufgaben wird Ihnen durch einen sogenannten „Ghost" angezeigt, wohin Sie Ihr Fahrzeug steuern sollen. Der Ghost stellt eine Kopie des zu steuerndes Fahrzeugs dar und wird halbtransparent schwarz dargestellt (s. Abb. unten). Versuchen Sie bei jeder Fahraufgabe die Position des Ghosts mit dem zu steuernden Fahrzeug einzuhalten, so dass Fahrzeug und Ghost möglichst deckungsgleich sind. Folgen sie dem Ghost *möglichst kontinuierlich und nicht ruckartig*.

Abb. 1: Fahrzeug und Ghost (schwarz) bei Geradeausfahrt und bei einer Rotation

Jeder Aufgabenblock (z.B. Geradeausfahrt oder Rotation) besteht aus mehreren Einzelaufgaben (z.B. Geradeausfahrt mit hoher Geschwindigkeit). Dabei wird jede Einzelaufgabe zweimal hintereinander ausgeführt.

Im Anschluss an jeden Aufgabenblock werden Sie gebeten verschiedene Fragebögen (z.B. zur Arbeitsbelastung) auszufüllen.

Zwischenfragebogen

Fragebogen zur Arbeitsbelastung (NASA-TLX)

Vp-Nr.: _____   Trial: _____   (vom Versuchsleiter auszufüllen)

Die folgenden Fragen beziehen sich auf die <u>Arbeitsbelastung im letzten Durchgang</u>.

Geistige Anforderungen   Wie viel geistige Anstrengung war bei der Informationsaufnahme und bei der Informationsverarbeitung erforderlich? War die Aufgabe leicht oder anspruchsvoll, einfach oder komplex, erfordert sie hohe Genauigkeit oder ist sie fehlertolerant?

sehr wenig   sehr viel

| | | | | | | | | | | | | | | | | | | | |

Körperliche Anforderungen   Wie viel körperliche Aktivität war erforderlich? War die Aufgabe leicht oder schwer, einfach oder anstrengend, erholsam oder mühselig?

sehr wenig   sehr viel

| | | | | | | | | | | | | | | | | | | | |

Zeitliche Anforderungen   Wie viel Zeitdruck empfanden Sie hinsichtlich der Häufigkeit oder dem Takt mit dem Aufgaben oder Aufgabenelemente auftraten? War die Abfolge langsam oder geruhsam oder schnell und hektisch?

sehr langsam   sehr schnell

| | | | | | | | | | | | | | | | | | | | |

Ausführung der Aufgaben   Wie erfolgreich haben Sie Ihrer Meinung nach die vom Versuchsleiter (oder Ihnen selbst) gesetzten Ziele erreicht? Wie zufrieden waren Sie mit Ihrer Leistung bei der Verfolgung der Ziele? *(0= Perfekt; 20 = Fehlschlag)*

Perfekt   **Fehlschlag**

| | | | | | | | | | | | | | | | | | | | |

Anstrengung   Wie hart mussten Sie arbeiten, um Ihren Grad an Aufgabenerfüllung zu erreichen?

sehr wenig   sehr viel

| | | | | | | | | | | | | | | | | | | | |

Frustration   Wie unsicher, entmutigt, irritiert, gestresst und verärgert (versus sicher, bestätigt, zufrieden, entspannt und zufrieden mit sich selbst) fühlten Sie sich während der Aufgabe?

sehr wenig   sehr viel

| | | | | | | | | | | | | | | | | | | | |

Beanspruchungsstruktur im Experiment (NASA-TLX)

Geben Sie bitte an, welche relativen Bedeutungen für die empfundene Gesamtbeanspruchung in allen Durchgängen die sechs Beanspruchungsdimensionen *Geistige Anforderungen, Körperliche Anforderungen, Zeitliche Anforderungen, Ausführung der Aufgaben, Anstrengung und Frustration* für Sie hatten.

Im Folgenden werden jeweils zwei der sechs Beanspruchungsdimensionen in verschiedenen Kombinationen gegenübergestellt. Geben Sie jeweils an, welche Beanspruchungsdimension für die Gesamtbeanspruchung, die Sie empfunden haben, bedeutsamer war. Es geht also nicht darum, wie hoch die Beanspruchung in den einzelnen Dimensionen war, sondern wie wichtig die jeweilige Dimension für das Gesamtempfinden war!

Bsp.: Wenn die geistigen Anforderungen, die die Aufgabe gestellt hat für die empfundene Gesamtbeanspruchung bedeutsamer waren als die Anstrengung, die Sie aufbringen mussten, dann kreuzen Sie wie folgt an:

Anstrengung		X	Geistige Anforderungen
Anstrengung			Ausführung der Aufgabe
Anstrengung			Frustration
Ausführung der Aufgabe			Frustration
Ausführung der Aufgabe			Geistige Anforderungen
Ausführung der Aufgabe			Zeitliche Anforderungen
Frustration			Geistige Anforderungen
Frustration			Körperliche Anforderungen
Frustration			Zeitliche Anforderungen
Geistige Anforderungen			Anstrengung
Geistige Anforderungen			Körperliche Anforderungen
Körperliche Anforderungen			Anstrengung
Körperliche Anforderungen			Ausführung der Aufgabe
Zeitliche Anforderungen			Anstrengung
Zeitliche Anforderungen			Geistige Anforderungen
Zeitliche Anforderungen			Körperliche Anforderungen

Gebrauchstauglichkeit des Bedienelements

System Usability Scale (SUS)   Bedingung_____

	Trifft gar nicht zu			Trifft sehr zu

1. Ich denke, dass ich dieses System gerne häufig nutzen würde.

| 1 | 2 | 3 | 4 | 5 |

2. Ich fand das System unnötig komplex.

| 1 | 2 | 3 | 4 | 5 |

3. Ich denke, das System war einfach zu benutzen.

| 1 | 2 | 3 | 4 | 5 |

4. Ich denke, ich würde die Hilfe eines Technikers benötigen, um das System benutzen zu können.

| 1 | 2 | 3 | 4 | 5 |

5. Ich halte die verschiedenen Funktionen des Systems für gut integriert.

| 1 | 2 | 3 | 4 | 5 |

6. Ich halte das System für zu inkonsistent.

| 1 | 2 | 3 | 4 | 5 |

7. Ich kann mir vorstellen, dass die meisten Leute sehr schnell lernen würden, mit dem System umzugehen.

| 1 | 2 | 3 | 4 | 5 |

8. Ich fand es sehr mühsam das System zu benutzen.

| 1 | 2 | 3 | 4 | 5 |

9. Ich fühlte mich bei der Nutzung des Systems sehr sicher.

| 1 | 2 | 3 | 4 | 5 |

10. Ich musste viele Dinge lernen, bevor ich das System nutzen konnte.

| 1 | 2 | 3 | 4 | 5 |

Abschlussfragebogen

Vp-Nr.:_____ Bedingung_____(vom Versuchsleiter
auszufüllen)

Teilnehmercode:
(vom Probanden auszufüllen)

erste 2 Buch-staben des Vornamens der Mutter	erste 2 Buch-staben des Vornamens des Vaters	Geburts-monat der Mutter	Geburts-monat des Vaters

Alter: _____   Jahre

Geschlecht: m w   (bitte ankreuzen)

Jahreskilometerleistung (Pkw):   ca. _____   km

	fast nie		1x pro Woche		täglich	
1. Wie häufig fahren Sie selbst einen Pkw?						
2. Wie häufig verrichten Sie körperliche Arbeit?						
	nie				häufig	
3. Wie häufig nutzen Sie einen Computer-Joystick?						
4. Wie häufig benutzen Sie eine SpaceMouse?						
5. Wie häufig nutzen Sie Flug- oder Fahr-simulationen am PC?						
Einschätzung der eigenen Fahrweise	gering				hoch	
6. Wie würden Sie Ihre Risikobereitschaft im Straßenverkehr einschätzen?						
	langsam/ vorsichtig				schnell/ sportlich	
7. Wie würden Sie Ihre Fahrweise einschätzen?						
	sehr				gar nicht	
8. Wie schwer fällt es Ihnen sich kurzfristig auf ein anderes Fahrzeug einzustellen?						
	sehr schlecht				sehr gut	
9. Wie würden Sie ihr Reaktionsvermögen im Vergleich zum durchschnittlichen Autofahrer einschätzen?						

**Vergleich der beiden Bedienkonzepte
(Joystick ohne vs. mit Spacemouse)** tl

Wie beurteilen Sie die nötige Konzentration zur Steuerung des Fahrzeugs mit…	gering						zu hoch
a) nur Joystick							
b) Joystick mit Spacemouse							
Wie häufig kam es vor, dass Sie bei Seitwärts- und Schrägfahrten übersteuerten?	sehr selten						sehr häufig
a) nur Joystick							
b) Joystick mit Spacemouse							
Wie schwierig war es, schnell zu reagieren?	sehr einfach						sehr schwierig
a) nur Joystick							
b) Joystick mit Spacemouse							
Mussten Sie auch nach längerer Benutzung erst überlegen, wie Sie einen Steuerwunsch mit dem System umsetzen?	Selten						Ständig
a) nur Joystick							
b) Joystick mit Spacemouse							
Wie gut wurden Sie bei den Fahraufgaben durch die beiden Bedienkonzepte unterstützt?	System wirkt störend						System unterstützt perfekt
a) nur Joystick							
c) Joystick mit Spacemouse							

	gar nicht						sehr
1. Wie sehr hat Sie der Leichtbauroboter während des Experiments gestört?							
2. Hatten Sie optimale Sicht auf den Monitor?							
3. Die Sitzposition war angenehm							
4. Die Armhaltung war angenehm							
5. Wurden Sie während des Experiments abgelenkt oder gestört?							

Simulator Sickness Questionnaire (nach Mehlitz, 2004)

Bitte füllen Sie folgenden Fragebogen aus, der verschiedene Symptome aufführt, die in Simulationsumgebungen auftreten können. Die Daten werden anonymisiert, d.h. ohne eine mögliche Zuordnung zu Ihrer Person, gespeichert. Falls Sie Fragen zu den einzelnen Symptomen haben, sprechen Sie bitte Ihren Testleiter an.

Symptom	**Ausprägung**			
(1) Allgemeines Unwohlsein	( ) nicht vorhanden	( ) etwas	( ) deutlich	( ) sehr stark
(2) Müdigkeit	( ) nicht vorhanden	( ) etwas	( ) deutlich	( ) sehr stark
(3) Kopfschmerzen	( ) nicht vorhanden	( ) etwas	( ) deutlich	( ) sehr stark
(4) Überanstrengte Augen	( ) nicht vorhanden	( ) etwas	( ) deutlich	( ) sehr stark
(5) Schwierigkeiten beim Scharfsehen	( ) nicht vorhanden	( ) etwas	( ) deutlich	( ) sehr stark
(6) Erhöhter Speichelfluss	( ) nicht vorhanden	( ) etwas	( ) deutlich	( ) sehr stark
(7) Schwitzen	( ) nicht vorhanden	( ) etwas	( ) deutlich	( ) sehr stark
(8) Übelkeit	( ) nicht vorhanden	( ) etwas	( ) deutlich	( ) sehr stark
(9) Konzentrationsschwierigkeiten	( ) nicht vorhanden	( ) etwas	( ) deutlich	( ) sehr stark
(10) Druckgefühl im Kopf	( ) nicht vorhanden	( ) etwas	( ) deutlich	( ) sehr stark
(11) Getrübtes Sehen	( ) nicht vorhanden	( ) etwas	( ) deutlich	( ) sehr stark
(12) Benommenheit bei geöffneten Augen	( ) nicht vorhanden	( ) etwas	( ) deutlich	( ) sehr stark
(13) Benommenheit bei geschlossenen Augen	( ) nicht vorhanden	( ) etwas	( ) deutlich	( ) sehr stark
(14) Schwindelgefühl	( ) nicht vorhanden	( ) etwas	( ) deutlich	( ) sehr stark
(15) Wahrnehmung des Magens	( ) nicht vorhanden	( ) etwas	( ) deutlich	( ) sehr stark
(16) Aufstoßen	( ) nicht vorhanden	( ) etwas	( ) deutlich	( ) sehr stark

Appendix C

Prototype phase

C.1   Static moment

The static analysis was followed to compare the torques generated by the new weight added by the systems. The general fomula to calculate a moment generated by a force F in a point G at a (perpendicular) distance d is:

$$M_G[Nm] = F \cdot d = P[kg] \cdot 9.8[m/s^2] \cdot d[m] \tag{C.1}$$

C.1.1   Direct drive

When no force is applied by the user in any of the directions ($\alpha = 0$), due to the symmetry of the system no torque is generated in the cardan joint, which will be our point G (and is stimated to be at a vertical distance of 0.06m). However, as soon as $\alpha \neq 0$, using C.1, the moment can be calculated. See Figure C.1 for angle and distance aclaration.

The maximum torque appears when $\alpha = \pm 20$ so:

$$M_G(max) = 0.8kg \cdot sen20 \cdot 9.8m/s^2 \cdot 0.06m \tag{C.2}$$

$$M_G(max) = 0.16kg \cdot m^2/s^2 = 0.16Nm \tag{C.3}$$

C.1.2   Indirect drive - Planetary gear

This case is similar to the direct drive case, the mass is centered, so only a torque is generated when $\alpha \neq 0$, and Figure C.1 also applies here. The maximum torque at G is when $\alpha = \pm 20$, so:

$$M_G(max) = (0.360 + 0.107)kg \cdot sen20 \cdot 9.8m/s^2 \cdot 0.06m \tag{C.4}$$

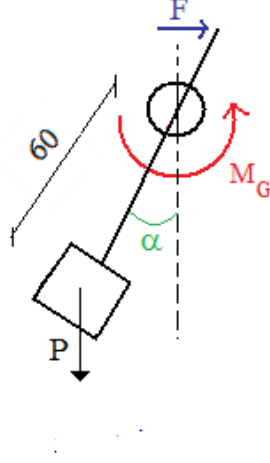$$M_G(max) = 0.094kg \cdot m^2/s^2 = 0.094Nm \tag{C.5}$$

Figure C.1: Distances (in cm) for cases C.1.1 and C.1.2

C.1.3 Indirect drive - Cable transmission

In this case, since the mass is not centered, a torque is generated even when $\alpha = 0$. Supposing the motor is placed in the back (if it is in the front the explanation would be analogous), the maximum torque appears at $\alpha = 20$ when steering forward, and the minimum when steering backwards and $\alpha = -20$. See Figure C.2 for angle and distance aclaration.

$$M_G(max) = P_p \cdot 9.8 \cdot d = 0.360kg \cdot cos\delta \cdot 0.06m \qquad (C.6)$$

$$M_G(max) = 0.360kg \cdot cos(90 - (\alpha + \beta)) \cdot 9.8m/s^2 \cdot 0.06m \qquad (C.7)$$

$$M_G(max) = 0.360kg \cdot cos(90 - 20 - atan(\frac{0.0375}{0.06})) \cdot 9.8m/s^2 \cdot 0.06m \quad (C.8)$$

$$M_G(max) = 0.360kg \cdot cos(90 - 20 - 32) \cdot 9.8m/s^2 \cdot 0.06m \qquad (C.9)$$

$$M_G(max) = 0.360kg \cdot cos38 \cdot 9.8m/s^2 \cdot 0.06m \qquad (C.10)$$

$$M_G(max) = 0.166kg \cdot m^2/s^2 = 0.166Nm \qquad (C.11)$$

The stimated minimum torque is also stimated:

$$M_G(min) = P_p \cdot 9.8 \cdot d = 0.360kg \cdot cos\delta \cdot 9.8m/s^2 \cdot 0.06m \qquad (C.12)$$
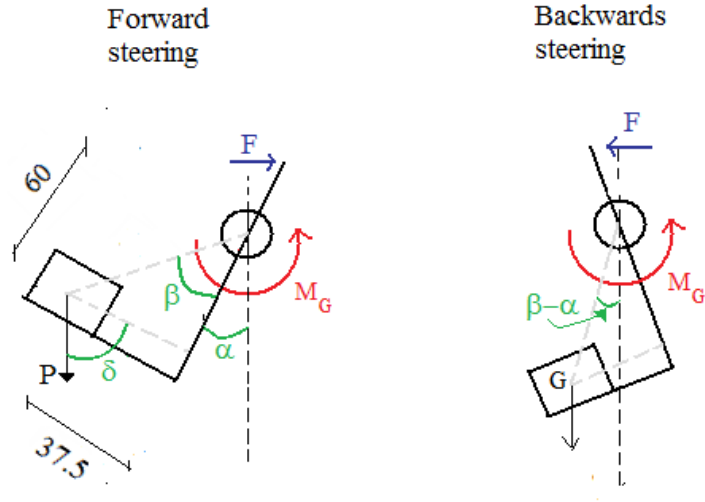
Figure C.2: Angles and distances (in cm) for case C.1.3

$$M_G(min) = 0.360kg \cdot cos(90 - (\beta - \alpha)) \cdot 9.8m/s^2 \cdot 0.06m \qquad \text{(C.13)}$$

$$M_G(min) = 0.360kg \cdot cos(90 - atan(\frac{0.0375}{0.06}) + 20) \cdot 9.8m/s^2 \cdot 0.06m \quad \text{(C.14)}$$

$$M_G(min) = 0.360kg \cdot cos(90 - 32 + 20) \cdot 0.06m \qquad \text{(C.15)}$$

$$M_G(min) = 0.360kg \cdot cos78 \cdot 9.8m/s^2 \cdot 0.06m \qquad \text{(C.16)}$$
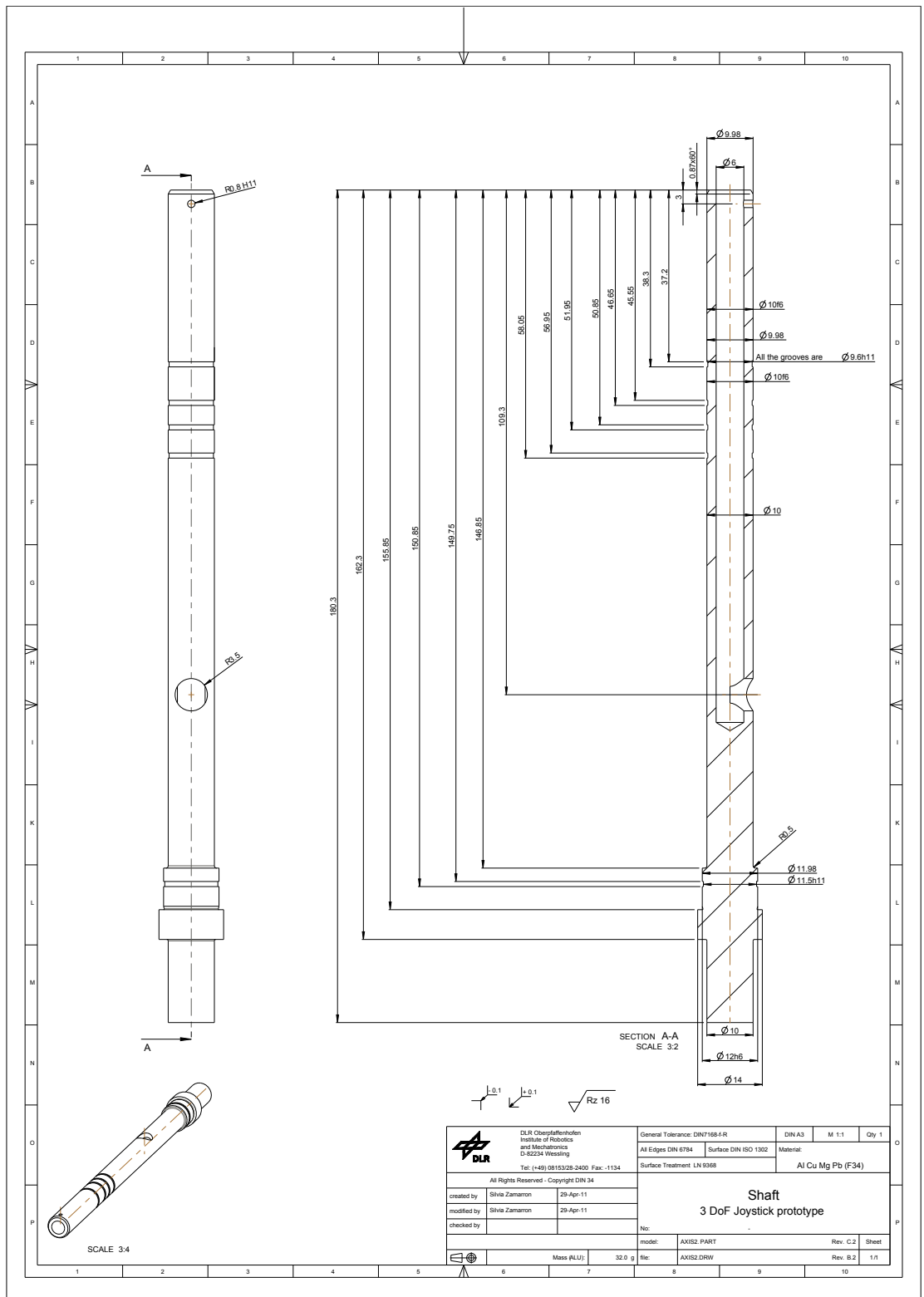
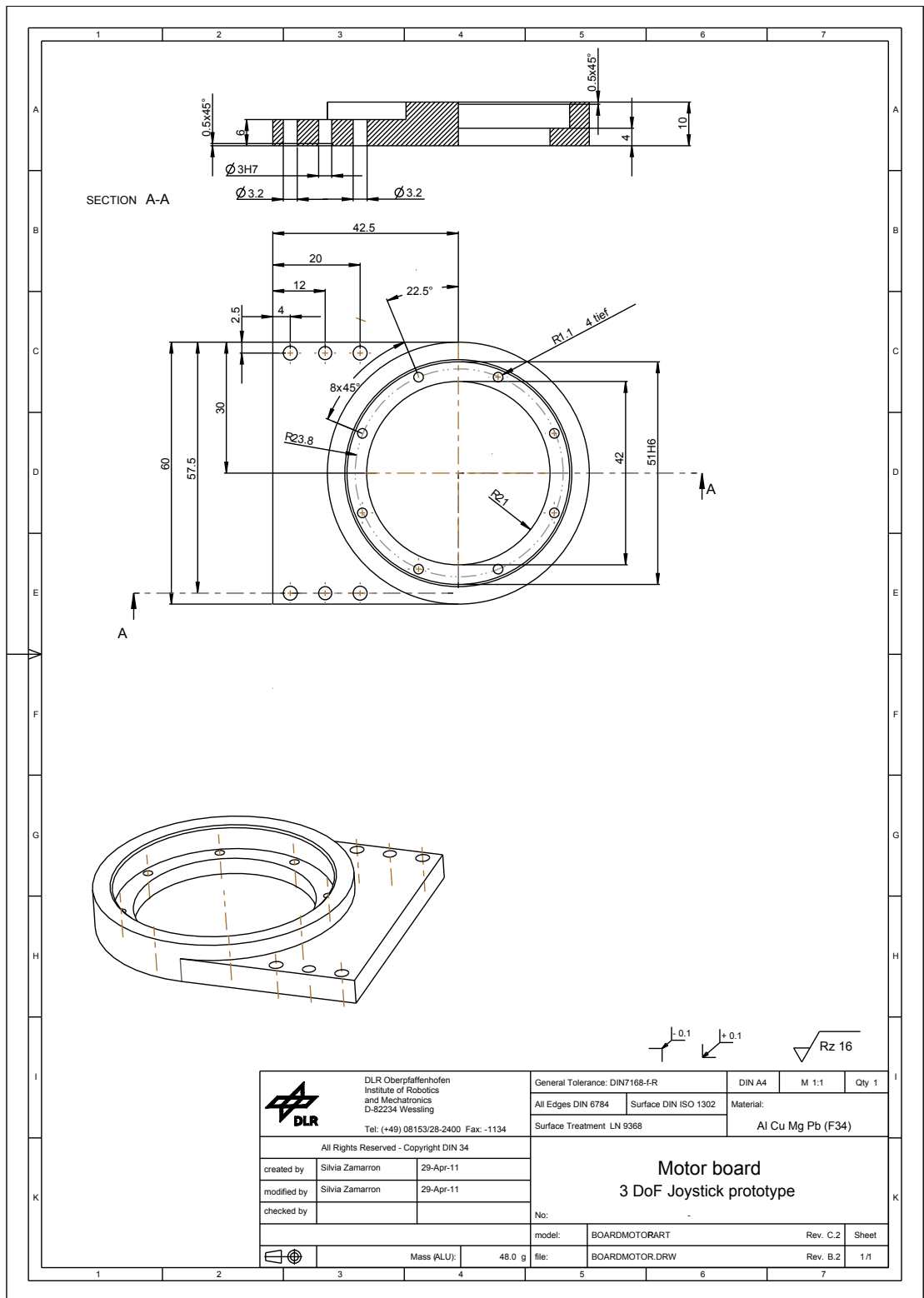$$M_G(min) = 0.044kg \cdot m^2/s^2 = 0.044Nm \qquad \text{(C.17)}$$

Appendix D

Final design

D.1 Drawings

The following pages contain the drawings of the parts submitted to the Workshop to be manufactured.

A

R0.8 H11

R3.5

A

SCALE 3:4

SECTION A-A
SCALE 3:2

Ø9.98
0.87x60°
Ø6
3
Ø10f6
Ø9.98
All the grooves are   Ø9.6h11
Ø10f6
Ø10
R0.5
Ø11.98
Ø11.5h11
Ø10
Ø12h6
Ø14

38.3
37.2
45.55
46.65
50.85
51.95
56.95
58.05
109.3
146.85
149.75
150.85
155.85
162.3
180.3

-0.1   +0.1   Rz 16

DLR Oberpfaffenhofen Institute of Robotics and Mechatronics D-82234 Wessling Tel: (+49) 08153/28-2400 Fax: -1134	General Tolerance: DIN7168-f-R		DIN A3	M 1:1	Qty 1
	All Edges DIN 6784	Surface DIN ISO 1302	Material:		
	Surface Treatment LN 9368		Al Cu Mg Pb (F34)		

All Rights Reserved - Copyright DIN 34

created by	Silvia Zamarron	29-Apr-11	Shaft 3 DoF Joystick prototype		
modified by	Silvia Zamarron	29-Apr-11			
checked by					
			No:	-	
			model:	AXIS2. PART	Rev. C.2	Sheet
Mass (ALU):	32.0 g	file:	AXIS2.DRW	Rev. B.2	1/1

SECTION A-A

0.5x45°

0.5x45°

6

4

10

Ø3H7

Ø3.2

Ø3.2

42.5

20

12

22.5°

R1.1 4 tief

2.5

4

8x45°

R23.8

R31

30

42

51H6

60

57.5

A

A

- 0.1   + 0.1   √ Rz 16

General Tolerance: DIN7168-f-R		DIN A4	M 1:1	Qty 1
All Edges DIN 6784	Surface DIN ISO 1302	Material:		
Surface Treatment LN 9368		Al Cu Mg Pb (F34)		

created by	Silvia Zamarron	29-Apr-11
modified by	Silvia Zamarron	29-Apr-11
checked by		

Motor board
3 DoF Joystick prototype

No: -

model:	BOARDMOTORPART	Rev. C.2	Sheet
file:	BOARDMOTOR.DRW	Rev. B.2	1/1

Mass (ALU):   48.0 g

104

SECTION B-B

SECTION A-A
SCALE 11:8

All radius are r=2.1

Rz 16

General Tolerance: DIN7168-f-R | DIN A4 | M 1:1 | Qty 1
All Edges DIN 6784 | Surface DIN ISO 1302 | Material:
Surface Treatment LN 9368 | Al Cu Mg Pb (F34)

created by	Silvia Zamarron	27-Apr-11
modified by	Silvia Zamarron	27-Apr-11
checked by		

Griffbolzen
3 DoF Joystick prototype

No: -

model: KRJ_GRIFFBOLZEN222.PART | Rev. --- | Sheet
Mass(ALCUMGPB_F34): 26.7 g | file: GRIFF.DRW | Rev. B.2 | 1/1

SECTION C-C

Ø 23H13
Ø 22H12
Ø 21H6
Ø 19

4.3
2.1
1
10.5
9.3
4

SECTION B-B
SCALE 3:2

5.5
0.5x45°
Ø 3H7
M3
21.5
14
Ø 3H7
6.5
0.5x45°
7.9
28
18.75
14
9.25
11
25
39
50

SECTION A-A

4.5
5
Ø 2.2
Ø 2H6
Ø 4.3
Ø 4.3
Ø 2.2
18.75
14
9.25
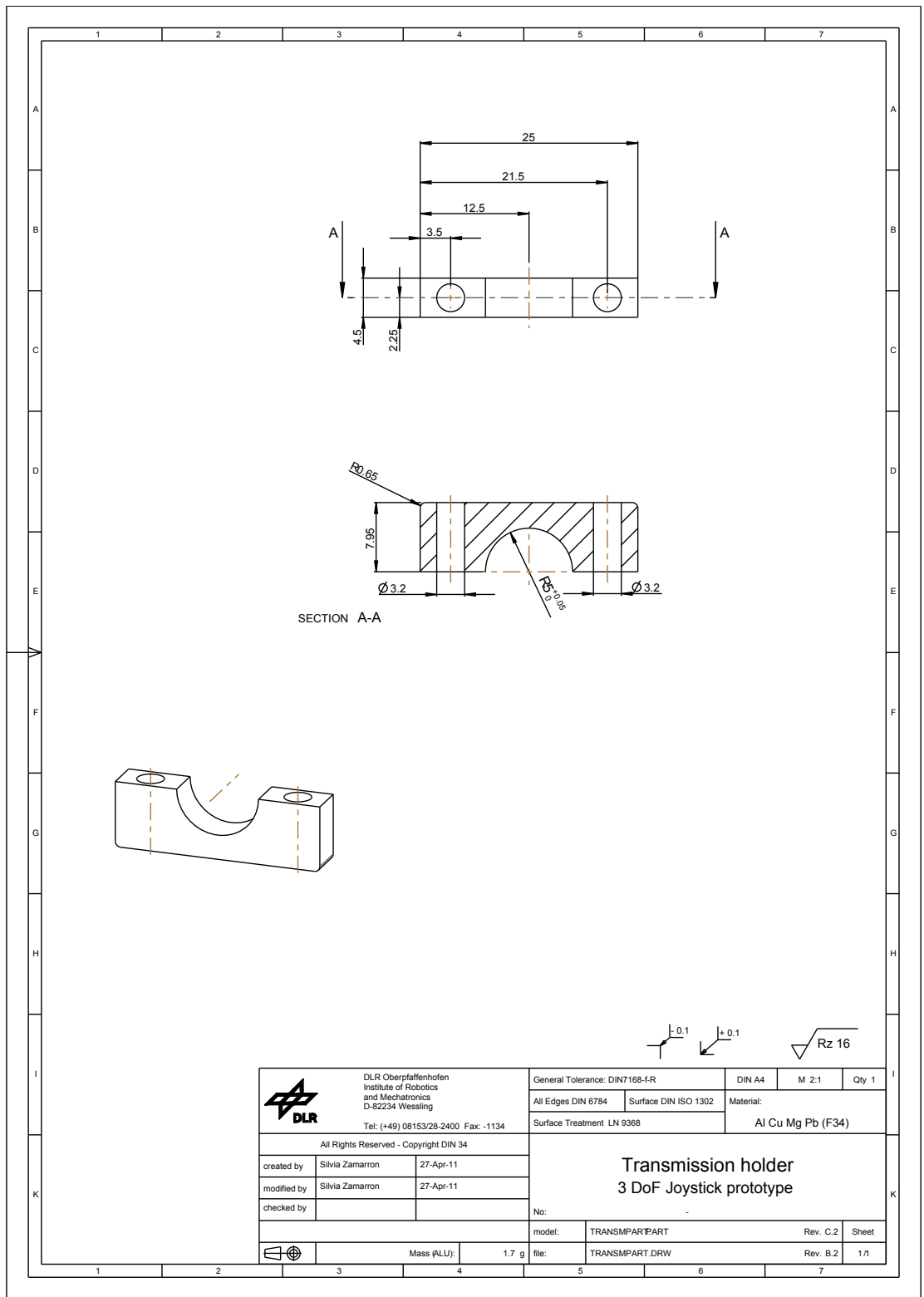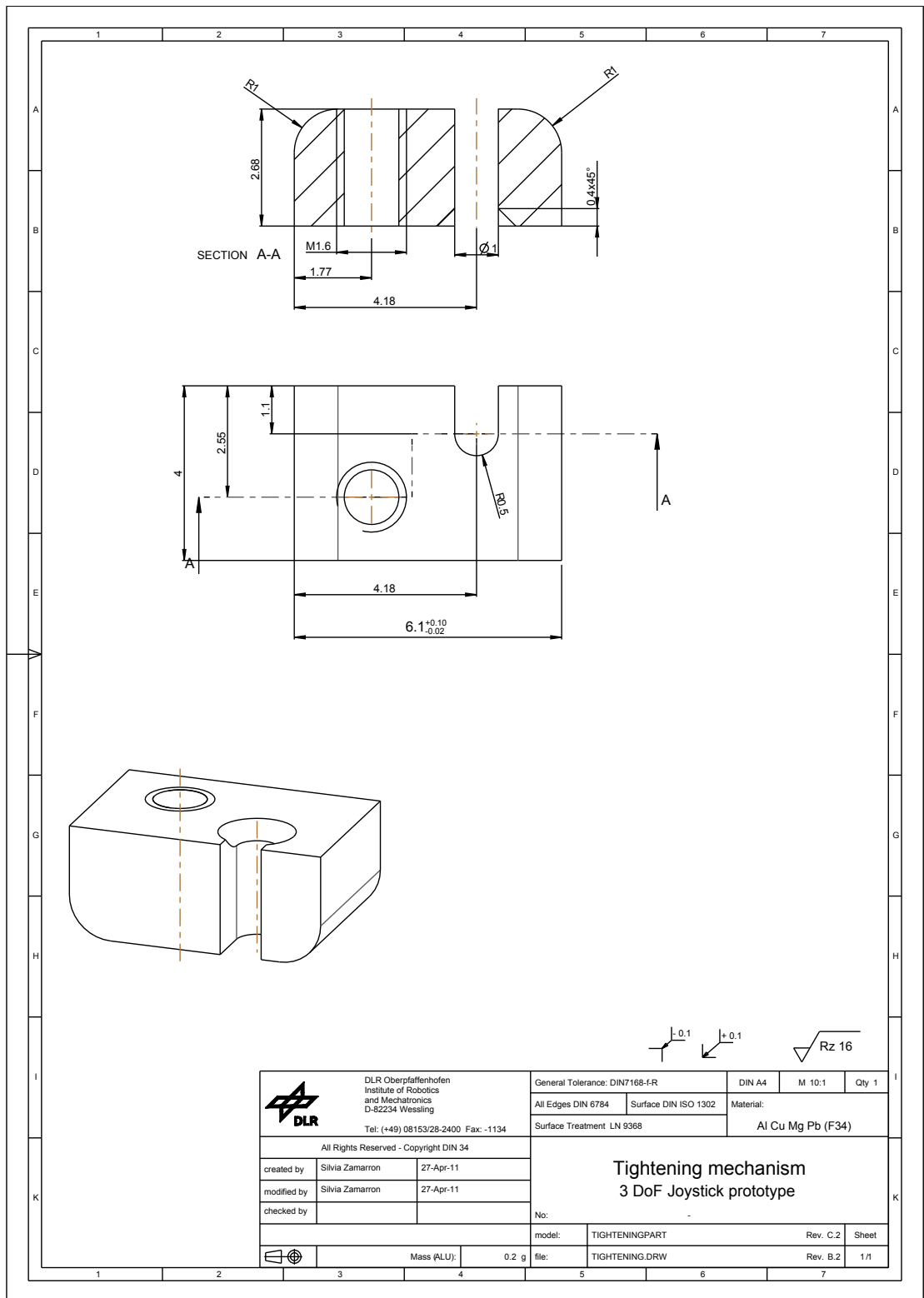
- 0.1   + 0.1   √ Rz 16

DLR Oberpfaffenhofen
Institute of Robotics
and Mechatronics
D-82234 Wessling
Tel: (+49) 08153/28-2400 Fax: -1134

General Tolerance: DIN7168-f-R		DIN A4	M 1:1	Qty 1
All Edges DIN 6784	Surface DIN ISO 1302	Material:		
Surface Treatment LN 9368		Al Cu Mg Pb (F34)		

Bearing board

3 DoF Joystick prototype

created by	Silvia Zamarron	27-Apr-11
modified by	Silvia Zamarron	27-Apr-11
checked by		

		No:	-	
		model:	BOARD3PART	Rev. C.2	Sheet
Mass (ALU):	29.1 g	file:	BOARD3.DRW	Rev. B.2	1/1

SCALE 5:2

SECTION A-A

DETAIL B
SCALE 3:1

DETAIL A
SCALE 3:1

SCALE 3:2

All radius r=1

Rz 16

32.95
14.45
9.5
12.5
6.5
6.5
4.5

29.56
26.2
25.2
22.45
21.45
8.25
6.38
5.09
115°
R25
155°
25
18.62
6.52
14.45
15.45
20.77
28.72
29.56
$10^{+0.03}$

2.25
M3
3.82
Ø 1.8
11
4.5
21.18
17.17
16.5
15
M3

25.2
24.75
21.7
20.76
15.45
14.45
7.95
16.5
12.5
10
8
SEE DETAIL A
SEE DETAIL B
19.35
20.2°

17.3
2.7
1

6.25
1.3
R2

1
R1.4
R0.3

SECTION A-A

General Tolerance: DIN7168-f-R
All Edges DIN 6784
Surface DIN ISO 1302
Surface Treatment LN 9368
DIN A3
M 1:1
Qty 1
Material:
Al Cu Mg Pb (F34)

created by | Silvia Zamarron | 29-Apr-11
modified by | Silvia Zamarron | 29-Apr-11
checked by

Transmission
3 DoF Joystick prototype

No: -
model: TRANSM_NEWPART | Rev. C.2 | Sheet
Mass (ALU): 10.9 g | file: TRANSM_NEW.DRW | Rev. B.2 | 1/1
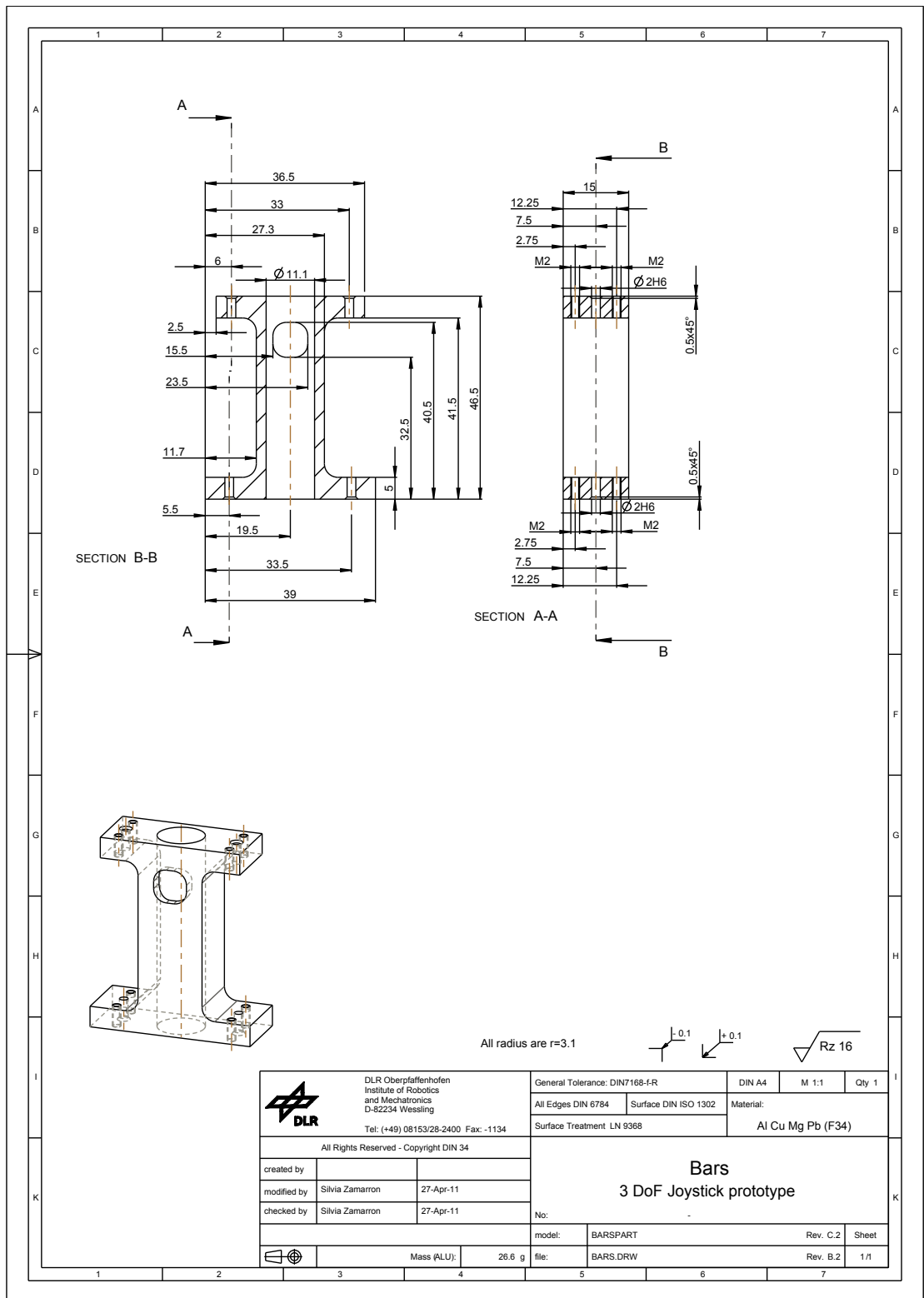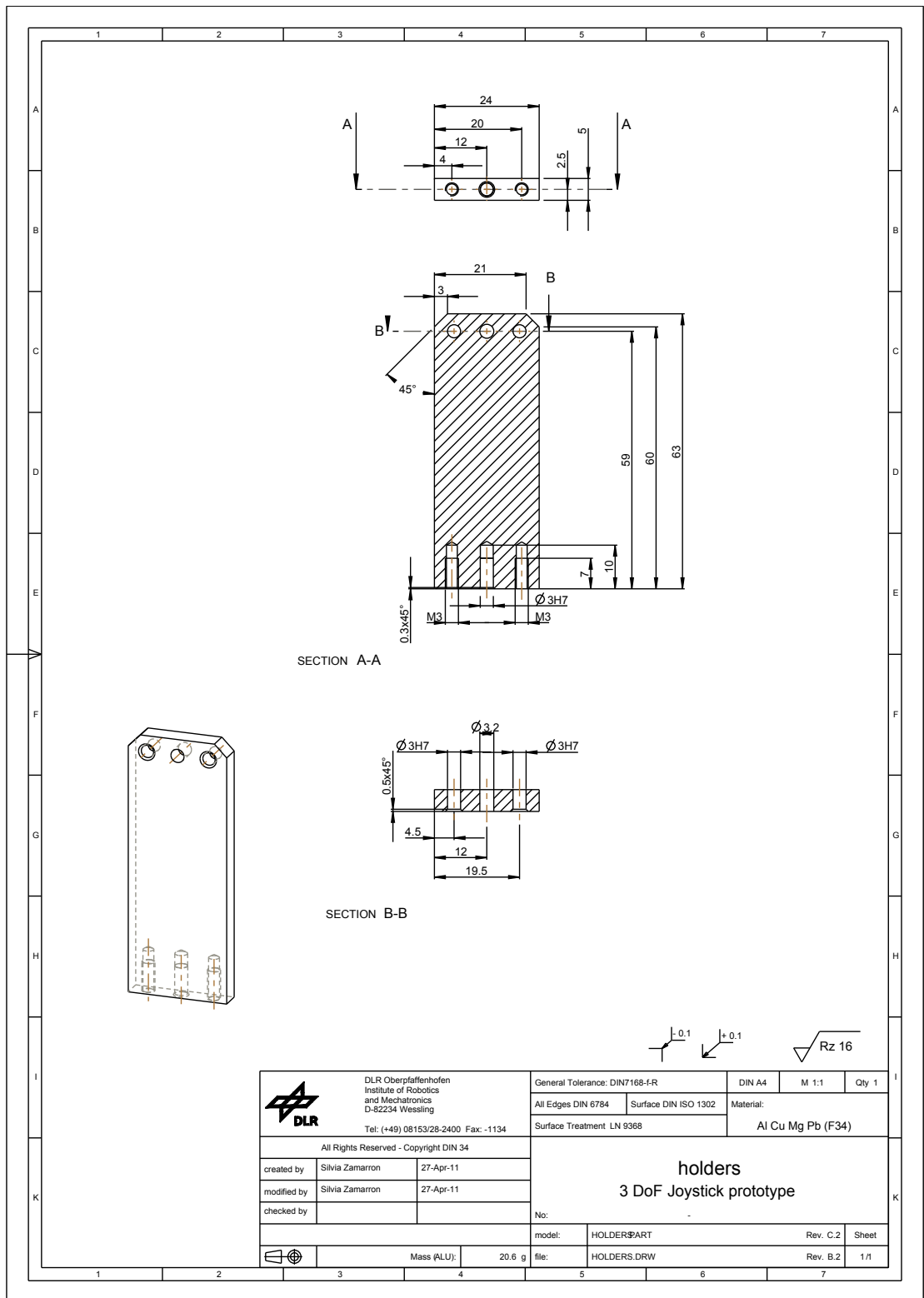
SECTION A-A

	DLR Oberpfaffenhofen Institute of Robotics and Mechatronics D-82234 Wessling Tel: (+49) 08153/28-2400 Fax: -1134	General Tolerance: DIN7168-f-R		DIN A4	M 2:1	Qty 1
		All Edges DIN 6784	Surface DIN ISO 1302	Material:		
		Surface Treatment LN 9368		Al Cu Mg Pb (F34)		
All Rights Reserved - Copyright DIN 34						
created by	Silvia Zamarron	27-Apr-11	Transmission holder			
modified by	Silvia Zamarron	27-Apr-11	3 DoF Joystick prototype			
checked by			No:	-		
			model:	TRANSMPART.PART	Rev. C.2	Sheet
		Mass (ALU):	1.7 g	file:	TRANSMPART.DRW	Rev. B.2	1/1

SECTION A-A

R1
R1

2.68

0.4x45°

M1.6

Ø1

1.77

4.18

1.1

2.55

4

R0.5

A

A

4.18

6.1 $^{+0.10}_{-0.02}$

- 0.1   + 0.1   Rz 16

General Tolerance: DIN7168-f-R		DIN A4	M 10:1	Qty 1
All Edges DIN 6784	Surface DIN ISO 1302	Material:		
Surface Treatment LN 9368		Al Cu Mg Pb (F34)		

created by	Silvia Zamarron	27-Apr-11
modified by	Silvia Zamarron	27-Apr-11
checked by		

Tightening mechanism
3 DoF Joystick prototype

No: -

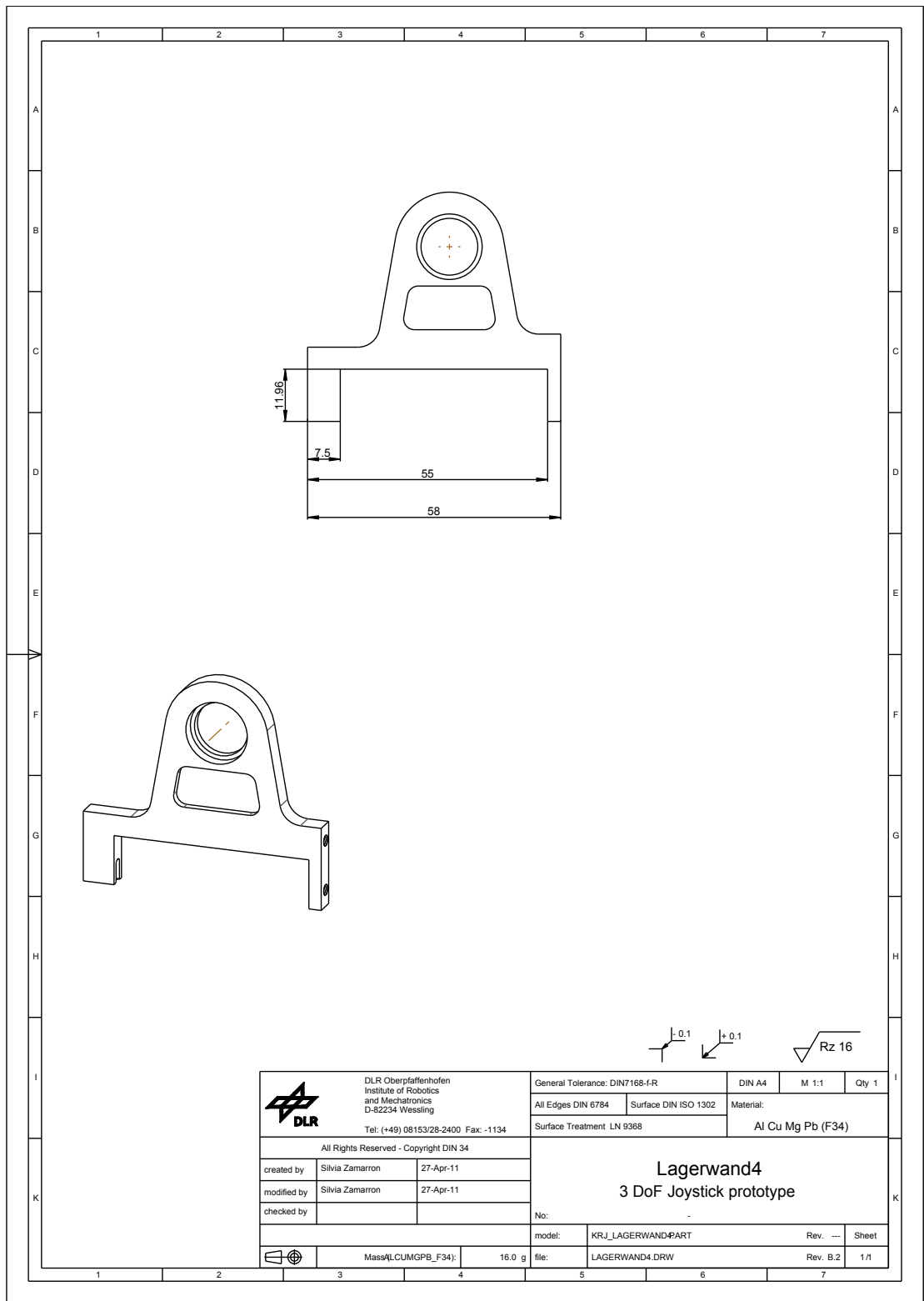| model:	TIGHTENINGPART	Rev. C.2	Sheet
Mass (ALU): 0.2 g	file: TIGHTENING.DRW	Rev. B.2	1/1

109

SECTION B-B

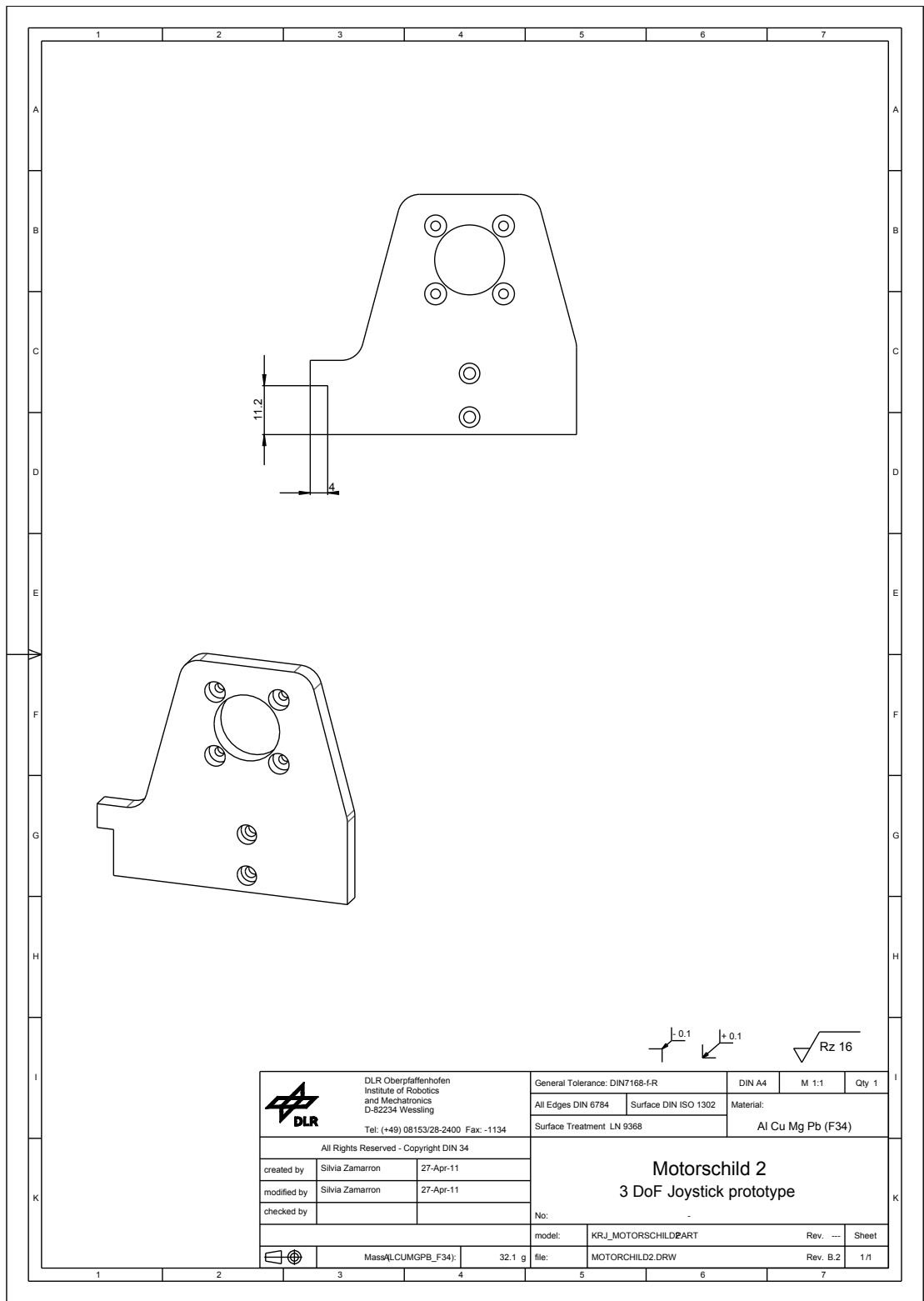SECTION A-A

All radius are r=3.1

Rz 16

	DLR Oberpfaffenhofen Institute of Robotics and Mechatronics D-82234 Wessling Tel: (+49) 08153/28-2400 Fax: -1134		General Tolerance: DIN7168-f-R		DIN A4	M 1:1	Qty 1
			All Edges DIN 6784	Surface DIN ISO 1302	Material:		
			Surface Treatment LN 9368		Al Cu Mg Pb (F34)		
All Rights Reserved - Copyright DIN 34							
created by				**Bars**			
modified by	Silvia Zamarron	27-Apr-11		3 DoF Joystick prototype			
checked by	Silvia Zamarron	27-Apr-11	No:	-			
			model:	BARSPART		Rev. C.2	Sheet
Mass (ALU):		26.6 g	file:	BARS.DRW		Rev. B.2	1/1

110

SECTION A-A

SECTION B-B

| | | DLR Oberpfaffenhofen Institute of Robotics and Mechatronics D-82234 Wessling | General Tolerance: DIN7168-f-R | | DIN A4 | M 1:1 | Qty 1 |

General Tolerance: DIN7168-f-R   DIN A4   M 1:1   Qty 1

All Edges DIN 6784   Surface DIN ISO 1302   Material:

Surface Treatment LN 9368

Al Cu Mg Pb (F34)

All Rights Reserved - Copyright DIN 34

created by	Silvia Zamarron	27-Apr-11
modified by	Silvia Zamarron	27-Apr-11
checked by		

holders
3 DoF Joystick prototype

No: -

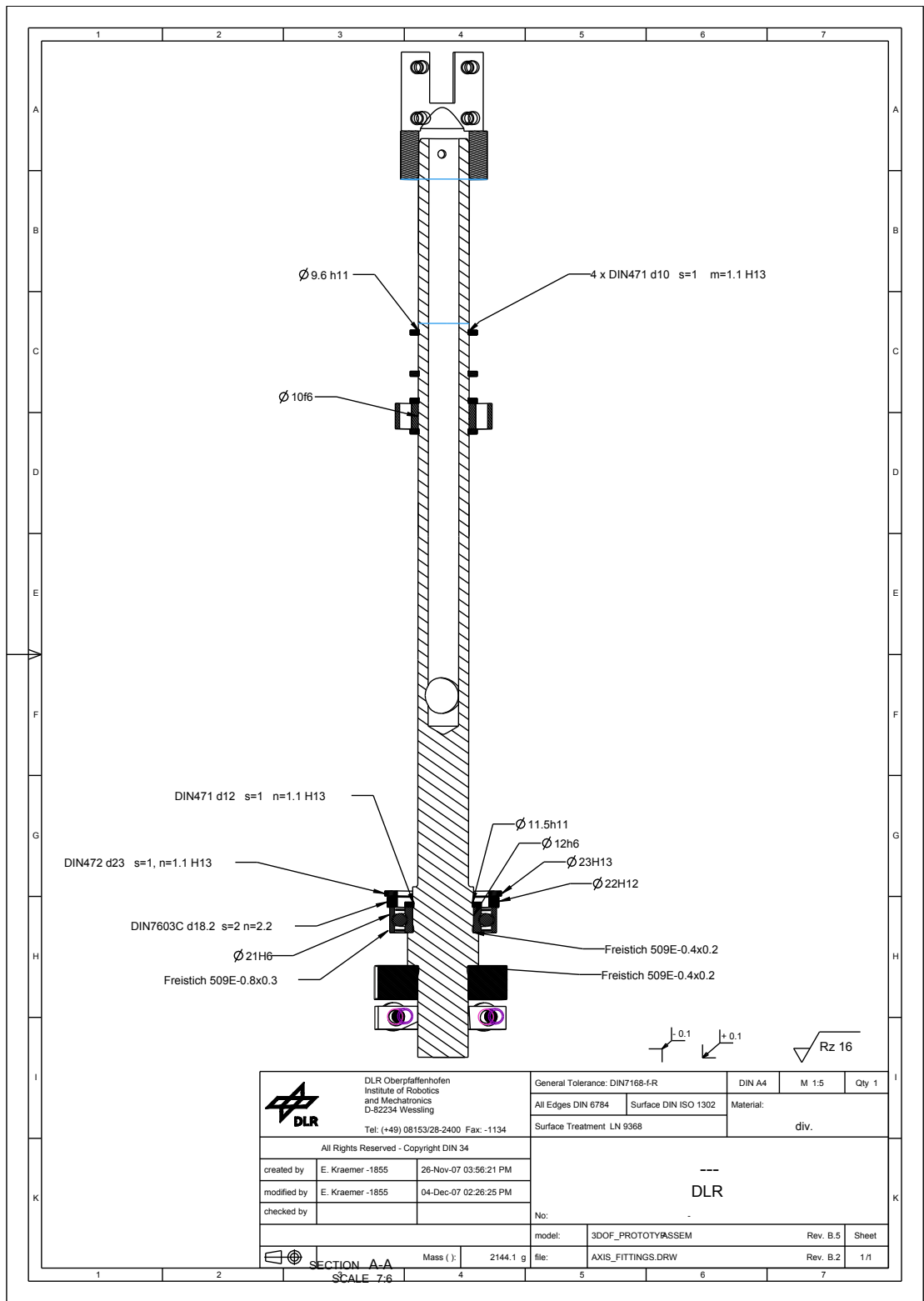| model: | HOLDERSPART | | Rev. C.2 | Sheet |
| Mass (ALU): | 20.6 g | file: | HOLDERS.DRW | Rev. B.2 | 1/1 |

111

193

142.5

119

67.9

All radius are r=3.1

- 0.1   + 0.1   √ Rz 16

	DLR Oberpfaffenhofen Institute of Robotics and Mechatronics D-82234 Wessling	General Tolerance: DIN7168-f-R		DIN A4	M 1:4	Qty 1
DLR		All Edges DIN 6784	Surface DIN ISO 1302	Material:		
	Tel: (+49) 08153/28-2400 Fax: -1134	Surface Treatment LN 9368		Al Cu Mg Pb (F34)		
All Rights Reserved - Copyright DIN 34						
created by	Silvia Zamarron	28-Apr-11		**Grundplatte**		
modified by	Silvia Zamarron	28-Apr-11		3 DoF Joystick prototype		
checked by			No:	-		
			model:	KRJ_GRUNDPLATTEPART	Rev. ---	Sheet
⊟⊕	Mass(ALCUMGPB_F34):	562.6 g	file:	GRUNDPLATTE.DRW	Rev. B.2	1/1

11.96

7.5

55

58

- 0.1   + 0.1   Rz 16

General Tolerance: DIN7168-f-R	DIN A4	M 1:1	Qty 1
All Edges DIN 6784	Surface DIN ISO 1302	Material:
Surface Treatment LN 9368	Al Cu Mg Pb (F34)

created by	Silvia Zamarron	27-Apr-11
modified by	Silvia Zamarron	27-Apr-11
checked by		

Lagerwand4
3 DoF Joystick prototype

No: -

model:	KRJ_LAGERWAND4.PART	Rev. ---	Sheet
Mass(ALCUMGPB_F34):	16.0 g	file:	LAGERWAND4.DRW	Rev. B.2	1/1

113

11.2

4

- 0.1   + 0.1   Rz 16

114

Ø 9.6 h11

4 x DIN471 d10 s=1   m=1.1 H13

Ø 10f6

DIN471 d12 s=1 n=1.1 H13

Ø 11.5h11
Ø 12h6
DIN472 d23 s=1, n=1.1 H13
Ø 23H13
Ø 22H12

DIN7603C d18.2 s=2 n=2.2
Freistich 509E-0.4x0.2
Ø 21H6
Freistich 509E-0.4x0.2
Freistich 509E-0.8x0.3

- 0.1   + 0.1   Rz 16

General Tolerance: DIN7168-f-R | DIN A4 | M 1:5 | Qty 1

All Edges DIN 6784 | Surface DIN ISO 1302 | Material:

Surface Treatment LN 9368 | div.

created by	E. Kraemer -1855	26-Nov-07 03:56:21 PM
modified by	E. Kraemer -1855	04-Dec-07 02:26:25 PM
checked by		

DLR

No: -

model: 3DOF_PROTOTYPASSEM   Rev. B.5   Sheet

file: AXIS_FITTINGS.DRW   Rev. B.2   1/1

Mass ( ):   2144.1 g

SECTION A-A
SCALE 7:6

115

D.2 Standarized elements

D.2.1 List of standarized elements

The following is the list of standarized elements contained in the mechanical system.

- Screws

    - 4 x DIN912 M03x12
    - 8 x DIN912 M02x06
    - 2 x DIN912 M03x10
    - 4 x DIN912 M02x12
    - 4 x DIN912 M02x10
    - 1 x DIN912 M16x10
    - 2 x DIN912 M03x16

- Pins

    - 6 x DIN7 d02 L=12
    - 4 x DIN7 d03 L=8

- Rings

    - 4 x DIN471 d10
    - 1 x DIN471 d12
    - 1 x DIN472 d23
    - 1 x DIN7606C 18.2x22x2

- Bearings

    - 1 x 61800-2z-SKF d=10, D=19
    - 1 x 61801-2z-SKF d=12, D=21

- cable: 1x D=0.6 AISI 316, construction 1x7CG007060

- ball: 2x C-type terminal d=2.3 CM004523

D.2.2 Displacement of the joining elements

The following figures show the exact displacement of all the joining elements (screws and pins).
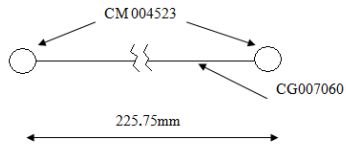
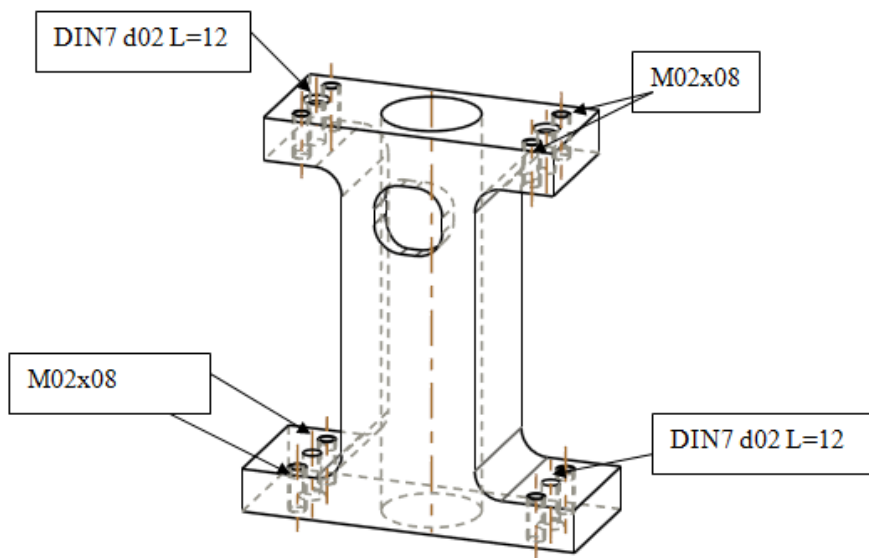Figure D.1: Representation of the cable and bars

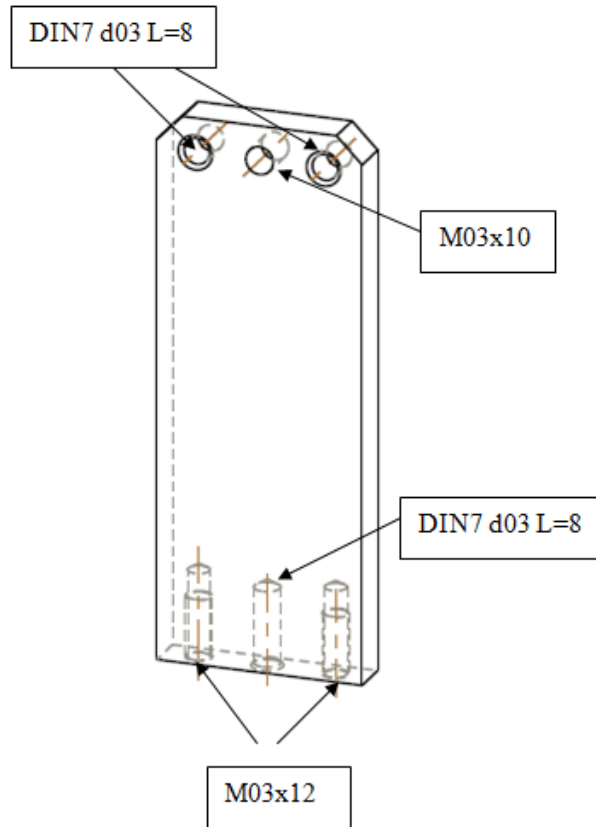

Figure D.2: Pins and screws at the 'Bars' part
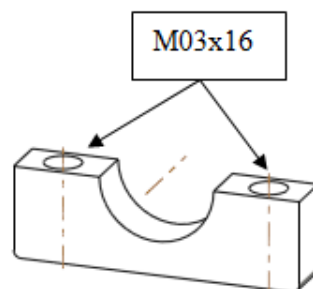
Figure D.3: Pins and screws at the 'Holders' part

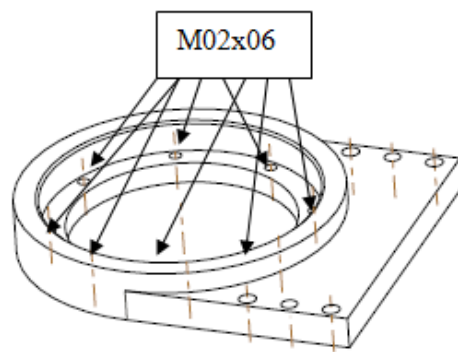Figure D.4: Pins and screws at the 'Transmission' part

Figure D.5: Pins and screws at the 'Motor board' part

Bibliography

[1] Oshima, H.; Tani, M.; Kobayashi, N.; Ishii, A.; Imai, K.: *Control for Four-Wheel Individual Steering and Four-Wheel Driven Electronic Vehicle*, Electrical Engineering in Japan, Vol. 153, No. 3, 2005.

[2] Christiansson, G. A. V.: *Introduction to Analysis and Control in Haptic Teleoperation*, Delft Haptics Laboratory, Delft University of Technology, 2007.

[3] Lichiardopol, S.: *A Survey on Teleoperation*, Technische Universiteit Eindhoven Department Mechanical Engineering, DCT report, Eindhoven, December, 2007.

[4] Lin, W. C.; Young, K. Y.: *Design of Force-Reflection Joystick System for VR-Based Simulation*, Journal of Information, Science and Engineering No. 23, 1421-1436 (2007).

[5] Ellis, R. E.; Ismaeil, O. M.; Lipsett, M. G.: *Design and evaluation of high-performance haptic interface*, Robotica vol 4 pp 321-327, 1996.

[6] Zhai, S.: *Human Performance in Six Degree of Freedom Input Control*, Department of Industrial Engineering. Toronto: University of Toronto, 1995.

[7] Burdea, G.C.: *Force and touch feedback for virtual reality*, Wiley-Interscience, 1 edition (August 3, 1996).

[8] Zhai, S.; Milgram, P.: *Human performance evaluation of isometric and elastic rate controllers in a 6 DOF tracking task*, Proc. of SPIE Vol.2057 Telemanipulator Technology, Boston, MA., USA.

[9] Maruping, P.: *The Design and Construction of a Large Scale- Force Feedback Joystick for the use in Physiotherapy*, University of Southren Queensland Faculty of Engineering and Surverying, 2009.

[10] Russo, M. A.: *The design and implementation of a three degree of freedom force output joystick*, Masachusssets Institute of Technology (MIT), Masther's Thesis (1990).

[11] Birglen, L.; Gosselin, C.; Pouliot N.; Monsarrat, B.; Laliberté, T.: *SHaDe, A New 3-DOF Haptic Device*, IEEE Transactions on Robotics and automation, Vol. 18, No. 2, April 2002.

[12] Millman, P.A.; Stanley, M.; Colgate, J. E.: *Design of a hogh performance haptic interface to virtual environments*, Proc. IEEE Virtual Reality Annual International Symposium, pp. 216-222, 1993.

[13] Lindemann, R.: *Construction and demonstration of a 9-string 6 DoF force reflecting joystick for telerobotics*, Proc. of NASA International Conference on Space Telerobotics, No. 4, pp. 55-63, 1989.

[14] Hanke, D.; Herbst, C.: *Active sidestick technology - a means for improving situational awareness*, Aerosp. Sci. Technol. 3 pp. 525-532, 1999.

[15] Black, G. T.; Moorhouse, D.J.: *Flying Qualities Design Requirements for Sidestick Controllers*, AFFDL-TR-79-3126, Oct. 1979.

[16] Andonian, B.; Rauch, W.; Bhise, V.: *Driver Steering Performance Using Joystick vs. Steering Wheel Controls*, Society of Automotive Engineering, SAE paper 2003-01-1108, 2003.

[17] Eckstein, L. 2001. *Entwicklung und Überprüfung eines Bedienkonzepts und von Algorithmen zum Fahren eines Kraftfahrzeugs mit aktiven Sidesticks* Fortschrittsberichte VDI-Reihe 12 Nr. 471. VDI-Verlag, Düsseldorf.

[18] The Boeing Company, 1999

[19] Mücke, S.: *Der Einfluß der Aufgabenschwierigkeit auf die Leistungsund Beanspruchungsbezogenen Potentiale aktiver Stellteile*, 54 (26NF) 2000/1 Z. Arb. Wiss., 2000.

[20] Mayer, A.: *Untersuchung über den Einfluss eines aktiven Bedienelements auf die menschliche Regelleistung*, Fortschritt-Berichte VDI-Reihe 17, No. 37, 1987.

[21] Peters, B.; Östlund, J.: *Manoeuvrability characteristics of cars operated by joysticks*, VTI meddelande 860A-1999, Swedish Road and Transport Research Institute (VTI), Linköping, Sweden, 1999.

[22] Peters, B.; Östlund, J.: *Joystick controlled driving for drivers with disabilities*, VTI rapport 506A-2005, Swedish Road and Transport Research Institute (VTI), Linköping, Sweden, 2005.

[23] Bünte, T.:*Human Machine Interface Concept for Interactive Motion Control of a Highly Maneuverable Robotic Vehicle*, DLR, 2011.

[24] *Institut für Robotik und Mechatronik. Knowledge for tomorrow*, DLR, 2010.

[25] Donges, E.:*A Two-Level Model of Driver Steering Behavior*, Human Factors. Vol 20. No 6. pp 691-708. 1978.

[26] Mischon, J.A.:*A critical view of driver behaviour models: What do we know, what should we do?* Proceedings of the International Symposium on Human Behaviour and Traffic Safety. Plenum, New York. 1985.

[27] Huang, H. M.:*Toward a Generic Model for Autonomy Levels for Unmanned Systems (ALFUS)*, Proceedings of the 2003 Performance Metrics for Intelligence Systems Workshop, Gaithersburg, MD, August 16-18, 2003.

[28] Hara, M.; Matthey, G.; Yamamoto, A.; Chapuis, D.; Gassert, R.; Bleuler, H.; Higuchi, T.: *Development of a 2-DOF Electrostatic Haptic Joystick for MRI/fMRI Applications*, 2009 IEEE International Conference on Robotics and Automation Kobe International Conference Center Kobe, Japan, May 12-17, 2009.

[29] Mazurkiewicz, J.: *The Basics of Motion Control-Part 1*, Baldor Electric co, Power transmission design, 1996.

[30] Eberle, S.; Ohndorf, A.; Faller, R.: *On-Orbit Servicing Mission Operations at GSOC*, SpaceOps 2010 Conference, Delivering on the Dream, Hosted by NASA Mars, 25 - 30 April 2010, Huntsville, Alabama.

[31] Martin, K. M.; Levin, M. D.; Braun, A.C.: *Force Feedback Transmission System*, United States Patent 6104382, August 2000.

[32] Martin, K. M.; Levin, M. D.; Rosenberg, B.; Moore, D. F.: *Mechanical and Force Force Feedback Transmission System*, United States Patent 6400352, June 2002.

[33] Martin, K. M.; Levin, M. D.; Braun, A.C.: *Method and apparatus for controlling force feedback interface system*, United States Patent 6400352, January 2006.

[34] Eiberger, O.; Haddadin, S.; Weis, M.; Albu-Schäffer, A.; Hirzinger, G.: *On Joint Design with Intrinsic Variable Compliance: Derivation of the DLR QA-Joint*, In Proceedings of ICRA'2010. pp.1687-1694.

[35] Cooper, R.; Spaeth, D.: *Variable Compliance Joystick with Compensation Algorithm*, United States Patent 0153370, June 2009.

[36] Petit, F.; Chalon, M.; Friedl, W.; Grebenstein, M.; Albu-Schaeffer, A.; Hirzinger, G.: *Bidirectional Antagonistic Variable Stiffness Actuation: Analysis, Design and Implementation*, 2010 IEEE International Conference on Robotics and Automation Anchorage Convention District May 3-8, 2010, Anchorage, Alaska, USA.

[37] Panzer, H.; Eiberger, O.; Grebenstein, M.; Schaefer, P.; Van der Smagt, P.: *Human motion range data optimizes anthropomorphic robotic hand-arm system design*, Proceedings of the 1998 IEEE International Conference on Robotics and Automation Leuven, Belgium o May 1998.

[38] *Uniones atornilladas*, ARATEC ingeniería.

[39] Kelly, A.: *A Vector Algebra Formulation of Kinematics of Wheeled Mobile Robots*, Carnegie Mellon University, 2010.

[40] Andreasson, J.; Bünte, T.: *Global Chassis Control Based on Inverse Vehicle Dynamics Models*, Proc. 19th IAVSD Symposium, Milan, Italy, 2005. Supplement to Vehicle System Dynamics, Volume 44, 2006.

[41] Siegwart, R.: *Mobile Robot Kinematics Requirements for Motion Control*, ETH Zurich.

[42] Wada, M.; Mori, S.: *Holonomic and Omnidirectional Vehicle with Conventional Tires*, Proceedings of the 1996 IEEE International Conference on Robotics and Automation Minneapolis, Minnesota - April 1996.

[43] Muñoz Martínez, V. F.; Gil-Gómez, G.; García Cerezo, A.:*Modelado cinemático y dinámico de un robot móvil omni-direccional*, Instituto Andaluz de Automática Avanzada y Robótica. Dpto. Ingeniería de Sistemas y Automática.

[44] Kozlowski, K.; Pazderski, D.: *Modelling and control of a 4-wheel skid-steering mobile robot*, Int. J. Appl. Math. Comput. Sci., 2004, Vol. 14, No. 4, 477-496.

[45] Lauria, M.; Nadeau, I.; Lepage, P.; Morin, Y.; Giguère, P.; Gagnon, F.; Létourneau, D.; Michaud, F.: *Design and Control of a Four Steered Wheeled Mobile Robot*, Proc. 32nd Annual Conference on Industrial Electronics, pp. 4020-4025, 2006.